Bio-Synthetic Emulsion Polymer Latexes for Adhesive Applications

Yujie Zhang

Thesis submitted to the

Faculty of Graduate and Postdoctoral Studies

In partial fulfilment of the requirements

For the degree of

Doctorate in Philosophy

Department of Chemical Engineering

Faculty of Engineering

University of Ottawa

uOttawa

Abstract

Petroleum resources are the dominant feedstock used in polymer production, however, with the depletion of petroleum resources and the associated environmental concerns, it is necessary to explore alternative renewable resources to produce polymeric materials. Using experimental grade starch nanoparticles (SNPs) provided by EcoSynthetix Inc. (Burlington, ON) we have replaced a significant amount of non-renewable feedstock to yield SNP-containing latexes for adhesive applications. Due to the hydrophilic nature of SNPs, they tend to reside in the water phase or, at best, at the particle-water interface. Thus, to maintain expected polymer performance, we encapsulated SNPs in the acrylic polymer latex particles. To achieve this, SNPs were modified by increasing their cross-link density, then by functionalizing with a sugar-based monomer, and finally, by tuning their hydrophobicity. The modified SNPs were then incorporated in a semi-batch emulsion polymerization to produce stable SNP-based latexes. To understand the effect of each SNP modification procedure, a series of controlled experiments was conducted. Stable and low viscosity latexes with up to 45 wt.% SNPs and 55 wt.% solids have been produced. TEM and STEM images confirmed the presence of a core-shell morphology (SNP core/acrylic polymer shell), and mass balance calculations suggested a significant degree of encapsulation of the SNPs in the latex particles. Crosslinker and chain transfer agent were then used to produce SNP-based latexes with a variety of latex and adhesive properties by manipulating the acrylic shell polymer microstructure.

Résumé

Les ressources pétrolières constituent la matière prédominante utilisée dans la production de polymères. Cependant, avec l'épuisement des ressources pétrolières ainsi que les préoccupations environnementales qui y sont associées, il est nécessaire d'explorer des ressources renouvelables en tant qu'alternatives dans la production de matériaux polymères.

Des nanoparticules d'amidon (NPA) de qualité expérimentale fournies par EcoSynthetix Inc. (Burlington, ON) furent utilisés pour remplacer une quantité significative de matières premières non-renouvelables afin de produire des latex à la NPA pour les applications adhésives. En raison des caractéristiques hydrophiles des NPA, ils ont tendance à demeurer dans la phase aqueuse, ou bien, au mieux, à l'interface particule-eau. Ainsi, pour maintenir la qualité et la performance attendue du polymère, nous avons encapsulés les NPA à l'intérieur des particules de latex acrylique.

Pour ce faire, les NPA ont d'abord été modifiées en augmentant leur densité de réticulation, puis, en fonctionnalisant avec un monomère à base de sucre, et finalement en ajustant leur hydrophobicité. Par la suite, les NPA modifiés ont été incorporés dans une polymérisation en émulsion semi-continue pour produire un latex stable à base de NPA.

À titre de comprendre l'effet de chaque procédure de modification des NPA, une série d'expériences contrôlés a été réalisé. Des latex stables à faible viscosité, contenant

jusqu'à 45 % en masse de NPA et 55 % en masse de solides ont été produits. Les images MET et METB ont bien confirmés la présence d'une morphologie noyau-coque (noyau de NPA / coque en polymère acrylique) et les calculs de bilans massiques démontrent un niveau important d'encapsulation des NPA dans les particules de latex. Des agents de réticulation en chaîne et de transfert ont ensuite été utilisés pour produire des latex à base de NPA avec une variété de latex et propriétés adhésives en manipulant la microstructure de la coquille polymère acrylique.

Dedication

I dedicate this thesis first and foremost to my grandparents, *Mrs. Xiufen Ma* and *Mr. Chengyu Bai*, for their enlightenment and abiding love, to my *parents* for their tremendous support in my education, my *sister* for always believing in me, my *husband* for his mutual understanding and support, and my *friends* for being there for me.

Statement of Contributions

I hereby declare that I am the sole author of this thesis. I performed the polymerization experiments, polymer characterization and all the associated data analysis.

I acknowledge Prof. Michael Cunningham from Queen's University and Dr. Niels Smeets previously from Ecosynthetix Inc., for their general guidance in the project.

The scientific guidance throughout the project and editorial comments of the written work were provided by my thesis supervisor Dr. Marc A. Dubé of the Department of Chemical and Biological Engineering at the University of Ottawa.

Yujie Zhang Date: 10/16/2019

Acknowledgement

I would like to express my heartfelt gratitude to my supervisor Dr. Marc A. Dubé for his patient guidance, considerable encouragement and support throughout this project and beyond. I wish to thank all the members in the Polymer Reaction Engineering group for their support and friendship.

I am thankful to Prof. Michael Cunningham from Queen's University and Dr. Niels Smeets previously from EcoSynthetix Inc., for their guidance, assistance and support throughout this project.

Financial support for this work through the Natural Sciences and Engineering Research Council (NSERC) of Canada, University of Ottawa and EcoSynthetix Inc. is gratefully acknowledged.

Table of Contents

Table of Figures

List of Tables

Nomenclature

Abbreviations

AA	Acrylic Acid
AESO	Acrylated-Epoxidized Soybean Oil
AIBN	Azobisisobutyronitrile
AMA	Allyl Methacrylate
AN	Acrylonitrile
APG	Alkyl Polyglycosides
ATR-FTIR	Attenuated Total Reflectance – Fourier Transform Infrared Spectroscopy
BA	Butyl Acrylate
BMA	Butyl Methacrylate
BPO	Benzoyl Peroxide
BVE	Butyl Vinyl Ether
CLA	Conjugated Linoleic Acid
CMC	Critical Micelle Concentration
CTA	Chain Transfer Agent
DDW	Deionized Distilled Water
DLS	Dynamic Light Scattering
DMA	Dynamic Mechanical Analysis

DSC	Differential Scanning Calorimetry
DVB	Divinylbenzene
EHA	2-Ethylhexyl Acrylate
FSM	Functionalized Sugar-based Monomer
HCl	Hydrochloric Acid
HLB	Hydrophilic/Lipophilic Balance
H-NMR	Proton Nuclear Magnetic Resonance Spectroscopy
HQ	Hydroquinone
IR	Infrared Spectroscopy
KPS	Potassium Persulfate
LIM	d-Limonene
MAnh	Maleic Anhydride
MMA	Methyl Methacrylate
M_w	Weight-Average Molecular Weight
$NaHCO_3$	Sodium Bicarbonate
NaOH	Sodium Hydroxide
NDM	1-Dodecanethiol
P_{de}	Phosphate Diester
P_{me}	Phosphate Monoester
PP	Pyrophosphate
PP_g	Grafted Pyrophosphate

PSA	Pressure Sensitive Adhesive
RAFT	Reversible Addition-Fragmentation Transfer
SDS	Sodium Dodecyl Sulfate
SNP	Starch Nanoparticle
STEM	Scanning Transmission Electron Microscope
STMP	Sodium Trimetaphosphate
STPP	Sodium Tripolyphosphate
$STPP_g$	Grafted Sodium Tripolyphosphate
STY	Styrene
TEM	Transmission Electron Microscopy
T_g	Glass Transition Temperature
THF	Tetrahydrofuran

Symbols

M_{dp}	Mass of dry polymer
M_l	Mass of latex
d_c	Radius of core
G'	Storage modulus
G"	Loss modulus
M_b	Mass of buffer
m_c	Mass of the core (SNPs)
M_i	Mass of initiator
M_p	Mass of polymer
M_s	Mass of SNPs
m_s	Mass of the shell (acrylic polymers)
M_{tm}	Mass of total monomer
M_w	Mass of DDW
δ	Shell thickness
ρ	Density

1. Introduction

Polymeric materials in their various forms (e.g., plastics, paints, and rubbers) play a significant role in every aspect of human life and there is no doubt that their technological impact has in many ways improved our standard of living. However, with the enormous growth of the polymer industry, non-negligible environmental consequences have surfaced. For example, synthetic polymers are not normally biologically degradable and this has led to their significant accumulation (about 22 to 43 percent of global plastics) in municipal landfill sites.[1] At the same time, many components in synthetic polymers such as residual monomers, catalysts and additives, which in most cases are toxic, can migrate into the environment and inevitably endanger the health of both wildlife and humans.

With growing concerns about the environmental impact of polymers, it is absolutely necessary to carry out immediate action to encourage the synthesis of more sustainable polymer products. To start with, a green synthesis pathway needs to be chosen. Emulsion polymerization is considered as a more sustainable and environmentally friendly way to produce a wide range of polymers because water is used as a suspending medium (as opposed to the use of a solvent): it not only eliminates the consumption of organic solvents, which are one of the main sources for volatile organic compounds (VOCs)[2], but also acts as an excellent heat sink to facilitate the control of reaction temperature during synthesis.

Even though emulsion polymerization is the better environmental choice over other polymer synthesis methods, considerable environmental concerns surrounding latex polymer production remain. Thus, it is of great importance to reconsider all aspects of emulsion polymerization technology to achieve a more effective pathway towards sustainable polymer products. To guide us towards a green emulsion polymerization technique, some principles can be used at the design stage. The 12 Principles of Green Chemistry are based on the fundamental science of chemistry to enable scientists to minimize or eliminate the environmental impact of chemical products and processes by reducing or eliminating hazardous chemicals, using renewable feedstocks and catalysts, and so on.[3] Recently, Dubé and Salehpour applied the 12 Principles of Green Chemistry to polymer production technology.[4]

Based on the 12 Principles of Green Chemistry, the use of renewable feedstocks is considered as the most effective means to achieve a green emulsion polymerization. Renewable monomers have been available for decades and are either obtained directly or derived from natural resources. Since natural resources consume CO_2 through photosynthesis, using natural resources as feedstock will slow CO_2 buildup in the atmosphere. In addition, not only are renewable monomers abundant, they also offer a wide variety of building blocks that may not exist in fossil-based resources. A common refrain is that bio-based polymers present poorer performance compared to those derived from petroleum-based monomers. However, by applying advanced polymer chemistry and reaction engineering techniques, one can optimize these new processes to achieve similar and sometimes better properties.

1.1. **Thesis Objectives**

Our hypothesis is that starch nanoparticles (SNPs) (provided by EcoSynthetix Inc. (Burlington, ON)) can be incorporated into core-shell (starch-polymer) latex particles by introducing vinyl groups (carbon-carbon double bonds) to promote binding of the starch to polymer (Figure 1.1). Ideally, these vinyl groups will copolymerize with a variety of vinyl monomers and form a "core-shell" structure and at the very least, form grafts with the polymer.

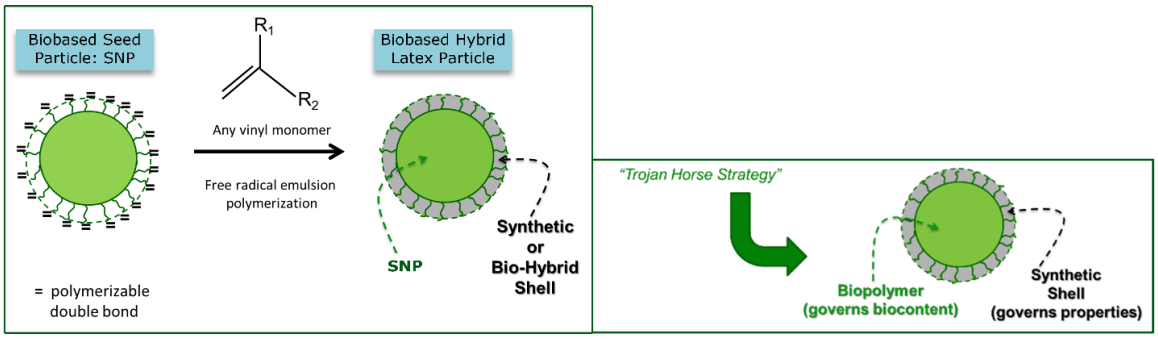

Figure 1.1 Concept of a polymerizable SNP to increase bio-content of latex emulsions.

Stable SNP-containing polymer latexes have been successfully produced in a previous project.[5] However, the desired core-shell particle morphology (i.e., starch core – synthetic polymer shell) was not obtained due to the hydrolysis of starch. To achieve core-shell particle morphology, experimental grade SNP provided by EcoSynthetix will be cross-linked and further modified by attaching vinyl groups to the surface. A "tie-layer" of organic monomer will then be polymerized onto the SNP surface to enhance its hydrophobicity. The SNP core particles will then be used in the production of core-shell particles via semi-batch emulsion polymerization. Once the core-shell morphology is

confirmed, we will then maximize the SNP loading in the product, and optimize adhesive properties.

1.2. **Thesis Outline**

This thesis contains seven chapters. After the introductory chapter, Chapter 2 provides fundamental background material on emulsion polymerization and pressure sensitive adhesives. Chapter 3 is a published literature review (i.e., a book chapter), which introduces approaches to sustainable polymer production via emulsion polymerization technology. Chapters 4, 5 and 6 consist of manuscripts published in refereed scientific journals. Chapter 4 provides the proof-of-principle study, where the core/shell (SNP core/acrylic shell) particle morphology was achieved using the modification methodologies we proposed. In Chapter 5, the effect of SNP loadings and latex solids on latex stability and properties is presented. Chapter 6 demonstrates our manipulation of adhesive properties of SNP-based latexes using cross-linker and chain transfer agent in the acrylic shell polymer formulations. Finally, Chapter 7 provides a summative discussion of the thesis, which includes the achievements of this work and some ideas on exploration of other potential applications of SNP-based latexes, and how to further improve the sustainability of SNP-based latexes.

1.3. **Challenges**

The main technical challenge in this project is to combine hydrophilic (SNP) and hydrophobic (synthetic polymer) materials. Typical core-shell particles are composed of a

hydrophilic shell and hydrophobic core, and this is more easily achieved because of the dispersion in water.[6,7] We are attempting to invert the core and shell elements from their more typical configuration. In addition, it's difficult to achieve perfect core surface coverage, high solids content and high SNP incorporation due to the limited reactivity of SNPs. However, it is possible to tackle these problems via chemical modification of the SNPs and adjustment of the reaction formulation.

References

[1] Worldwatch Institute, Global Plastic Production Rises, Recycling Lags | Worldwatch Institute, (2015). http://www.worldwatch.org/global-plastic-production-rises-recycling-lags-0 (accessed July 19, 2016).

[2] E. and C.C.C. Government of Canada, Environment and Climate Change Canada - Environmental Indicators - Air Pollutant Emissions, (2016). https://www.ec.gc.ca/indicateurs-indicators/default.asp?lang=en&n=E79F4C12-1 (accessed June 28, 2016).

[3] P.T. Anastas, Green chemistry: theory and practice, Oxford University Press, Oxford; New York, 1998.

[4] M.A. Dubé, S. Salehpour, Applying the Principles of Green Chemistry to Polymer Production Technology, Macromol. React. Eng. 8 (2014) 7–28.

[5] S. Cummings, Novel Methods for the Production of Bio-Synthetic Latex, PhD Thesis, University of Ottawa.

[6] D.C. Sundberg, A.P. Casassa, J. Pantazopoulos, M.R. Muscato, B. Kronberg, J. Berg, Morphology development of polymeric microparticles in aqueous dispersions. I. Thermodynamic considerations, J. Appl. Polym. Sci. 41 (1990) 1425–1442.

[7] J.M. Stubbs, D.C. Sundberg, Core-shell and other multiphase latex particles—confirming their morphologies and relating those to synthesis variables, J. Coat. Technol. Res. 5 (2008) 169–180.

2. Literature Review

2.1. Emulsion Polymerization

Emulsion polymerization is a heterogeneous free radical polymerization process to produce polymer latexes. In general, an emulsion polymerization system comprises relatively hydrophobic monomer (e.g., styrene), water soluble initiator (e.g., potassium persulfate), water and surfactant (e.g., sodium dodecyl sulfate).[1–4] There are a broad range of monomers that have been applied in emulsion polymerization, for instance, styrene, butyl acrylate, methyl methacrylate, butadiene, and acrylonitrile. Because the polymers produced are relatively hydrophobic, an extremely large oil-water interfacial area is generated as the particle nuclei form and grow in size with the progress of the polymerization. In order to prevent the interactive latex particles from coagulating, the addition of surfactants is necessary. Surfactants can be physically absorbed on the particle surface or chemically incorporated on to the particle surface. In general, three types of surfactants are available to stabilize polymer latexes: electrostatic surfactants (ionic surfactants) (e.g., sodium dodecyl sulfate), steric surfactants (e.g., poly(ethylene oxide) nonylphenyl ether) and electrosteric surfactants, which provide both electrostatic and steric stabilization mechanisms, such as a 'hairy layer' of poly(acrylic acid) grafted to polymer chains. Each surfactant can be used separately or by combining them.[3,5,6]

Typically, at the beginning of the polymerization, the emulsion polymerization system contains a large amount of monomer droplets (1-10 μm in diameter, 10^{12}-10^{14} dm^{-3} in number) dispersed in the continuous aqueous phase with the help of surfactants. When the surfactant concentration in the continuous aqueous phase exceeds its critical micelle concentration (CMC), monomer-swollen micelles (5-10 nm in diameter, 10^{19}-10^{21} dm^{-3} in number) will also be present. Only a small amount of relatively hydrophobic monomer is dissolved in the continuous aqueous phase or exists in the micelles (if present).[2] Polymerization is initiated by adding water soluble initiator, which will then decompose and react with limited monomer molecules in the continuous aqueous phase. This is followed by the generation of latex particles (0.05-1 μm in diameter, 10^{16}-10^{18} dm^{-3} in number) via different possible particle nucleation mechanisms. According to the micellar nucleation mechanism proposed by Smith and Ewart, the monomer-swollen micelles capture the free radicals in the continuous aqueous phase and generate particles.[7–9] Other nucleation mechanisms such as homogeneous nucleation may also be present. Monomer droplets serve as monomer reservoirs and are not considered as effective nucleation sites considering their relatively small surface area compared to the monomer-swollen micelles. Polymer latexes composed of a great number of particles (10^{1}-10^{3} nm in diameter) dispersed in a continuous aqueous phase can be produced using this technique.

Emulsion polymerization is widely used to synthesize a broad range of polymer products for various applications such as synthetic rubbers, coatings, adhesives, binders, thermoplastics and so on. In emulsion polymerization, each particle acts as an individual

polymerization site and free radicals are segregated among the discrete particles, this significantly reduces the possibility of bimolecular termination of the free radicals and eventually leads to a faster polymerization rate and higher molecular weight.[10]

Emulsion polymerization processes can be implemented in batch, semi-batch and continuous operating modes. The main difference between those modes is the residence time distribution of the growing particles within the reactor. Batch emulsion polymerization is commonly used in the laboratory to develop new latex products and study emulsion polymerization mechanisms. In industry, most latex products are produced via semi-batch or continuous emulsion polymerization processes to avoid heat transfer issues present in large-scale reactors. Semi-batch and continuous processes also provide more operational flexibility to manufacture latex polymers with controlled polymer composition and particle morphology.[2]

2.1.1. **Particle Nucleation Mechanism**

Typically, in emulsion polymerization, most particles are generated in a short period (on the order of seconds to minutes compared to a 4-hour total polymerization time) immediately after the addition of initiator. However, the short particle nucleation period will determine the number and size of those polymer particles per unit volume of water.[11,12] This will have a significant influence not only on the polymerization kinetics, but also on the final latex properties (e.g., film formation, rheology, gloss, etc.).[1] Thus, in order to be able to produce polymer latexes with desired properties, it is necessary to develop an understanding of the particle nucleation mechanism. Up to now, several

theories on the nucleation mechanism have been proposed and tested. In this section we will discuss three well-recognized particle nucleation mechanisms: micellar nucleation[9], homogeneous nucleation[13] and coagulative nucleation[14].

Micellar Nucleation

Harkins[15–17], Smith and Ewart[7–9], and Gardon[18,19] developed the currently accepted theory of particle formation based on the oligomeric radicals captured by monomer-swollen micelles. When the surfactant concentration exceeds its critical micelle concentration (CMC), monomer-swollen micelles (5-10 nm in diameter, 10^{19}-10^{21} dm^{-3} in number) are formed. With the addition of water-soluble initiator, the initiator will decompose and quickly react with monomers dissolved in the continuous aqueous phase to produce oligomeric radicals. With the increase of chain length of the oligomeric radicals by monomer addition, they become increasingly hydrophobic and eventually enter the monomer-swollen micelles. Considering the extremely large oil-water interfacial area of the monomer-swollen micelles, the capture of the oligomeric radicals is principally by the micelles; these become polymer particles. Given the fact that monomer droplets have relatively small oil-water interfacial area, the possibility for monomer droplets to capture radicals is low; thus, the monomer droplets mainly act as monomer reservoirs. Particles will continue to grow by the absorption of monomers diffusing from the monomer droplets. Free surfactants in the continuous aqueous phase will absorb on the surface of particles to further stabilize the particles.

Homogeneous Nucleation

Priest[20], Roe[21], Fitch and Tsai[1,13] proposed a homogeneous nucleation mechanism, which would be responsible for particle formation when the surfactant concentration is below the CMC. As the initiators decompose, monomers dissolved in the continuous aqueous phase are initiated and then propagate. With the growing chain length of the oligomeric radicals, the radicals become increasingly water-insoluble until they reach a critical chain length and phase separate. Then, the hydrophobic oligomeric radicals will tend to coil up and form a particle nucleus in the continuous aqueous phase. Afterwards, limited flocculation may occur between unstable particle nuclei to reduce the oil-water interfacial area, and surfactant (if there is any) will adsorb on the particle's surface. Normally, the homogeneous nucleation mechanism dominates the emulsion polymerization of relatively hydrophilic monomers (e.g., methyl methacrylate) or in the absence of monomer-swollen micelles.

Coagulative Nucleation

Coagulative nucleation is another recognized mechanism other than micellar and homogeneous nucleation. This mechanism, proposed by Lichti et al[14] and Feeney et al[22,23] is based on particle size distribution data during the particle nucleation stage. They suggested that the rate of particle formation increased to a maximum and then decreased until the end of the particle nucleation stage. Precursor particles generated either by homogeneous nucleation (where oligomeric radicals coil up and form a particle), or by micellar nucleation (where monomer-swollen micelles capture oligomeric radicals and generate particles) at the beginning of the nucleation stage are highly unstable in nature,

so those particles tend to coagulate quickly with each other to reduce the oil-water interfacial area. Mature latex particles are generated by the coagulation of precursor particles, but not by growth of precursor particles via polymerizing monomers. In addition, the total number of mature particles per unit volume of water is mainly dominated by the available surfactant in the continuous aqueous phase.

2.1.2. **Emulsion Polymerization Kinetics**

In conventional emulsion polymerization, there are three intervals. Interval I is the nucleation stage, where particles are generated via the mechanisms described above. In this stage, the rate of polymerization increases, along with the number of particles and the particle size. The beginning of Interval II coincides with the disappearance of the monomer-swollen micelles. The number of particles remains constant and particles grow as the monomer droplets provide monomer to the particles via diffusion through the continuous aqueous phase. Most of the monomers are consumed in this particle growth stage (10 to 60% monomer conversion). The monomer concentration within each particle remains constant due to the establishment of a thermodynamic equilibrium made possible by the rapid diffusion of monomer from the monomer droplets. The polymerization rate in this stage is likely to be constant. Monomer droplet depletion indicates the beginning of interval III, where the remaining monomers polymerize until the end of polymerization. Particle size may slightly decrease due to shrinkage at this stage.

2.2. **Pressure Sensitive Adhesives**

Pressure sensitive adhesives (PSAs) are soft viscoelastic polymers that can stick to almost any surface upon contact at room temperature.[24,25] PSAs typically require light pressure to stick, and do not involve any chemical reaction or physical changes. PSAs have been used in applications such as tapes, labels, packaging, and many others. Commercial PSAs are dominated by acrylic polymers, styrenic block copolymers and natural rubber. In general, PSAs can be produced from solution, emulsion latexes and hot melts. However, emulsion-based PSAs are more favored as water is used as a dispersing media rather than a potentially toxic solvent.

PSA performance is usually evaluated by tack, peel strength and shear strength.[24] Tack is the force that allows an adhesive to detach from a substrate upon contact under light or no pressure. Peel strength is defined as the force needed to peel away a strip of PSA coated film with standard dimensions from a substrate at a standard peel rate and angle. Shear strength is the measurement of shear deformation under constant shear stress, and is related to the internal or cohesive strength of the PSA.

To obtain PSAs with superior viscoelastic properties, polymer composition, molecular weight and structure should be finely tuned. One main requirement is that the glass transition temperature (T_g) of the PSAs should be 25-45 ^oC lower than usage temperature.[25] Normally, with the increase of chain length (from 4 to 12), T_g of its homopolymers decreases and peel strength increases.[26] Acrylate monomers with long alkyl chain lengths enhance tack, while those with short alkyl chain lengths influence cohesive strength.[24] In addition, monomers with polar groups may exhibit strong

cohesion due to hydrogen bonding. To improve the shear strength of PSAs, cross-linker and filler can be added.[27] An interesting conundrum arises in latex-based PSAs is that generally, increasing the shear strength of a PSA leads to a reduction in peel strength and tack.[26] Significant experimental effort has been made to overcome this conundrum.[28,29]

References

1. Fitch, R. M. Polymer Colloids, Academic Press, 1997.
2. Chern, C. S. *Prog. Polym. Sci.*, 2006, **31**, 443–486.
3. Thickett, S. C., Gilbert, R. G. *Polymer*, 2007, **48**, 6965–6991.
4. Chern, C.-S. Principles and applications of emulsion polymerization, Hoboken, N.J., 2008.
5. Zecha, H. *Acta Polym.*, 1981, **32**, 582–582.
6. Dunn, A. S. *Br. Polym. J.*, 1986, **18**, 278–278.
7. Smith, W. V. *J. Am. Chem. Soc.*, 1948, **70**, 3695.
8. Smith, W. V. *J. Am. Chem. Soc.*, 1949, **71**, 4077–4082.
9. Smith, W. V., Ewart, R. H. *J. Chem. Phys.*, 1948, **16**, 592–599.
10. Gilbert, R. G. Emulsion polymerization: a mechanistic approach, Academic Press, c1995, London; San Diego, 1995.
11. Hergeth, W., Lebek, W., Kakuschke, R., Schmutzler, K. *Makromol. Chem.*, 1991, **192**, 2265–2275.
12. Hergeth, W.-D., Lebek, W., Stettin, E., Witkowski, K., Schmutzler, K. *Makromol. Chem.*, 1992, **193**, 1607–1621.
13. Fitch, R. M. *Br. Polym. J.*, 1973, **5**, 467–483.
14. Lichti, G., Gilbert, R. G., Napper, D. H. *J. Polym. Sci. Polym. Chem. Ed.*, 1983, **21**, 269–291.
15. Harkins, W. D. *J. Chem. Phys.*, 1945, **13**, 381.
16. Harkins, W. D. *J. Chem. Phys.*, 1946, **14**, 47–48.
17. Harkins, W. D. *J. Am. Chem. Soc.*, 1947, **69**, 1428–1444.
18. Gardon, J. L. *J. Polym. Sci. [A1]*, 1968, **6**, 623–641.
19. Gardon, J. L. *J. Polym. Sci. [A1]*, 1968, **6**, 643–664.
20. Priest, W. J. *J. Phys. Chem.*, 1952, **56**, 1077–1082.
21. Roe, C. P. *Ind. Eng. Chem.*, 1968, **60**, 20.
22. Feeney, P. J., Napper, D. H., Gilbert, R. G. *Macromolecules*, 1984, **17**, 2520–2529.

23. Feeney, P. J., Gilbert, R. G., Napper, D. H. *J. Colloid Interface Sci.*, 1985, **107**, 159–173.
24. Jovanović, R., Dubé, M. A. *J. Macromol. Sci. Part C*, 2004, **44**, 1–51.
25. Costantino Creton *Pp 434-439*, 2003, **MRS Bulletin**, 434.
26. Connelly, R. W., Parsons, W. F., Pearson, G. H. *J. Rheol. 1978-Present*, 1981, **25**, 315–328.
27. Wang, T., Lei, C.-H., Dalton, A. B., Creton, C., Lin, Y., Fernando, K. a. S., Sun, Y. P., Manea, M., Asua, J. M., Keddie, J. L. *Adv. Mater.*, 2006, **18**, 2730–2734.
28. Qie, L., Dubé, M. A. *J. Appl. Polym. Sci.*, 2012, **124**, 349–364.
29. Fonseca, G. E., McKenna, T. F., Dubé, M. A. *Chem. Eng. Sci.*, 2010, **65**, 2797–2810.

3. “Green” Emulsion Polymerization Technology

Chapter 3 contains a book chapter entitled “Green” Emulsion Polymerization Technology”, which was published in the book “Polymer Reaction Engineering of Dispersed Systems” in Advances in Polymer Science by Springer on May 17, 2017.

“Green” Emulsion Polymerization Technology

Yujie Zhang, Marc Arnold Dubé

_____

Department of Chemical and Biological Engineering,

Centre for Catalysis Research and Innovation,

University of Ottawa, 161 Louis Pasteur Pvt.,

Ottawa, Ontario, Canada K1N 6N5

_____

Abstract

The polymer industry is dominated by the use of petroleum-based feedstock and due to increased awareness, the related environmental consequences have provided the impetus for change. Emulsion polymerization is considered as a more sustainable technique for the manufacture of polymeric materials because of its use of water as a dispersing medium. To further improve the sustainability of emulsion polymerization technology, the 12 Principles of Green Chemistry and Engineering were used as a guideline towards the design of a greener process. The most obvious and effective approach is to use renewable, bio-based feedstock in emulsion polymerization

formulations. In addition, maximizing energy efficiency, preventing waste and pollution, and minimizing the potential for accidents also figure prominently.

Keywords: emulsion polymerization, sustainability, renewable feedstock

Introduction

Polymeric materials in their various forms (e.g., plastics, paints, and rubbers) play a significant role in every aspect of human life and there is no doubt that their technological impact has in many ways improved our standard of living. However, with the enormous growth of the polymer industry, non-negligible environmental consequences have surfaced. For example, synthetic polymers are not normally biologically degradable and this has led to their significant accumulation (about 22 to 43 percent of global plastics) in municipal landfill sites (Worldwatch Institute 2015). According to the U.S. National Institute of Health, about 44% of seabird species are known to have ingested synthetic polymers mistakenly and the same thing has happened to 267 marine species (Laist 1997). At the same time, many components in synthetic polymers such as residual monomers, catalysts and additives, which in most cases are toxic, can migrate into the environment and inevitably endanger the health of both wildlife and humans. In addition, there is great concern about emissions of air pollutants (e.g., carbon dioxide (CO_2), methane (CH_4), and volatile organic compounds (VOCs)) which are involved in the production and waste management of synthetic polymers. Since the Industrial Revolution, greenhouse gas emissions have been on the increase (Figure 3.1). This matter has captured world attention, and as of June 24 2016, 177 countries including the European Union have

signed the Paris Agreement, which aims to cut greenhouse gas emissions worldwide and limit global warming to below 2 ℃ by 2030 (United Nations 2016).

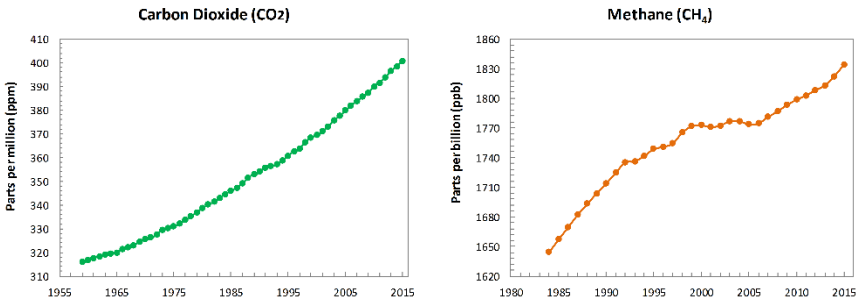

Figure 3.1 Major greenhouse gases trend since the Industrial Revolution (US Department of Commerce)**.**

With growing concerns about the environmental impact of polymers, it is absolutely necessary to carry out immediate action to encourage the synthesis of more sustainable polymer products. To start with, a green synthesis pathway needs to be chosen. Emulsion polymerization is considered as a more sustainable and environmentally friendly way to produce a wide range of polymers because water is used as a suspending medium (as opposed to the use of a solvent): it not only eliminates the consumption of organic solvents, which are one of the main sources for VOCs (Figure 3.2) (Government of Canada 2016), but also acts as an excellent heat sink to facilitate the control of reaction temperature during synthesis. Typical emulsion polymerization formulations contain several components (e.g., monomer, initiator, surfactant, and buffer) (Table 3.1) that will influence final polymer properties (Jovanović and Dubé 2004). Polymers manufactured by emulsion polymerization can be found in various applications, for instance, paints and coatings, adhesives, plastics and synthetic rubber. In 2015, the global emulsion polymer

market was around $33.30 billion (US$), and is expected to grow continuously in the near future (Grand View Research 2016).

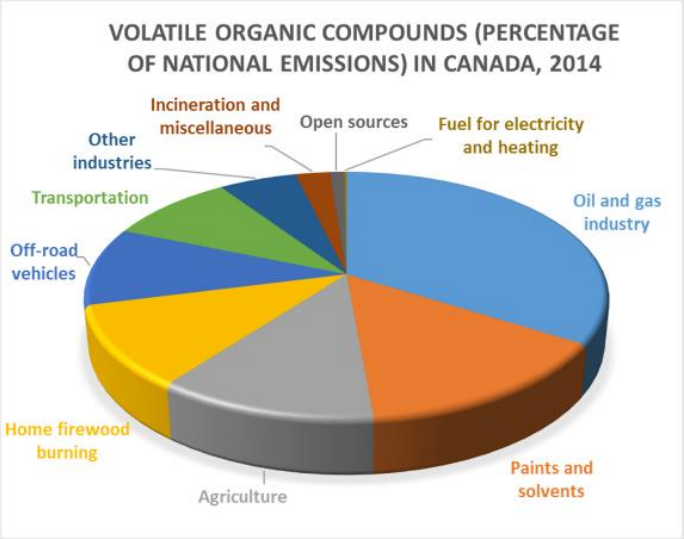

Figure 3.2 Distribution of VOCs emissions in Canada by source, 2014 (Government of Canada 2016).

Table 3.1 Typical emulsion polymerization formulation.

Component	Chemical	Weight (g)
Monomer	Butyl Acrylate (BA)	120
Solvent	Deionized Water	300
Initiator	Potassium Persulfate (KPS)	1
Surfactant	Sodium Dodecyl Sulfate (SDS)	10
Buffer	Sodium Carbonate	0.5

Even though emulsion polymerization is considered to be the better environmental choice over other polymer synthesis methods, considerable environmental concerns surrounding latex polymer production remain. Thus, it is of great importance to

reconsider all aspects of emulsion polymerization technology to achieve a more effective pathway towards sustainable polymer products. In order to guide us towards a greener emulsion polymerization technique, some principles can be used at the design stage. The 12 Principles of Green Chemistry (Figure 3.3) are based on the fundamental science of chemistry to enable scientists to minimize or eliminate the environmental impact of chemical products and processes by reducing or eliminating hazardous chemicals, using renewable feedstocks and catalysts, and so on (Anastas 1998). These twelve principles have also been expressed from an engineering perspective (Figure 3.4) (Anastas and Zimmerman 2003). These principles have been applied by scientists and engineers in different fields of studies to pursue more sustainable solutions. Recently, Dubé and Salehpour applied the 12 Principles of Green Chemistry to polymer production technology (Dubé and Salehpour 2014).

In this chapter, the 12 Principles of Green Chemistry and Engineering will be applied to conventional emulsion polymerization techniques to design a greener path to polymer manufacture. The use of these principles implies that we need to design not only less hazardous chemicals and products, but also more sustainable processes. A number of these principles (2, 8 and 9) are addressed well in polymerization processes in general and will not be addressed here. The use of safer solvents (principle 5) is evidently addressed in emulsion polymerization, a water-based process. To begin with, we will focus on possible renewable alternatives for some main components in the emulsion polymerization formulation. This will address principles 3, 4 and 7 (i.e., less hazardous synthesis, designing benign chemicals and products, and using renewable feedstock), and

in an indirect way, principle 10 (designing degradable products). We then turn to the development of a more sustainable emulsion polymerization from a process technology point-of-view: how to prevent waste (principle 1), how to maximize energy efficiency (principle 6), real-time analysis (principle 11) and how to minimize the potential for accidents (principle 12).

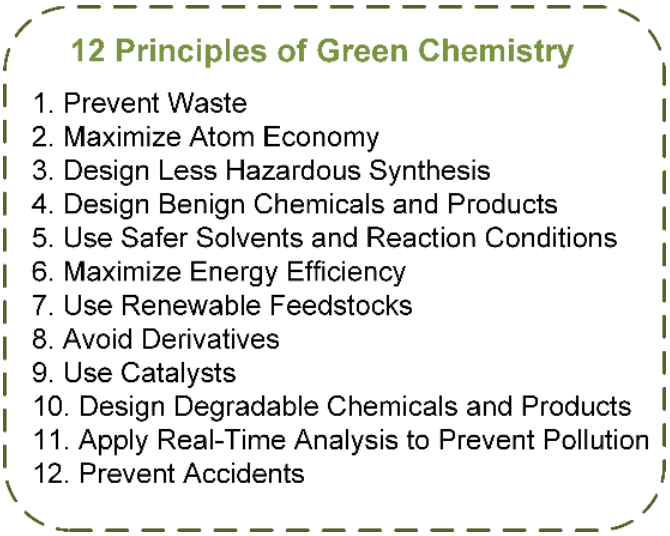

Figure 3.3 The 12 Principles of Green Chemistry (Anastas 1998).

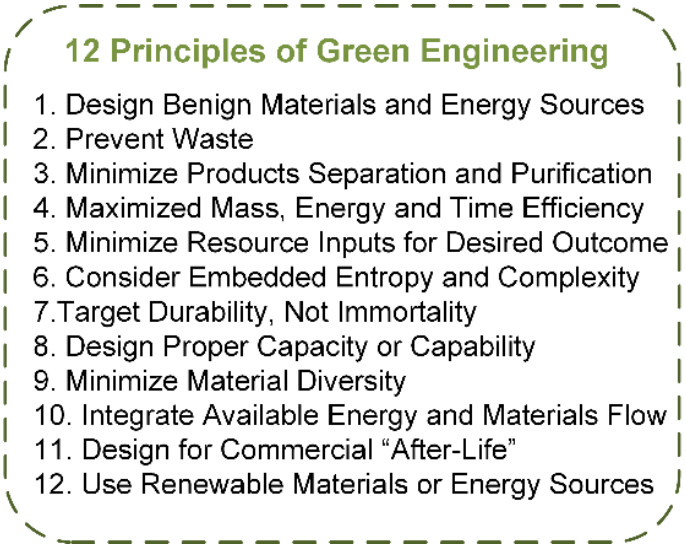

Figure 3.4 The 12 Principles of Green Engineering (Anastas and Zimmerman 2003).

Design of Green Chemicals and Products

According to the "12 Principles of Green Chemistry", in order to achieve green emulsion polymer products, chemicals involved in emulsion formulations (e.g., monomer, surfactant, and initiator) should be less hazardous and be derived from renewable sources. Here, we will focus on emulsion polymerization formulations and review possible alternative "green" components to develop a more sustainable product. Monomer is the most plentiful ingredient in emulsion polymerizations and we therefore provide a more comprehensive review for this component. Other components such as surfactant, cross-linker, chain transfer agent, initiator, and buffer, are addressed more briefly.

Monomer

Monomers, the main component in emulsion polymerization formulations (Table 1), typically comprise 30-60% of the total latex mass (Odian 2004). The monomers undergo free radical polymerization, which implies the presence of at least one vinyl group in the monomer structure. Otherwise, the principle monomer in the formulation requires a relatively low water solubility to form particles, lest the reaction proceeds as an aqueous solution polymerization. To achieve desired polymer properties, a multi-monomer mixture (i.e., co-monomers) is commonly used in emulsion polymerization.

In general, monomers used in emulsion polymerization are obtained from fossil-based resources. Around 7% of global fossil fuel production is diverted for plastics manufacture (Williams and Hillmyer 2008). With the uneven distribution and depletion of fossil resources, there is no guarantee for a stable price and supply chain and, as noted earlier,

numerous environmental concerns arise from the use of this non-renewable feedstock. At the same time, petroleum-derived monomers are usually toxic and pose a potential health risk due to exposure of personnel working with these materials. For instance, the exposure to acrylic monomers can lead to clinical symptoms and some of the monomers are possibly carcinogenic to humans (Autian 1975; 2002; Leggat and Kedjarune 2003). To create safer products and work environments, it is essential to pursue less toxic alternatives to the monomers used currently. Many renewable monomers, being derived from plants, are non-toxic; however, the origin of a material and its toxicity are not necessarily correlated.

Renewable monomers have been available for decades and are either obtained directly or derived from natural resources. Since natural resources consume CO_2 through photosynthesis, using natural resources as feedstock will slow CO_2 buildup in the atmosphere. In addition, not only are renewable monomers abundant, they also offer a wide variety of building blocks that may not exist in fossil-based resources. A common refrain is that bio-based polymers present poorer performance compared to those derived from petroleum-based monomers. However, by applying advanced polymer chemistry and reaction engineering techniques, one can optimize these new processes to achieve similar and sometimes better properties. Economic feasibility of these processes is also of concern. Often, raw material prices for bio-based feedstock are low, but in the event of extensive purification and derivatization, feedstock costs could become significant. It should be made clear that despite being renewably sourced, all aspects of

production of the material (e.g., cultivation, downstream modification) should be considered when assessing the "greenness" of a monomer.

Renewable monomers can be classified in various categories depending on their source (Table 3.2) (Belgacem and Gandini 2008a). However, only monomers containing vinyl groups and having low water solubility are appropriate for emulsion polymerization. Among those renewable monomers, some can be applied directly in emulsion polymerization after a simple extraction or purification process (e.g., limonene) (Zhang and Dubé 2014a). Some renewable monomers may require minor modification (e.g., conjugated linolenic acid) (Zhang et al. 2015); and some may have to be greatly modified to produce "new" monomers. In the latter case, modification costs and sustainability of the derivatization process must be balanced with the renewability of the initial feedstock. Research on the use of renewable monomers in emulsion polymerization is not extensive, thus we are providing a review of renewable monomers, which have either been studied in or show promise for application in emulsion polymerization.

Table 3.2 Categorized renewable monomers.

Compound Category	Monomers
Terpenes	Limonene, α-pinene, β-pinene, myrcene
Vegetable oils	Linoleic acid, linolenic acid
Sugars	Anhydroalditols, aldonic acids, lactones
Polysaccharide	Starch, cellulose*
Furan	Furfural, hydroxymethylfurfural
Rosin	Abietic acid, pimaric acid

*Starch and cellulose are, of course, polymers already and are used frequently as fillers, surfactants or in graft polymerization, but in this context, we refer to their use as macromonomers.

Terpenes

Terpenes are a large group of compounds existing mainly in plants (e.g., conifers, citrus fruits) that share the same isoprene building block (Silvestre and Gandini 2008; Wilbon et al. 2013). Terpene monomers that consist of two isoprene units with the molecular formula $C_{10}H_{16}$ are classified as monoterpenes (Figure 3.5). Monoterpenes are extremely diverse due to their variety of molecular backbone structures, stereoisomers and derivatives. Many monoterpenes have been used as fragrances, in foods as additives, and as green solvents. Since most monoterpenes (e.g., limonene, α-pinene) contain double bonds, they can be utilized as potential starting materials to produce polymers.

Studies have shown that many monoterpenes can be polymerized via cationic initiation, nevertheless, a limited number can undergo free radical polymerization in emulsion (Roberts and Day 1950; Silvestre and Gandini 2008; Zhang 2014). The presence of allylic C-H bonds in monoterpenes makes it difficult to homopolymerize those monomers using free radical polymerization. Free radical homopolymerization of monoterpenes leads to fairly low molecular weight polymers (Ramos et al. 1998; Singh and Kamal 2012). However, copolymerization offers greater opportunity for incorporation of monoterpenes in emulsion polymerization.

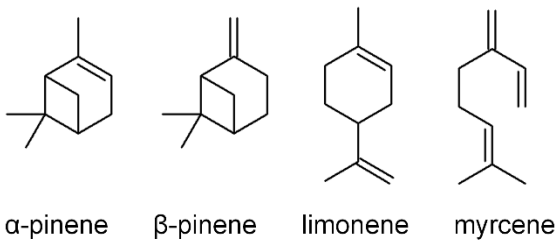

Figure 3.5 Monoterpene monomers.

Pinene

Pinene is a monoterpene with a bicyclic molecular structure (Fig. 5). α-Pinene (α-PIN) and β-pinene (β-PIN) are two isomers available in nature, and both can be obtained from conifers or other non-coniferous plants by steam-distillation (Lincoln and Lawrence 1984; Wilbon et al. 2013). Many pinene derivatives (e.g., 3-carene, myrcene, and limonene) can be obtained by isomerization of pinene (Corma et al. 2007).

Free radical polymerization of α-PIN and β-PIN were investigated using azobisisobutyronitrile (AIBN) as initiator at 60 ℃ (Ramos et al. 1998). Only oligomers were produced from attempts to homopolymerize both isomers. However, when α-PIN and β-PIN were copolymerized with methyl methacrylate (MMA) and styrene (STY), relatively high molecular weight polymers were obtained (Table 3.3). It was shown that α-PIN is more reactive than β-PIN, which may result from the different isomers of the propagating radicals. β-PIN was successfully copolymerized with pentafluorostyrene using benzoyl peroxide (BPO) as initiator at 70 ℃ (Paz-Pazos and Pugh 2006). Furthermore, reversible addition-fragmentation transfer (RAFT) radical copolymerization of β-PIN with methyl acrylate (Wang et al. 2006), acrylonitrile (Li et al. 2006), *n*-butyl acrylate (BA) (Li et al. 2007) and *n*-phenylmaleimide (Yamamoto and Matsumoto 2012) were conducted. The estimated reactivity ratios of β-PIN in all of the above cases are close to zero, which implies that β-PIN tends to react with other monomers but not with itself. All of the above work suggests that both α-PIN and β-PIN can be considered as alternatives to produce more sustainable polymeric materials via emulsion polymerization, and more specifically, emulsion copolymerization.

Table 3.3 Overall conversion and weight-average molecular weight (M_w) data (T = 60 °C) (Ramos et al. 1998).

Polymer	Conversion (wt. %)	M_w
Poly(α-PIN)	6	850
Poly(β-PIN)	5	880
Poly(α-PIN-co-MMA)	40	53,200
Poly(β -PIN-co-MMA)	21	11,600
Poly(α-PIN-co-STY)	7	25,800
Poly(β -PIN-co-STY)	5	25,300

Limonene

Limonene is a monocyclic terpene derived from citrus fruit oils and many other essential oils. Since limonene is a chiral monomer, there are two isomers: *d*-limonene ((+)-limonene) and *l*-limonene ((-)-limonene). Most naturally occurring limonene is *d*-limonene, which is obtained from citrus fruit oils via distillation. Limonene is a common additive in cosmetics, food and medicines due to its pleasant orange odor (H. Surburg 2006). Also, limonene is used extensively as a green solvent for cleaning purposes (Inamuddin 2012).

Two carbon double bonds in limonene suggest the possibility of free-radical polymerization. Similar to pinene, limonene presents some challenges to its homopolymerization. Free radical copolymerization of *d*-limonene and *l*-limonene with maleic anhydride was first presented in 1994, and alternating copolymers were produced using AIBN or BPO as initiators (Maślińska-solich et al. 1994). Attempts to copolymerize limonene with styrene (Sharma and Srivastava 2004), acrylonitrile (Sharma and Srivastava

2003) and vinyl acetate (Sharma and Srivastava 2007) in solution polymerization have been reported but conversions were limited to 20 wt.%.

Recent investigations of the bulk copolymerization of *d*-limonene (LIM) with butyl methacrylate (BMA) (Zhang and Dubé 2014a), 2-ethylhexyl acrylate (EHA) (Zhang and Dubé 2014b) and BA (Ren et al. 2015) led to the production of homogeneous copolymers with relatively high molecular weights (>100,000). Nevertheless, it was revealed that a significant degradative chain transfer mechanism manifests itself in all systems, and this led to limited monomer conversions and lower molecular weight. Using the reactivity ratios estimated from that work, one can employ a semi-batch monomer feed policy in emulsion polymerization to increase *d*-limonene incorporation (Dube et al. 1997).

Limonene (and limonene derived from pinenes) can be dehydrogenated to *α*-methyl styrene, which can be polymerized via a free-radical mechanism.(Horrillo-Martínez et al. 2010; Bolton et al. 2014) Limonene-derived α-methyl styrene has been used to produce sustainable thermoplastic elastomers with improved mechanical properties.(Bolton et al. 2014)

Vegetable Oils

Vegetable oils are triglycerides (Figure 3.6) extracted from plants (e.g., soybean, sunflower, and peanut) via mechanical or chemical extraction. For centuries, many vegetable oils have been used in cooking, cosmetics and personal care products. In addition, many oils have been incorporated into coatings, inks, lubricants and wood treatment products. In 2016, the total world major vegetable oil production was 186.17

million metric tons (United State Department of Agriculture 2016). The annual production of each major vegetable oil and the major producers are listed in Table 3.4. Vegetable oils have become good candidates as a renewable resource to produce polymeric materials because of their abundance, large variety and, of course, their functionality, which could lead to direct polymerization or straightforward derivatization.

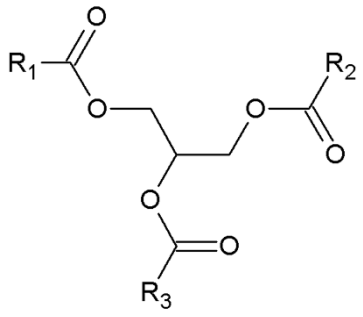

R: fatty acid chain

Figure 3.6 General structure of triglyceride.

Table 3.4 Major vegetable oils world production in 2016 (United State Department of Agriculture 2016).

Oil	Annual Production (Million Metric Tons)	Main Oil Producer
Palm	65.50	Indonesia
Soybean	53.82	China
Rapeseed	26.50	European Union
Sunflower seed	16.24	Ukraine
Palm kernel	7.66	Indonesia
Peanut	5.54	China
Cottonseed	4.50	China
Coconut	3.41	Philippines
Olive	3.01	European Union

The physical and chemical properties of vegetable oils may vary according to their species. In general, each vegetable oil contains a mixture of triglycerides with different fatty acid chains that may have carbon chain lengths between 14 to 22 and 0 to 5 double bonds, or some other functional groups (e.g., epoxy rings, hydroxyl moieties and ether groups) (Belgacem and Gandini 2008b). The chain length, the number of double bonds and their positions will have an important effect on the oil properties as well. Via transesterification using an alcohol, triglycerides can be converted to fatty acids (or fatty esters) and glycerol. The presence of double bonds in vegetable oils as well as in the fatty acids (or fatty esters) derived from them, opens up possibilities for their application as renewable monomers in emulsion polymerization. In Figure 3.7, some representative fatty acids with double bonds existing in vegetable oils are shown.

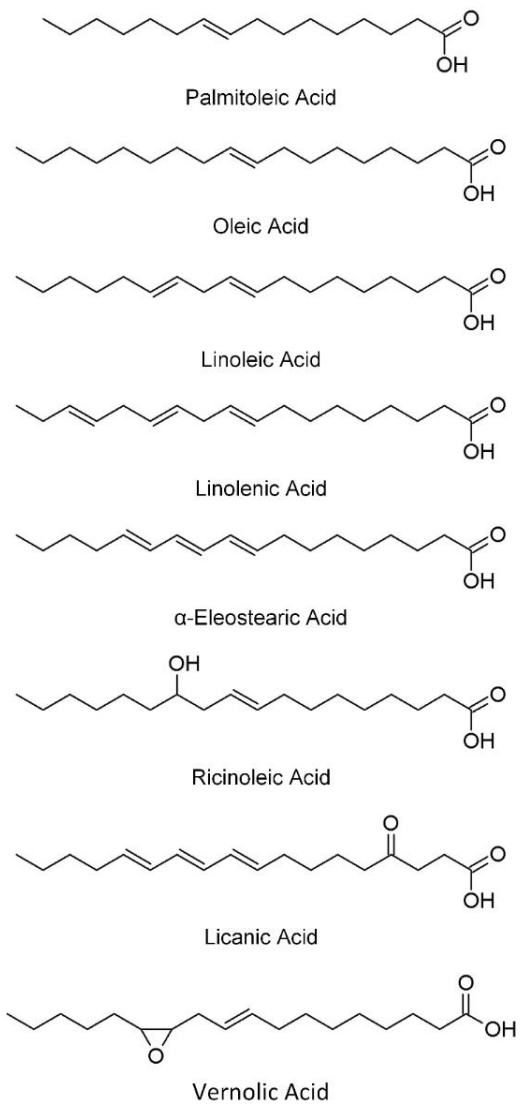

Figure 3.7 Fatty acids with double bonds.

Direct Use of Vegetable Oils

Vegetable oils relatively rich in double bonds (e.g., tung oil, linseed oil, and soybean oil) can be used in polymerization directly or after slight modification (e.g., conjugation). A small amount of tung oil (0.025-0.7 wt.%) was successfully copolymerized with styrene using a combination of free radical initiators to obtain better molding properties (Ingram et al. 1967). More significant tung oil quantities were used in a bulk copolymerization with

styrene (Fernandez and Conde 1983) and between 30 to 50 wt.% tung oil was used in a terpolymerization with STY and divinylbenzene (DVB) (Li and Larock 2003).

Highly conjugated linseed oil was reacted with STY and DVB at concentrations ranging from 30 to 70 wt.% at 85-160 ℃.Fully cured thermosets that contain approximately 35-85% cross-linked materials were produced (Kundu and Larock 2005). Terpolymerization of fully conjugated linseed oil with acrylonitrile (AN) and DVB was performed in bulk. From 30 to 75 wt.% conjugated linseed oil was used in the polymerization, and thermosets with a maximum oil incorporation of 96 wt.% were produced (Henna et al. 2007).

Modified Vegetable Oils

To improve vegetable oil incorporation in polymers, a more substantial modification of the vegetable oil can be performed (e.g., epoxidation, transesterification, and malination).

Macromonomers were produced via inter-transesterification of castor oil and linseed oil, followed by esterification with acrylic acid (Gultekin et al. 2000). The homopolymerization of these macromonomers proved difficult due to steric hindrance of the macromonomer structure. However, copolymerization with STY was successful, and copolymers with good film properties were produced. A similar approach was used to produce macromonomers by first reacting with glycerol and then transesterification with MMA; these were also copolymerized with STY (Akbas et al. 2003).

Soybean oil and sunflower oil were bromoacrylated with the addition of acrylic acid (AA) and N-bromosuccinimide (Figure 3.8) (Eren and Küsefoğlu 2004). Bromoacrylation was

conducted under room temperature with the addition of *N*-Bromosuccinimide and acrylic acid. However due to limited yield (75% for soybean oil, 55% for sunflower oil), an extra step is needed to remove unreacted monomers. The bromoacrylated soybean and sunflower oils were then copolymerized with STY. The bromoacrylated soybean oil yielded rigid polymer, whereas the sunflower oil yielded soft polymer. It should also be noted that N-bromosuccinimide does present as a chemical hazard and this reduces the "greenness" of the approach.

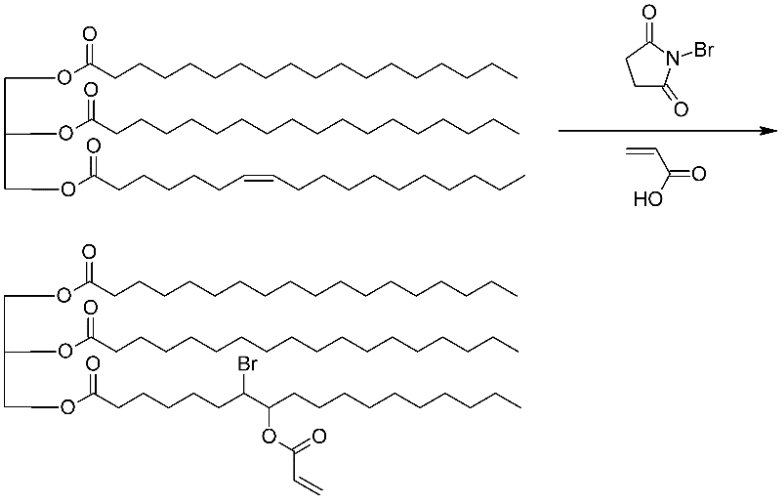

Figure 3.8 Synthesis of bromoacrylated triglycerides.

Acrylated-epoxidized soybean oil (AESO) (Figure 3.9), a well-studied modified vegetable oil, was produced in two steps: epoxidation of soybean oil, and then acrylation using acrylic acid (Hernandez and Vigueras 2013). The level of acrylation greatly influenced the mechanical properties of AESO. Photopolymerization of AESO resulted in a high yield of crosslinked polymer in a relatively short time frame (Pelletier et al. 2006). AESO has been copolymerized with BMA to manufacture electrically conductive polymer composites

(Hernandez and Vigueras 2013) and has also been used in pressure-sensitive adhesive formulations (Ahn et al. 2013).

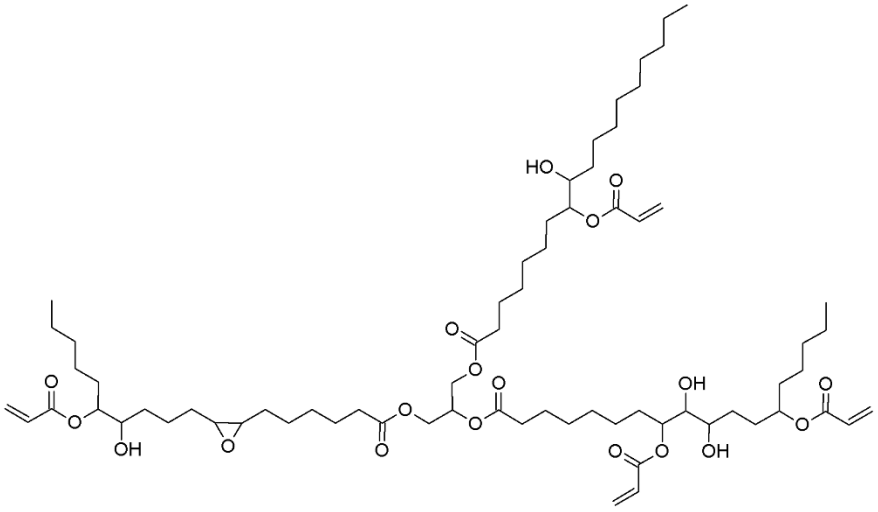

Figure 3.9 Example structure of AESO.

Soybean oil and castor oil were also modified by the alcoholysis reaction with polyol followed by malination with maleic anhydride (Can et al. 2006a, b). The resulting macromonomers were copolymerized with STY to yield a thermoset polymer.

Monomers Derived from Vegetable Oils

Beyond the direct use or modification of vegetable oils, there are many examples of monomer production using a transesterification or other similar reactions (e.g., glycerol, fatty acids, and fatty esters). These monomers and their derivatives are yet another alternative for application in emulsion polymerization.

Fatty Acids and Their Derivatives

As discussed above, fatty acids derived from vegetable oils normally contain long carbon chains, double bonds or other functional groups. Those with double bonds (Figure 3.7)

can be used directly in emulsion polymerization. For example, conjugated linoleic acid (CLA) was successfully used in bulk and emulsion polymerization (Roberge and Dubé 2016a, b). CLA was used as a bulk co- and terpolymer with BA and STY, and in emulsion as a CLA/BA/STY terpolymer. Application of emulsion terpolymer latex films as a pressure-sensitive adhesive was demonstrated with up to 30 wt.% CLA content in the latex.

Saturated fatty acids can be used in emulsion after derivatization such as hydrogenation to fatty alcohols (Vendamme et al. 2014). Further reaction with AA (which also can be derived from natural resources) can yield bio-based acrylic monomers (Wool and Bunker 2003; Çayli and Meier 2008; Anderson et al. 2011); 2-Octonal derived from ricinoleic acid, a product of castor oil transesterification, was used to produce 2-octyl methacrylate for latex-based adhesives.(Anderson et al. 2011)

Glycerol and Its Derivatives

Glycerol is the backbone of triglycerides and can be obtained by hydrolysis or transesterification of triglycerides from plant and animal resources. As the by-product of biodiesel, the production of glycerol is expected to exceed market demand six-fold by 2020 (Christoph et al. 2000). Glycerol has been used either in monomer or polymer form in the food, cosmetics and pharmaceuticals industries (Salehpour and Dubé 2011).

Glycerol (Fig. 10) is a polyol compound, and cannot be used directly as a monomer in emulsion. However, its derivatives (Fig. 10) obtained by modifying the alcohol groups in its structure can be used in free radical polymerization (Liu et al. 2010; Zhang and Grinstaff 2014). Normally, these can be modified via acrylation, alkylation, chlorination,

dehydration, and so on (Hernandez and Vigueras 2013). Free radical and living polymerization of glycerol-based monomers have been reviewed recently (Pham et al. 2013). Some examples include glycerol dimethacrylate (Figure 3.10) copolymerized with STY and 4-vinyl-pyrrole (Roice and Pillai 2005; Vijitha et al. 2009); and solketal methacrylate (Fig. 10) copolymerized with *tert*-butyl methacrylate, 2-(N,N-dimethylamino) ethyl methacrylate and 2-bromoethyl methacrylate (Miranda and Ford 2005). In addition, glycerol can be converted to allyl alcohol, which can further undergo free-radical polymerization.(Iio et al. 2007; Liu et al. 2010)

There is no doubt that various derivatized glycerol monomers can be developed and used in emulsion polymerization. Nevertheless, the modification of glycerol may come at significant economic and environmental cost.

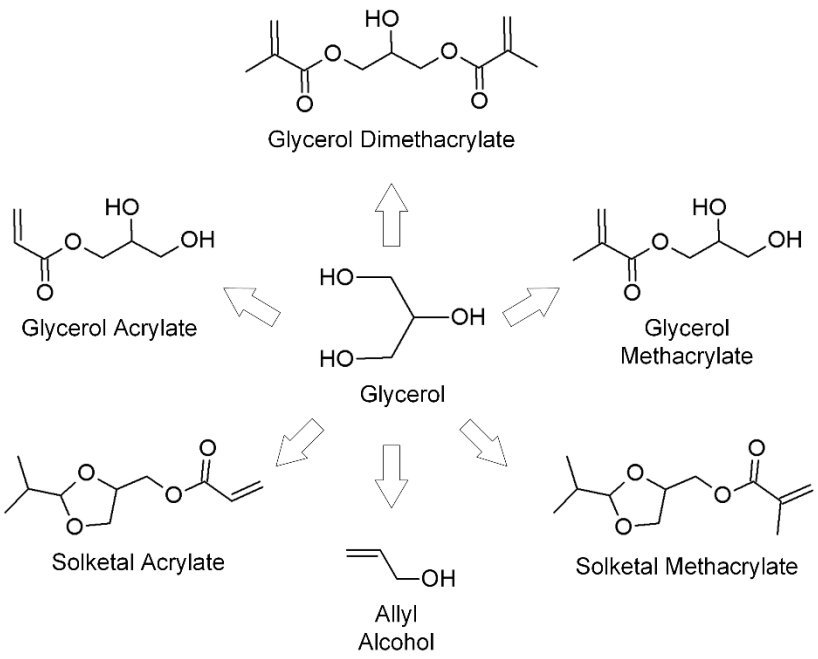

Figure 3.10 Glycerol and its derivatives.

Sugar-Based Monomers

Sugars are carbohydrates existing in the tissues of many plants (e.g., grapes, banana, sweet potato, and yam), and are normally extracted from sugar beets and sugar cane. In 2016, global sugar production was 169 million metric tons (United States Department of Agriculture 2016b). Sugars are abundant and possess an enormous variety of structures with multi-functional groups (Galbis et al. 2016). Nevertheless, their multi-functionality generally needs to be reduced to avoid undesired by-products. Polymerization of sugar-based monomers often yields atactic polymers but greater stereoregularity can be achieved (Galbis and García-Martín 2008).

Generally, sugar-based monomers are used to produce polyesters (Lavilla et al. 2012a, b; Wu et al. 2012), polycarbonates (Feng et al. 2012; Engler et al. 2015) and polyurethanes (Boyer et al. 2013; Begines et al. 2015) via step-growth polymerization. However, some of those monomers can be modified for application in emulsion polymerization.

AA is a monomer often added to emulsion formulations to improve latex stability and film properties (Reyes-Mercado et al. 2008). AA is produced commercially from petroleum-sourced propylene. However, it is possible to obtain AA through fermentation of sugars via several pathways. (Figure 3.11) One method involves first obtaining lactic acid by fermentation, and then dehydrating the lactic acid to produce AA (Datta and Henry 2006; Xu et al. 2006). In 2011, the Dow Chemical Company and OPX Biotechnologies Inc., announced the development of a process using fermentation of sugar-based 3-

hydroxypropionic acid (Guzman 2012; Dishisha et al. 2015). A more recent report involves the metathesis transformation of sugar-based fumaric acid (Burk et al. 2012).

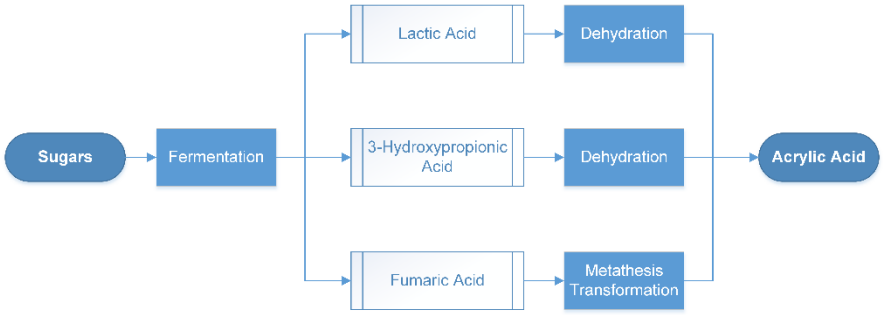

Figure 3.11 Pathways to sugar-based AA.

It is also possible to derive sugar-based acrylic and methacrylic monomers which can be applied in emulsion. *n*-Butanol is an important building block that can be derived from the fermentation of sugars and starches (Green 2011). Though it cannot be directly used in emulsion polymerization, it can be used to produce bio-based BA via acrylation using AA (Vendamme et al. 2014). Bio-based MMA can be produced via fermentation of sugar cane (Guzman 2013), or using sugar-based isobutyric acid (University of Minnesota). Other acrylic and methacrylic monomers have been obtained using various sugar-based building blocks (e.g., isosorbide, hydroxymethylfurfural) (Bloom and Venkitasubramanian 2009). For instance, a sugar-based monomer 5-butoxymethyl furfuryl alcohol can be reacted with methyl acrylate using Lipase B enzyme (Nuvozyme 435) as catalysts to produce 5-butoxymethylfurfuryl acrylate (Figure 3.12), which can be later polymerized in emulsion.

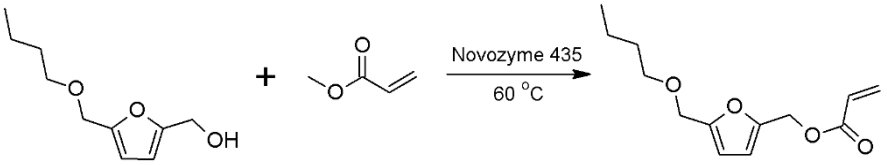

Figure 3.12 Reaction to produce 5-butoxymethylfurfuryl acrylate.

Another technology developed by EcoSynthetix Inc. introduced sugar-based vinyl monomers that can be used in emulsions (Bloembergen et al. 1999, 2001). In this technology, an aldose sugar is converted to alkyl polyglycosides (APG), and then APG is reacted with maleic anhydride to produce sugar-based vinyl monomers. The sugar-based vinyl monomers were successfully applied in emulsion polymerization formulations with monomers such as BA, MMA and vinyl acetate. This invention was targeted for application in coatings, adhesives, and toners, in paper and paperboard products.

Other Bio-Sourced Monomers

The use of terpenes, vegetable oils, sugars and their derivatives for emulsion polymerization is an emerging field of research. As shown in Table 3.2, a great many other possibilities exist. In all cases, however, the cost and compositional variability of the source material and the cost of derivation, if necessary, must be considered for the selection of these materials. At the same time, the replacement of a petroleum-based monomer in the reaction formulation will most certainly lead to significant process modification to achieve similar or improved properties.

Surfactants

Surfactant (or stabilizer) is an essential component in emulsion polymerization to achieve stable latex particles and lower latex viscosity. Typical surfactants contain both a hydrophilic group (polar head group) and a hydrophobic group (alkyl chain) in their structure. They can be physically absorbed on the particle surface or chemically incorporated onto the surface. In general, there are three types of surfactants: electrostatic surfactants (ionic surfactants) (e.g., sodium dodecyl sulfate), steric surfactants (e.g., poly(ethylene oxide) nonylphenyl ether) and electrosteric surfactants, which provide both electrostatic and steric mechanisms (Zecha 1981; Dunn 1986; Thickett and Gilbert 2007). Each surfactant can be used separately or as a mixture, although anionic surfactants are used most frequently.

The surfactant type will dictate the amount of surfactant required in the emulsion formulation. For example, anionic surfactant is normally used at a concentration of 0.2 to 3 wt.% in water, while non-ionic surfactant is used in amounts of 2 to 10 wt.% (Odian 2004). Commonly used surfactants are considered toxic to marine organisms, and may result in bioaccumulation (Liwarska-Bizukojc et al. 2005; Kronberg et al. 2014). Due to their relatively high cost and effect on latex application properties, minimization of surfactant concentration in emulsion formulations is highly desired.

Surfactants are produced from both petroleum and natural resources, but mostly from the former. Nevertheless, driven by environmental concerns, there is a growing trend towards the development and use of renewable and less-hazardous surfactants

(Kronberg et al. 2014). Surfactants that are entirely derived from natural resources are commercially available; the most popular of these are shown in Table 3.5.

Table 3.5 Some commercially available renewable surfactants.

Category	Supplier	Application	Global Production (ton/yr)*
Alkyl polyglycosides	Dow Chemical Company, BASF, DuPont, E. I. du Pont de Nemours and Company, Cognis, AkzoNobel, Clariant, Shanghai Fine Chemicals and LG Household & Health Care	Household detergents, personal care, cosmetics, industrial cleaners and agricultural chemicals	>90,000
Sorbitan esters	Dupont, BASF, SABO, SEPPIC, Kao,Vantage, Clariant, Lonza, Croda	Food, pharmaceutical and cosmetic products	25,000
Sucrose esters	BASF, Evonik Industries, P&G Chemicals, Croda International Plc, Sisterna B.V., Mitsubishi Chemical Holdings Corporation, Dai-Ichi Kogyo	Food and beverage additives, personal care, detergents and cleansers	<10, 000

*References are cited in the text.

Alkyl Polyglycosides

Alkyl polyglycosides (APG) (Figure 3.13) are manufactured completely from natural resources and have been under development for over 30 years. The hydrophobic parts of APG are fatty alcohols with chain lengths from 8 to 16 derived from vegetable oils (e.g., coconut oil, palm oil, and rapeseed oil), while the hydrophilic parts are glucose derived from starch, potatoes, sugars and so on. In general, APG are mixtures of isomers, and are

characterized based on the alkyl chain length and the degree of oligomerization (Rybinski and Hill 1998; Holmberg 2003). Commercially available APG has a degree of oligomerization from 1.3 to 1.6.

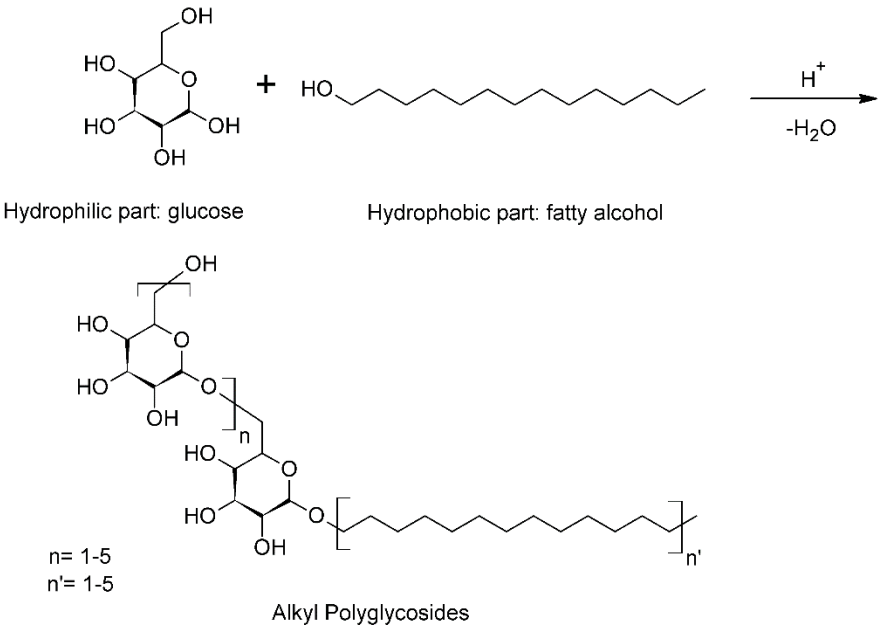

Figure 3.13 Synthesis of alkyl polyglycosides.

APG is supplied by many companies (Benvegnu et al. 2008; Hill 2010) with a global production of over 90,000 tons (Table 3.5).(Global Market Insights 2016) Industrial production of APG normally contains several stages (Figure 3.14). The first stage is acetalization of glucose with fatty alcohols. The acetylization process differs depending on the source of glucose. For anhydrous glucose, direct acetalization can be applied, while for glucose syrup and starch, butanolysis is conducted prior to transacetalization with fatty alcohols. A neutralization stage follows to terminate the acetalization reaction. Because excess fatty alcohol is needed for acetalization, a distillation stage is used to remove and recycle excess fatty alcohols. Additional refining (e.g., bleaching,

stabilization) is sometimes necessary. The APG production process is solvent-free, has high yields and low emissions, which makes it industrially and environmentally favorable.

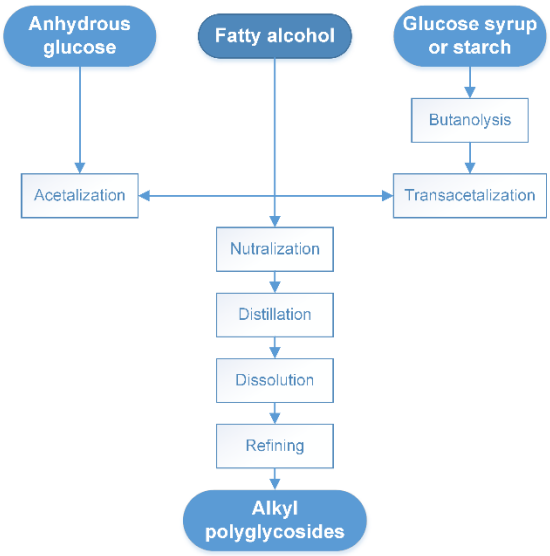

Figure 3.14 Production of alkyl polyglycosides.

Beyond the favorable nature of the APG production process, APG are not toxic to humans and are compatible with skin and eyes (Aulmann and Sterzel 1996). APG have been applied as household detergents, personal care products, and cosmetics, to name a few (Rybinski and Hill 1998).

APG have been used as non-ionic surfactants in emulsion polymerizations. APG with different degrees of oligomerization (1.6 to 4.0) and alkyl chain lengths (8 to 14) were tested in the semi-batch emulsion copolymerization of vinyl acetate and BA (Lazaridis et al. 2001). The degree of oligomerization and alkyl chain length of APG affected latex particle stability. As with typical non-ionic surfactants, with increasing APG concentration, latex particle size decreased, while particle stability increased. However, this only applied

up to a certain APG concentration beyond which destabilization occurred. APG was also used in BA/MMA seeded emulsion polymerization as a replacement for nonylphenol ethoxylates (NPEOs).(Chen 2012) Similar effects of APG concentration on particle size and latex stability were shown. In addition, the increasing APG concentration was shown to decrease the water-resistance of the latex film.

Mixtures of APG along with other green non-ionic or anionic surfactants were also studied (Klima et al. 2000; Maver and Krasnansky 2001). APG with alkyl chain lengths between 9 and 11, and degree of oligomerization of 1.6 were used. APG (4 to 40 wt.%) were mixed with fatty alcohol ethoxylate (20 to 76 wt.%) as a surfactant mixture. As a result, much less surfactant was used to achieve a stable latex with excellent mechanical properties (Klima et al. 2000). Mixtures of APG and a traditional surfactant were used in the production of a wide range of emulsion polymers (e.g., BA, MMA, and EHA), and improved block resistance of the latex film was achieved (Maver and Krasnansky 2001).

Sorbitan Esters

Sorbitan esters are non-ionic surfactants made from sorbitol (hydrophilic part, derived from glucose) and fatty acids (hydrophobic part, derived from fat or vegetable oils). (Figure 3.15) Sorbitan esters are biodegradable and safe to use on humans; they have been used in food, cosmetics and pharmaceutical products. Sorbitan esters are industrially manufactured via two approaches. The first approach involves the dehydration of sorbitol to produce sorbitan, followed by transesterification of sorbitan with fatty acids (Stockburger 1981; Hoydonckx et al. 2004). In the other approach, sorbitol

is directly esterified with fatty acids using acid or base catalysts at relatively high temperatures (200 to 250 °C) (Milstein 1992; Ellis et al. 1998). Both methods yield mixtures of sorbitan fatty acid esters (commercially named 'Span') with different degrees of esterification. The chain length and amount of fatty acid used, as well as the degree of esterification influences the hydrophilic/lipophilic balance (HLB) (ranging from 1 to 8). Sorbitan fatty acid esters can be further reacted with ethylene oxide to produce polyethoxylated sorbitan esters (commercially named 'Tween') with HLB values ranging from 10 to 17 (Falbe 1987). The main suppliers of sorbitan esters report an annual global production of over 25,000 tons (Table 3.5) (Benvegnu et al. 2008; Global Market Insights 2016).

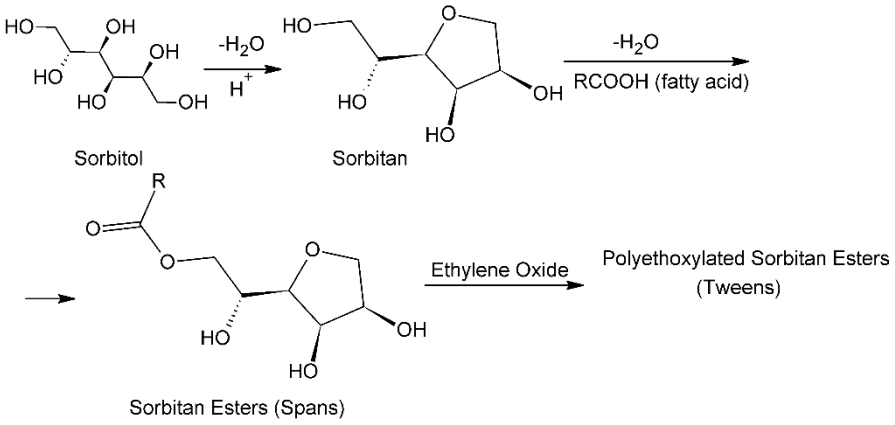

Figure 3.15 Synthesis of sorbitan esters.

Spans and Tweens with different HLB values have been successfully applied in emulsion polymerization. Spans are efficient surfactants used in water-in-oil high internal phase emulsion systems (Kovačič et al. 2012; Silverstein 2014). Tweens are generally applied in oil-in-water emulsion systems and are more commonly used in conventional emulsion polymerization (Capek and Chudej 1999; Yao et al. 2014; Giovannoli et al. 2015). Spans

and Tweens can be used together or as a combination with other traditional surfactants at different ratios to obtain certain HLB values (Clark 1988; Zhang et al. 2007; Wan et al. 2010; Ramli et al. 2013). In general, a combination of Spans and Tweens with a low and high HLB value may work better in comparison to a single surfactant. An appropriate HLB value is required to achieve a latex stability and this value can be obtained through experiment (Wan et al. 2010). Spans and Tweens with unsaturated alkyl chains tend to provide better stability for the emulsion polymerization of unsaturated monomers (Mollet and Grubenmann 2000).

Sucrose Esters

Sucrose is a carbohydrate existing in many plants (e.g., sugar cane, beet). By attaching fatty acid chains derived from vegetable oils to sucrose (Fig. 16), sucrose esters can be produced. Sucrose esters are thus, non-ionic surfactants derived completely from natural resources. In general, the production of sucrose esters poses challenges due to the high functionality of sucrose as well as its high sensitivity to temperature. Sucrose esters can be produced via transesterification of sucrose with fatty acid methyl esters (Figure 3.16), or via esterification with fatty acids (Osipow et al. 1956; Reuben et al. 1973; Parker et al. 1976). Both pathways yield mixtures of sucrose esters with various degrees of esterification, and offer sucrose esters with a broad range of HLB values. Sucrose esters have been used as food and beverage additives, and can be found in personal care products, detergents and cleansers. In 2015, the sucrose esters market was estimated at 55.7 million US dollars and is expected to reach 74.6 million US dollars by 2020 (Markets

and Markets 2016). The major sucrose ester manufacturers are listed in Table 5 (Hill 2010; Markets and Markets 2016).

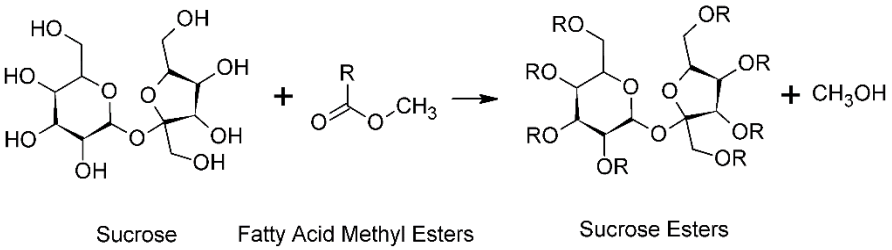

Figure 3.16 Synthesis of sucrose esters with fatty acid methyl esters.

It is possible to use sucrose esters in emulsion polymerization, though limited publications on the subject can be found. Sucrose esters were successfully used in a patent to make pH-neutral pressure sensitive adhesives (Crandall and Nelson 1995). From 2 to 10 wt.% sucrose esters based on the total polymer weight were added as non-ionic surfactants to stabilize non-ionic monomers in emulsion formulations. HLB values ranging from 12 to 18 gave the best performance. Sucrose esters have also been studied in water-in-oil emulsions to produce water-absorbent resins (Nagasuna et al. 1990). To stabilize water-soluble unsaturated monomers (e.g., AA, sodium acrylate), generally 0.5 to 10 wt.% sucrose esters relative to monomer weight was needed, and sucrose esters with HLB values between 2 and 6 were preferred.

Other Components

Compared with monomers and surfactants, relatively smaller amounts of other components (e.g., cross-linker, chain transfer agent, initiator, and buffer) are used in emulsion formulations (Table 3.1). Typically, these components are mostly consumed during the reaction and thus, their environmental impact would be limited. Nonetheless,

replacement of some of these components with less-hazardous and natural-based chemicals is an area of active interest.

Some cross-linkers derived from renewable resources have been used in polymer synthesis to replace conventional cross-linkers (Oprea 2009; Ma et al. 2014; Lan et al. 2014). Castor oil was used as a trifunctional cross-linker to produce polyurethane elastomers and the morphology changes with castor oil concentration were investigated (Oprea 2009). In soybean oil-based coatings, gallic acid (Figure 3.17), which can be extracted from gallnuts, oak bark, tea leaves and other plants, was used (Ma et al. 2014). Another natural-based cross-linker 3-hydroxy-N,N-bis(2-hydroxyethyl)butanamide (HBHBA) (Figure 3.17) was tested in the production of polyurethane foams as a replacement for conventional cross-linker diethanolamine and offered better mechanical properties (Lan et al. 2014). Bio-based materials containing vinyl groups, which may be suitable for cross-linking, are generally less reactive. Pripol™ is an example of a commercial renewable cross-linker. Pripol 1009 (di-acid) and Pripol 1040 (tri-acid) are derived from vegetable oils; both have been used to produce thermosetting resins with epoxidized linseed oil.(Supanchaiyamat et al. 2012; Ding et al. 2015)

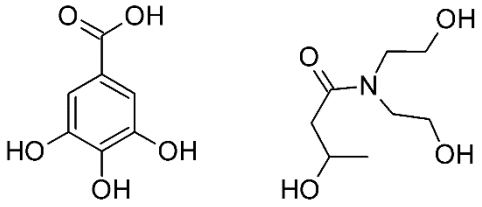

Gallic Acid HBHBA

Figure 3.17 Natural-based cross-linkers.

α-Pinene and *d*-limonene have shown potential as renewable chain transfer agents (Mathers et al. 2006; Mathers and Damodaran 2007; Zhang and Dubé 2014a). Investigations on the copolymerization of *d*-limonene revealed its dramatic degradative chain transfer effects on conversion, copolymer composition and molecular weights, which makes it a renewable alternative as a chain transfer agent (Zhang and Dubé 2014a).

Initiators not only increase polymerization rate, but are also used as "chasers" to consume residual monomer (Clark 1995). Though relatively small amounts of initiators are used, in some cases, their toxicity is non-negligible (Nomura et al. 2006). To eliminate the environmental effects of initiators, either less-hazardous or highly efficient initiators should be chosen. Alternative initiation methods can also be used (discussed below). Buffers (e.g., sodium bicarbonate) used in emulsion polymerization are normally not of concern.

The often-present multi-functionality of renewable monomers can be explored to develop their potential as cross-linkers, chain transfer agents and so on. Furthermore, transition from petroleum-based monomers to renewable alternatives may open up possibilities to apply other less-hazardous materials because of the additional functionality often present in bio-based monomers.

Design of a Green Emulsion Polymerization Process

The use of less hazardous and renewable alternatives is an obvious approach towards achieving a "greener" emulsion polymerization. However, sustainability or "green-ness"

of a process goes well beyond replacement of toxic and/or non-renewable materials. Upon further inspection of the 12 Principles of Green Chemistry and Engineering (Dubé and Salehpour 2014), some important engineering issues in emulsion polymerization emerge. These include how to prevent waste, how to maximize energy efficiency, and how to minimize the potential for accidents; which are explored below. Nevertheless, other principles should still be considered during process design and other engineering tools (e.g., life cycle assessment) can be applied to evaluate the environmental impact of the entire process (Caillol 2014).

Prevent Waste

The primary source of waste generated in emulsion polymerization are residual monomers and off-spec production material. To remove residual monomers, various techniques can be employed, which can be classified as chemical methods or physical methods (Araújo et al. 2002). Chemical methods are typically geared to further reaction of unreacted monomers. This can be achieved by increasing temperature (Oka et al. 1999), adding extra initiator towards the end of the reaction (Heider et al. 1992), or adding reactive monomers (Minematsu et al. 1981). Physical methods include distillation (Humme et al. 1983), supercritical devolatilization (Aerts et al. 2011), spray-drying (Schull and Arnoldi 1998) and stripping (Heinze et al. 1981). These techniques can be used alone or in combination depending on final product specifications. Cost and impact on final product properties should also be considered. Off-spec material can result from impurities in the monomer and other components, inefficient mixing, or inconsistent heat transfer. Impurities can be carefully avoided by purification of chemicals, while others can

be prevented by regular maintenance and calibration (Salehpour and Dubé 2011). Process control techniques (Copelli et al. 2011) and some real-time analysis tools (Fonseca et al. 2009) can be used as well to prevent off-spec material. In any case, one can make process operating and reaction formulation choices at the design stage to minimize the amount of residual monomer.

Maximize Energy Efficiency

In general, polymerizations are performed under isothermal conditions to obtain consistent polymer properties (Odian 2004). As polymerization reactions are extremely exothermic, to control the reaction temperature, a great deal of energy is consumed. In emulsion polymerization, the aqueous medium acts as a heat sink to more easily control polymerization temperature. In large-scale reactors, challenges in heat transfer and due to fouling may still be present. To maximize energy efficiency and make better use of the heat produced during polymerization, one can adopt approaches such as adiabatic polymerization or alternative initiation techniques.

Adiabatic Polymerization

Adiabatic polymerization is a polymerization process that involves no external heating or cooling system, or in some cases, only involves heating at the initial stages of the process (Chen and Reichert 1993; Goikoetxea et al. 2008). This technique employs the heat generated during polymerization and is often applied to fast reactions; as a result, both reaction time and energy costs are reduced. Normally, initiators requiring relatively low temperatures (e.g., redox initiators) are used. By controlling the initiator and chain

transfer agent concentrations, polymers with a range of desired properties can be achieved (Chen and Reichert 1993; Wang et al. 2016).

Adiabatic polymerizations have been successfully applied to bulk and solution free radical polymerization, and thorough thermodynamic and kinetic studies were conducted (Tonoyan et al. 1973; Pohl and Rodriguez 1981; Thomson 1986; Chen and Reichert 1993; Garg et al. 2014). Very recently, adiabatic emulsion polymerization was investigated using a reaction calorimeter (Wang 2013). Redox initiators (hydrogen peroxide and ascorbic acid) were used at ambient temperatures to polymerize BMA, a monomer with a relatively high reaction rate. Both batch and semi-batch processes were studied to investigate the influence of adiabatic conditions on the nucleation stage. Compared with conventional emulsion polymerization conditions, a shorter reaction time and less energy were needed.

Initiation Methods

Thermal initiators are generally used in emulsion polymerization, however, some other initiation methods are available. Photo-induced emulsion polymerizations were studied and were considered as an energy-efficient method with a lower risk of latex destabilization (Turro et al. 1980; Mah et al. 2002; Chemtob et al. 2010). The polymerization rate and polymer molecular weight can be controlled by changing the light intensity and irradiation time (Chemtob et al. 2010). Microwave irradiation is another initiation method used in emulsion polymerization, which provides higher polymerization rates, higher yields and a shorter reaction time (Zhu et al. 2003; Aldana-García et al. 2005;

Ergan et al. 2015). Ultrasonication has also been studied (Chou and Stoffer 1999; Cheung and Gaddam 2000; Xia et al. 2003; Bhanvase et al. 2012; Korkut and Bayramoglu 2014). Ultrasound power, pulse ratio and probe diameter have been shown to influence polymerization yields and polymer properties (Korkut and Bayramoglu 2014). Ultrasound irradiation can be used in large scale latex production and shows more promise than some other methods (Cheung and Gaddam 2000; Bhanvase et al. 2012).

It is worth mentioning that the initiation methods mentioned above are normally used at room temperature, but one can combine these methods with adiabatic polymerization to achieve even higher energy efficiencies.

Apply Real-Time Analysis to Prevent Pollution

To better tune polymer product properties, minimize by-product formation and prevent pollution, real-time analysis tools can be used in a feedback control loop. There are various real-time analysis tools available (e.g., calorimetry, infrared (IR) spectroscopy and Raman spectroscopy), and these have been widely used in polymer production to monitor polymerization parameters (e.g., temperature, pH, and composition) (Fonseca et al. 2009). In general, real-time analysis tools are cost-effective, non-invasive and environmental-friendly. Development of real-time analysis tools in emulsion polymerization are relatively slower and more difficult because of the thermodynamic instability of the latex particles (Chien and Penlidis 1990). However, there are some tools that have been successfully developed and employed in emulsion systems (e.g., calorimetry, IR spectroscopy). Some other tools are still under development, for example,

particle size analysis is of particular interest in emulsion polymerization, but reliable real-time analysis is still not available.

Calorimetry

Reaction calorimetry has been widely used to monitor polymerization by tracking the heat generated during the reaction. The heat generation is closely correlated to monomer conversion and polymerization kinetics, which makes reaction calorimetry a useful tool to predict conversion, polymerization rate and so on (Fonseca et al. 2009). Reaction calorimetry is ideal for on-line polymerization monitoring, as it is non-invasive, robust and fast (Elizalde et al. 2005).

There are three types of reaction calorimetry: heat-flow calorimetry, heat-balance calorimetry and power-compensation calorimetry (Gesthuisen et al. 2005; Fonseca et al. 2009). Heat-flow calorimetry measures the heat flow between the reactor and cooling jacket. It is of great sensitivity, thus, is more applicable to lab-scale reactors due to the significant temperature difference between the reaction mixture and cooling jacket (Frauendorfer et al. 2010). Heat-balance calorimetry performs energy balances based on the heat transfer of the cooling fluid and is less sensitive to temperature changes resulting from the slow flow rates of cooling fluids (Fonseca et al. 2009). Power-compensation calorimetry uses a heater to achieve a constant temperature by varying the power. This technique is not commonly used in the polymer industry as cooling is not available, however, it can be effective at high pressure conditions (Wang et al. 2003; Liu et al. 2005).

Heat-flow calorimetry has been extensively used in batch and semi-batch emulsion polymerization as an on-line analysis tool (De Buruaga et al. 1997; Lamb et al. 2005; Elizalde et al. 2005; Rincón et al. 2013, 2014). With the data collected using calorimetry, monomer conversion and copolymer composition were estimated and compared with data obtained by gravimetry and other conventional methods. It has also been used to monitor polymerization kinetics (De La Rosa et al. 1999; Elizalde et al. 2005), molecular weight (Vicente et al. 2001) and nucleation (Blythe et al. 1999a, b, c). This technique can be very helpful in adiabatic polymerization to measure the heat generation during polymerization and maximize energy efficiency (Wang et al. 2016).

IR Spectroscopy

IR spectroscopy has been developed for use in emulsion polymerization to provide information on molecular structure and polymerization kinetics (Fonseca et al. 2009). IR bands have three regions: near- (wave number from 14000 to 400 cm-1), mid- (wave number from 4000 to 400 cm-1), and far-IR (wave number from 400 to 400 cm-1). Near-IR can excite overtone or harmonic vibrations, while mid-IR can detect fundamental molecular vibrations.

Near-IR was successfully used in-line and *in situ* to monitor conversion and molecular weight in emulsion polymerization, however numerous challenges were encountered (Vieira et al. 2002). Attenuated total reflectance (ATR)-Fourier transform infrared (FTIR) spectroscopy is more commonly used to monitor emulsion polymerization. In-line ATR-FTIR can detect residual monomers, estimate monomer conversion and copolymer

composition in emulsion polymerization (Hua and Dubé 2002; Dubé and Li 2010; Poljanšek et al. 2013; Roberge and Dubé 2016c). Results obtained via ATR-FTIR often correlates well with those determined by conventional methods.

Prevent Accidents

In emulsion polymerization, the aqueous medium often prevents thermal runaway, however, potential for accidents still exists. Accidents may happen during feedstock transport and storage, polymer synthesis or when dealing with final products (Dubé and Salehpour 2014). As mentioned above, less-hazardous and renewable chemicals are far less likely to lead to hazardous situations. For example, when handling and transporting bio-based chemicals, personal protective gear, while always necessary, would be less critical in the face of low or non-existent material toxicity. During the polymerization process, the reaction temperature and pressure should be closely monitored; process control methods or equipment can be implemented in the process. For instance, early warning detection systems can be used (Ampelli et al. 2006; Ampelli and Maschio 2012). Reactor fouling, which is an important concern for emulsion polymerizations, may change heat transfer characteristics over time. Mixing also plays an important role in heat transfer and fouling, efficient mixing tools should be chosen to maintain constant temperature. Regular equipment maintenance and inspection should be performed to prevent fouling and detect any equipment failure (failure in cooling systems or feed pumps) that may cause accidents.

Concerns regarding final products are mainly in the event of fire, in which case hazardous chemicals may be released to the environment. This is typically prevented with the use of fire retardants or oxygen scavengers (Morgan and Gilman 2013). The use of bio-based feedstock may mitigate the need for such additives.

Conclusion

Emulsion polymerization is often touted as a more sustainable technique to manufacture polymer materials. While this is true, considerable efforts are still required to minimize the environmental impact of the process and the products. The 12 Principles of Green Chemistry and Engineering establish a framework for designing green products and processes. All of the principles should be taken into consideration when designing a green product or process. Here, we chose selected principles based on their applicability to emulsion polymerization technology. To design green chemicals and products, the use of renewable feedstocks (principle 6 in the 12 Principles of Green Chemistry) to replace their petroleum-based counterparts is recommended. Various renewable monomers and their potential for use in emulsion polymerization has been reviewed. The use of renewable feedstocks is probably the most effective means to achieve a green emulsion polymerization. Application of other principles such as maximizing energy efficiency, using real-time analysis to prevent pollution, preventing waste and accidents, may also have a significant impact on moving towards a green emulsion polymerization.

In all cases, the 12 Principles of Green Chemistry and Engineering should be actively considered when designing emulsion polymerization processes. Inevitably, there will be trade-offs when applying different principles, but an evaluation tool such as life cycle assessment, would greatly assist in making the most sustainable choices. In other words, the consideration of producing emulsion-based polymers should lead to a scenario of least overall impact on the environment. The 12 Principles of Green Chemistry and Engineering are an appropriate guide along the way.

References

Aerts M, Meuldijk J, Kemmere M, Keurentjes J (2011) Residual monomer reduction in polymer latex products by extraction with supercritical carbon dioxide. Macromol Symp 302:297–304. doi: 10.1002/masy.201000052

Ahn BK, Sung J, Rahmani N, et al (2013) UV-curable, high-shear pressure-pensitive adhesives derived from acrylated epoxidized soybean oil. J Adhes 89:323–338. doi: 10.1080/00218464.2013.749102

Akbas T, Beker ÜG, Güner FS, et al (2003) Drying and semidrying oil macromonomers. III. Styrenation of sunflower and linseed oils. J Appl Polym Sci 88:2373–2376. doi: 10.1002/app.11638

Aldana-García MA, Palacios J, Vivaldo-Lima E (2005) Modeling of the Microwave Initiated Emulsion Polymerization of Styrene. J Macromol Sci Part A 42:1207–1225. doi: 10.1080/10601320500189505

Ampelli C, Di Bella D, Maschio G, Russo A (2006) Calorimetric study of the inhibition of runaway reactions during methylmethacrylate polymerization processes. J Loss Prev Process Ind 19:419–424. doi: 10.1016/j.jlp.2005.10.003

Ampelli C, Maschio G (2012) Investigation of thermal runaway in semibatch chemical reactors by an early warning detection device. AIDIC Servizi S.r.l., pp 1–1

Anastas PT (1998) Green chemistry: theory and practice. Oxford University Press, New York

Anastas PT, Zimmerman JB (2003) Design through the 12 principles of green engineering. Environ Sci Technol 37:94–101

Anderson KS, Lewandowski KM, Fansler DD, et al (2011) 2-octyl (meth)acrylate adhesive composition. US Patent 7,893,179, 22 Feb 2011

Araújo PHH, Sayer C, Giudici R, Poço JGR (2002) Techniques for reducing residual monomer content in polymers: A review. Polym Eng Sci 42:1442–1468. doi: 10.1002/pen.11043

Aulmann W, Sterzel W (1996) Toxicology of alkyl polyglycosides. In: Hill K, Rybinski W von, Stoll G (eds) Alkyl polyglycosides. Wiley-VCH Verlag GmbH, pp 151–167

Autian J (1975) Structure-toxicity relationships of acrylic monomers. Environ Health Perspect 11:141–152. doi: 10.2307/3428337

Begines B, Zamora F, de Paz MV, et al (2015) Polyurethanes derived from carbohydrates and cystine-based monomers. J Appl Polym Sci. doi: 10.1002/app.41304

Belgacem MN, Gandini A (2008a) Monomers, polymers and composites from renewable resources. Elsevier, Oxford

Belgacem MN, Gandini A (2008b) Materials from vegetable oils: Major sources, properties and applications. In: Gandini A (ed) Monomers, polymers and composites from renewable resources. Elsevier, Amsterdam, pp 39–66

Benvegnu T, Plusquellec D, Lemiègre L (2008) Surfactants from renewable sources: synthesis and applications. In: Gandini A (ed) Monomers, polymers and composites from renewable resources. Elsevier, Amsterdam, pp 153–178

Bhanvase BA, Pinjari DV, Sonawane SH, et al (2012) Analysis of semibatch emulsion polymerization: Role of ultrasound and initiator. Ultrason Sonochem 19:97–103. doi: 10.1016/j.ultsonch.2011.05.016

Bloembergen S, McLennan IJ, Narayan R (1999) Sugar based vinyl monomers and copolymers useful in repulpable adhesives and other applications. US Patent 5,872,199, 16 Feb 1999

Bloembergen S, McLennan IJ, Narayan R (2001) Environmentally friendly sugar-based vinyl monomers useful in repulpable adhesives and other applications. US Patent 6,242,593, 5 Jun 2001

Bloom PD, Venkitasubramanian P (2009) Monomers and polymers from bioderived carbon. US Patent 20,090,018,300, 8 Jul 2008

Blythe PJ, Klein A, Sudol ED, El-Aasser MS (1999a) Enhanced droplet nucleation in styrene miniemulsion polymerization. 3. Effect of shear in miniemulsions that use cetyl alcohol as the cosurfactant. Macromolecules 32:4225–4231. doi: 10.1021/ma981977f

Blythe PJ, Klein A, Sudol ED, El-Aasser MS (1999b) Enhanced droplet nucleation in styrene miniemulsion polymerization. 2. Polymerization kinetics of homogenized emulsions containing predissolved polystyrene. Macromolecules 32:6952–6957. doi: 10.1021/ma981976n

Blythe PJ, Morrison BR, Mathauer KA, et al (1999c) Enhanced droplet nucleation in styrene miniemulsion polymerization. 1. Effect of polymer type in sodium lauryl sulfate/cetyl alcohol miniemulsions. Macromolecules 32:6944–6951. doi: 10.1021/ma981975v

Bolton JM, Hillmyer MA, Hoye TR (2014) Sustainable Thermoplastic Elastomers from Terpene-Derived Monomers. ACS Macro Lett 3:717–720. doi: 10.1021/mz500339h

Boyer A, Lingome CE, Condassamy O, et al (2013) Glycolipids as a source of polyols for the design of original linear and cross-linked polyurethanes. Polym Chem 4:296–306. doi: 10.1039/c2py20588b

Burk MJ, Pharkya P, Dien SJV, et al (2012) Methods for the synthesis of olefins and derivatives. US Patent 20,120,094,341, 19 Apr 2012

Caillol S (2014) Lifecycle assessment and green chemistry: a look at innovative tools for sustainable development. In: Hamaide T, Deterre R, Feller J-F (eds) Environmental impact of polymers. John Wiley & Sons, Inc., pp 65–89

Can E, Wool RP, Küsefoğlu S (2006a) Soybean- and castor-oil-based thermosetting polymers: Mechanical properties. J Appl Polym Sci 102:1497–1504. doi: 10.1002/app.24423

Can E, Wool RP, Küsefoğlu S (2006b) Soybean and castor oil based monomers: synthesis and copolymerization with styrene. J Appl Polym Sci 102:2433–2447. doi: 10.1002/app.24548

Capek I, Chudej J (1999) On the fine emulsion polymerization of styrene with non-ionic emulsifier. Polym Bull 43:417–424. doi: 10.1007/s002890050630

Çayli G, Meier MAR (2008) Polymers from renewable resources: Bulk ATRP of fatty alcohol-derived methacrylates. Eur J Lipid Sci Technol 110:853–859. doi: 10.1002/ejlt.200800028

Chemtob A, Kunstler B, Croutxé-Barghorn C, Fouchard S (2010) Photoinduced miniemulsion polymerization. Colloid Polym Sci 288:579–587. doi: 10.1007/s00396-010-2190-1

Chen L (2012) Application of green commercial surfactant in preparing purely acrylic latex via semi-continuous seeded emulsion polymerization. J Surfactants Deterg 16:197–202. doi: 10.1007/s11743-012-1373-9

Chen M, Reichert K-H (1993) Studies on free radical polymerization by adiabatic reaction calorimetry. Polym React Eng 1:145–170. doi: 10.1080/10543414.1992.10744426

Cheung HM, Gaddam K (2000) Ultrasound-assisted emulsion polymerization of methyl methacrylate and styrene. J Appl Polym Sci 76:101–104. doi: 10.1002/(SICI)1097-4628(20000404)76:1<101::AID-APP13>3.0.CO;2-F

Chien DCH, Penlidis A (1990) On-line sensors for polymerization reactors. J Macromol Sci Part C 30:1–42. doi: 10.1080/07366579008050904

Chou HCJ, Stoffer JO (1999) Ultrasonically initiated free radical-catalyzed emulsion polymerization of methyl methacrylate (i). J Appl Polym Sci 72:797–825. doi: 10.1002/(SICI)1097-4628(19990509)72:6<797::AID-APP7>3.0.CO;2-Z

Christoph R, Schmidt B, Steinberner U, et al (2000) Glycerol. In: Ullmann's Encyclopedia of Industrial Chemistry. Wiley-VCH Verlag GmbH & Co. KGaA

Clark E (1988) Inverse emulsion polymerization with sorbitan fatty acid esters and ethoxylated alcohol. US Patent 4,764,574, 16 Aug 1988

Clark JH (1995) Chemistry of waste minimization. Blackie Academic & Professional, New York

Copelli S, Derudi M, Sempere J, et al (2011) Emulsion polymerization of vinyl acetate: Safe optimization of a hazardous complex process. J Hazard Mater 192:8–17. doi: 10.1016/j.jhazmat.2011.04.066

Corma A, Iborra S, Velty A (2007) Chemical routes for the transformation of biomass into chemicals. Chem Rev 107:2411–2502. doi: 10.1021/cr050989d

Crandall MD, Nelson RL (1995) Nonionic, pH-neutral pressure sensitive adhesive. US Patent 4,424,122, 13 Jun 1995

Datta R, Henry M (2006) Lactic acid: recent advances in products, processes and technologies — A review. J Chem Technol Biotechnol 81:1119–1129. doi: 10.1002/jctb.1486

De Buruaga IS, Echevarría A, Armitage PD, et al (1997) On-line control of a semibatch emulsion polymerization reactor based on calorimetry. AIChE J 43:1069–1081. doi: 10.1002/aic.690430420

De La Rosa LV, Sudol ED, El-Aasser MS, Klein A (1999) Emulsion polymerization of styrene using reaction calorimeter. II. Importance of maximum in rate of polymerization. J Polym Sci Part Polym Chem 37:4066–4072

Ding C, Shuttleworth PS, Makin S, et al (2015) New insights into the curing of epoxidized linseed oil with dicarboxylic acids. Green Chem 17:4000–4008. doi: 10.1039/C5GC00912J

Dishisha T, Pyo S-H, Hatti-Kaul R (2015) Bio-based 3-hydroxypropionic- and acrylic acid production from biodiesel glycerol via integrated microbial and chemical catalysis. Microb Cell Factories 14:200. doi: 10.1186/s12934-015-0388-0

Dubé MA, Li L (2010) In-Line Monitoring of SBR Emulsion Polymerization Using ATR-FTIR Spectroscopy. Polym-Plast Technol Eng 49:648–656. doi: 10.1080/03602551003664909

Dubé MA, Salehpour S (2014) Applying the principles of green chemistry to polymer production technology. Macromol React Eng 8:7–28. doi: 10.1002/mren.201300103

Dubé MA, Soares J, Penlidis A, Hamielec AE (1997) Mathematical modeling of multicomponent chain-growth polymerizations in batch, semibatch, and continuous reactors: A review. Ind Eng Chem Res 36:966–1015

Dunn AS (1986) Polymeric stabilization of colloidal dispersions. Polym Int J 18:278–278. doi: 10.1002/pi.4980180420

Elizalde O, Azpeitia M, Reis MM, et al (2005) Monitoring emulsion polymerization reactors: Calorimetry versus Raman spectroscopy. Ind Eng Chem Res 44:7200–7207. doi: 10.1021/ie050451y

Ellis JMH, Lewis JJ, Beattie RJ (1998) Manufacture of fatty acid esters of sorbitan as surfactants. WO Patent 1,998,004,540, 5 Feb 1998

Engler AC, Ke X, Gao S, et al (2015) Hydrophilic polycarbonates: promising degradable alternatives to poly(ethylene glycol)-based stealth materials. Macromolecules 48:1673–1678. doi: 10.1021/acs.macromol.5b00156

Eren T, Küsefoğlu SH (2004) Synthesis and polymerization of the bromoacrylated plant oil triglycerides to rigid, flame-retardant polymers. J Appl Polym Sci 91:2700–2710. doi: 10.1002/app.13471

Ergan BT, Bayramoğlu M, Özcan S (2015) Emulsion polymerization of styrene under continuous microwave irradiation. Eur Polym J 69:374–384. doi: 10.1016/j.eurpolymj.2015.06.021

Falbe J (ed) (1987) Surfactants in consumer products. Springer Berlin Heidelberg, Berlin

Feng J, Zhuo R-X, Zhang X-Z (2012) Construction of functional aliphatic polycarbonates for biomedical applications. Prog Polym Sci 37:211–236. doi: 10.1016/j.progpolymsci.2011.07.008

Fernandez AM, Conde A (1983) Monomer reactivity ratios of tung oil and styrene in copolymerization. In: Jr CEC, Sperling LH (eds) Polymer applications of renewable-resource materials. Springer US, pp 289–302

Fonseca GE, Dubé MA, Penlidis A (2009) A critical overview of sensors for monitoring polymerizations. Macromol React Eng 3:327–373. doi: 10.1002/mren.200900024

Frauendorfer E, Wolf A, Hergeth W-D (2010) Polymerization online monitoring. Chem Eng Technol 33:1767–1778. doi: 10.1002/ceat.201000265

Galbis JA, de Gracia Garcia-Martin M, Violante de Paz M, Galbis E (2016) Synthetic Polymers from Sugar-Based Monomers. Chem Rev 116:1600–1636. doi: 10.1021/acs.chemrev.5b00242

Galbis JA, García-Martín MG (2008) Chapter 5 - Sugars as Monomers A2 - Belgacem, Mohamed Naceur. In: Gandini A (ed) Monomers, Polymers and Composites from Renewable Resources. Elsevier, Amsterdam, pp 89–114

Garg DK, Serra CA, Hoarau Y, et al (2014) Analytical solution of free radical polymerization: applications-implementing nonisothermal effect. Macromolecules 47:8514–8523. doi: 10.1021/ma501964h

Gesthuisen R, Krämer S, Niggemann G, et al (2005) Determining the best reaction calorimetry technique: theoretical development. Comput Chem Eng 29:349–365. doi: 10.1016/j.compchemeng.2004.10.009

Giovannoli C, Passini C, Anfossi L, et al (2015) Comparison of binding behavior for molecularly imprinted polymers prepared by hierarchical imprinting or pickering emulsion polymerization. J Sep Sci 38:3661–3668. doi: 10.1002/jssc.201500511

Global Market Insights (2016) Alkyl polyglucosides (APG) biosurfactants biosurfactants market size. https://www.gminsights.com/industry-analysis/alkyl-polyglucosides-apg-biosurfactants-market. Accessed 7 Sep 2016

Goikoetxea M, Heijungs R, Barandiaran MJ, Asua JM (2008) Energy efficient emulsion polymerization strategies. Macromol React Eng 2:90–98. doi: 10.1002/mren.200700042

Government of Canada E and CCC (2010) Environment and climate change Canada - environmental indicators - air pollutant emissions. https://www.ec.gc.ca/indicateurs-indicators/default.asp?lang=en&n=E79F4C12-1. Accessed 28 Jun 2016

Grand View Research (2016) Emulsion polymer market size and share (industry report 2022). http://www.grandviewresearch.com/industry-analysis/emulsion-polymer-market. Accessed 4 Jul 2016

Green EM (2011) Fermentative production of butanol—the industrial perspective. Curr Opin Biotechnol 22:337–343. doi: 10.1016/j.copbio.2011.02.004

Gultekin M, Beker U, Güner FS, et al (2000) Styrenation of castor oil and linseed oil by macromer method. Macromol Mater Eng 283:15–20. doi: 10.1002/1439-2054(20001101)283:1<15::AID-MAME15>3.0.CO;2-I

Guzman D de (2012) Bio-acrylic acid on the way. In: Green Chem. Blog. http://greenchemicalsblog.com/2012/09/01/5060/. Accessed 17 Aug 2016

Guzman D de (2013) Bio-MMA development expands. In: Green Chem. Blog. http://greenchemicalsblog.com/2013/03/14/bio-mma-development-expands/. Accessed 17 Aug 2016

H. Surburg JP B. Kurt, J. (2006) Common fragrance and flavor materials. In: Common fragrance and flavor materials. WILEY-VCH, Weinheim, p 52

Heider L, Storck G, Weintz H-J (1992) Preparation of polymers from olefinically unsaturated monomers. US Patent 5,087,676, 11 Feb 1992

Heinze C, Botsch F, Wolff H (1981) Process and device for continuously treating with gases aqueous dispersions of polyvinyl chloride. US Patent 4,301,275, 17 Nov 1981

Henna PH, Andjelkovic DD, Kundu PP, Larock RC (2007) Biobased thermosets from the free-radical copolymerization of conjugated linseed oil. J Appl Polym Sci 104:979–985. doi: 10.1002/app.25788

Hernandez S, Vigueras E (2013) Acrylated-epoxidized soybean oil-based polymers and their use in the generation of electrically conductive polymer composites. In: El-Shemy H (ed) Soybean- bio- active compounds. InTech, pp 231-263

Hill K (2010) Surfactants based on carbohydrates and proteins for consumer products and technical applications. In: Kjellin M, Johansson I (eds) Surfactants from renewable resources. John Wiley & Sons, Ltd, pp 63–84

Holmberg K (2003) Novel surfactants: preparation, applications, and biodegradability, 2nd ed., and expanded.. MDekker, New York

Horrillo-Martínez P, Virolleaud M-A, Jaekel C (2010) Selective Palladium-Catalyzed Dehydrogenation of Limonene to Dimethylstyrene. ChemCatChem 2:175–181. doi: 10.1002/cctc.200900200

Hoydonckx HE, Vos DED, Chavan SA, Jacobs PA (2004) Esterification and transesterification of renewable chemicals. Top Catal 27:83–96. doi: 10.1023/B:TOCA.0000013543.96438.1a

Hua H, Dubé MA (2002) In-Line Monitoring of Emulsion Homo- and Copolymerizations Using Atr-Ftir Spectrometry. Polym React Eng 10:21–39. doi: 10.1081/PRE-120002903

Humme G, Plato H, Ott K-H, et al (1983) Process for the removal of residual monomers from ABS polymers. US Patent 4,399,273, 16 Aug 1983

Iio K, Kobayashi K, Matsunaga M (2007) Radical polymerization of allyl alcohol and allyl acetate. Polym Adv Technol 18:953–958. doi: 10.1002/pat.870

Inamuddin M Ali, (2012) Green solvents. I, Properties and application in chemistry. Springer, New York

Ingram AR, Zupanc AJ, Nicholson HL (1967) Expandable styrene polymers. US Patent 3,359,219, 19 Dec 1967

Jovanović R, Dubé MA (2004) Emulsion-based pressure-sensitive adhesives: A review. J Macromol Sci Part C 44:1–51. doi: 10.1081/MC-120027933

Klima R, Pippin WH, Natale M, et al (2000) Alkylpolyglycoside containing surfactant blends for emulsion polymerization. US Patent 6,117,934, 12 Sep 2000

Korkut I, Bayramoglu M (2014) Various aspects of ultrasound assisted emulsion polymerization process. Ultrason Sonochem 21:1592–1599. doi: 10.1016/j.ultsonch.2013.12.028

Kovačič S, Matsko NB, Jerabek K, et al (2012) On the mechanical properties of HIPE templated macroporous poly(dicyclopentadiene) prepared with low surfactant amounts. J Mater Chem A 1:487–490. doi: 10.1039/C2TA00546H

Kronberg B, Holmberg K, Lindman B (2014) Environmental and health aspects of surfactants. In: Surface chemistry of surfactants and polymers. John Wiley & Sons, Ltd, pp 49–64

Kundu PP, Larock RC (2005) Novel conjugated linseed oil-styrene-divinylbenzene copolymers prepared by thermal polymerization. 1. Effect of monomer concentration on the structure and properties. Biomacromolecules 6:797–806. doi: 10.1021/bm049429z

Laist DW (1997) Impacts of Marine Debris: Entanglement of Marine Life in Marine Debris Including a Comprehensive List of Species with Entanglement and Ingestion Records. In: Coe JM, Rogers DB (eds) Marine Debris. Springer New York, pp 99–139

Lamb DJ, Fellows CM, Morrison BR, Gilbert RG (2005) A critical evaluation of reaction calorimetry for the study of emulsion polymerization systems: Thermodynamic and kinetic aspects. Polymer 46:285–294. doi: 10.1016/j.polymer.2004.11.026

Lan Z, Daga R, Whitehouse R, et al (2014) Structure–properties relations in flexible polyurethane foams containing a novel bio-based crosslinker. Polymer 55:2635–2644. doi: 10.1016/j.polymer.2014.03.061

Lavilla C, Alla A, de Ilarduya AM, et al (2012a) Carbohydrate-based copolyesters made from bicyclic acetalized galactaric acid. J Polym Sci Part Polym Chem 50:1591–1604. doi: 10.1002/pola.25930

Lavilla C, Alla A, Martínez de Ilarduya A, et al (2012b) Bio-based poly(butylene terephthalate) copolyesters containing bicyclic diacetalized galactitol and galactaric acid: Influence of composition on properties. Polymer 53:3432–3445. doi: 10.1016/j.polymer.2012.05.048

Lazaridis N, Alexopoulos AH, Kiparissides C (2001) Semi-batch emulsion copolymerization of vinyl acetate and butyl acrylate using oligomeric nonionic surfactants. Macromol Chem Phys 202:2614–2622. doi: 10.1002/1521-3935(20010801)202:123.0.CO;2-E

Leggat PA, Kedjarune U (2003) Toxicity of methyl methacrylate in dentistry. Int Dent J 53:126–131. doi: 10.1111/j.1875-595X.2003.tb00736.x

Li A-L, Wang X-Y, Liang H, Lu J (2007) Controlled radical copolymerization of β-pinene and n-butyl acrylate. React Funct Polym 67:481–488. doi: 10.1016/j.reactfunctpolym.2007.03.002

Li A-L, Wang Y, Liang H, Lu J (2006) Controlled radical copolymerization of β-pinene and acrylonitrile. J Polym Sci Part Polym Chem 44:2376–2387. doi: 10.1002/pola.21316

Li FK, Larock RC (2003) Synthesis, structure and properties of new tung oil-styrene-divinylbenzene copolymers prepared by thermal polymerization. Biomacromolecules 4:1018–1025. doi: 10.1021/bm034049j

Lincoln DE, Lawrence BM (1984) The volatile constituents of camphorweed, heterotheca subaxillaris. Phytochemistry 23:933–934. doi: 10.1016/S0031-9422(00)85073-6

Liu J, Tai H, Howdle SM (2005) Precipitation polymerisation of vinylidene fluoride in supercritical CO2 and real-time calorimetric monitoring. Polymer 46:1467–1472. doi: 10.1016/j.polymer.2004.12.015

Liu Y, Tüysüz H, Jia C-J, et al (2010) From glycerol to allyl alcohol : iron oxide catalyzed dehydration and consecutive hydrogen transfer. Chem Commun 46:1238–1240. doi: 10.1039/B921648K

Liwarska-Bizukojc E, Miksch K, Malachowska-Jutsz A, Kalka J (2005) Acute toxicity and genotoxicity of five selected anionic and nonionic surfactants. Chemosphere 58:1249–1253. doi: 10.1016/j.chemosphere.2004.10.031

Ma S, Jiang Y, Liu X, et al (2014) Bio-based tetrafunctional crosslink agent from gallic acid and its enhanced soybean oil-based UV-cured coatings with high performance. RSC Adv 4:23036. doi: 10.1039/c4ra01311e

Mah S, Koo D, Jeon H, Kwon S (2002) Photo-induced emulsion polymerization of vinyl acetate in the presence of poly(oxyethylene)10 nonyl phenyl ether ammonium sulfate, an anionic emulsifier (I). J Appl Polym Sci 84:2425–2431. doi: 10.1002/app.10531

Markets and Markets (2016) Sucrose esters market by application, form, region - 2020. http://www.marketsandmarkets.com/Market-Reports/sucrose-esters-market-191170937.html. Accessed 12 Sep 2016

Maślińska-solich J, Kupka T, Kluczka M, Solich A (1994) Optically active polymers, 2. Copolymerization of limonene with maleic anhydride. Macromol Chem Phys 195:1843–1850. doi: 10.1002/macp.1994.021950531

Mathers RT, Damodaran K (2007) Renewable chain transfer agents for metallocene polymerizations: The effects of chiral monoterpenes on the polyolefin molecular weight and isotacticity. J Polym Sci Part -Polym Chem 45:3150–3165. doi: 10.1002/pola.22111

Mathers RT, McMahon KC, Damodaran K, et al (2006) Ring-opening metathesis polymerizations in d-limonene: A renewable polymerization solvent and chain

transfer agent for the synthesis of alkene macromonomers. Macromolecules 39:8982–8986. doi: 10.1021/ma061699h

Maver TL, Krasnansky R (2001) Aqueous coating composition with improved block resistance containing alkyl polyglycoside surfactant mixtures. US Patent 6,117,934, 12 Sep 2000

Milstein N (1992) Improved esterification of oxyhydrocarbon polyols and ethers thereof, and products therefrom. WO Patent 1,992,000,947, 23 Jan 1992

Minematsu H, Matsumoto K, Saeki T, Kishi A (1981) Low residual monomer α-methylstyrene-acrylonitrile copolymers and ABS blends therefrom. US Patent 4,294,946, 13 Oct 1981

Miranda LN, Ford WT (2005) Binary copolymer reactivity of tert-butyl methacrylate, 2-(N,N-dimethylamino)ethyl methacrylate, solketal methacrylate, and 2-bromoethyl methacrylate. J Polym Sci Part Polym Chem 43:4666–4669. doi: 10.1002/pola.20939

Mollet H, Grubenmann A (2000) Emulsions – Properties and production. In: Formulation Technology. Wiley-VCH Verlag GmbH, pp 59–104

Morgan AB, Gilman JW (2013) An overview of flame retardancy of polymeric materials: application, technology, and future directions. Fire Mater 37:259–279. doi: 10.1002/fam.2128

Nagasuna K, Namba T, Miyake K, et al (1990) Production process for water-absorbent resin. US Patent 4.973,362, 27 Nov 1990

Nomura Y, Teshima W, Kawahara T, et al (2006) Genotoxicity of dental resin polymerization initiators in vitro. J Mater Sci Mater Med 17:29–32. doi: 10.1007/s10856-006-6326-2

Odian G (2004) Principles of polymerization. John Wiley & Sons, Inc., New Jersey

Oka T, Tsubota K, Shinjo T, et al (1999) Process for preparing solvent-type acrylic pressure-sensitive adhesives and medical pressure-sensitive adhesive. US Patent 5,886,122, 26 May1996

Oprea S (2009) Synthesis and Properties of Polyurethane Elastomers with Castor Oil as Crosslinker. J Am Oil Chem Soc 87:313–320. doi: 10.1007/s11746-009-1501-5

Osipow L, Snell FD, York WC, Finchler A (1956) Methods of preparation fatty acid esters of sucrose. Ind Eng Chem 48:1459–1462. doi: 10.1021/ie51400a026

Parker KJ, Khan RA, Mufti KS (1976) Process of making sucrose esters. US Patent 3,996,206, 7 Dec 1976

Paz-Pazos M, Pugh C (2006) Synthesis of optically active copolymers of 2,3,4,5,6-pentafluorostyrene and β-pinene with low surface energies. J Polym Sci Part Polym Chem 44:3114–3124. doi: 10.1002/pola.21392

Pelletier H, Belgacem N, Gandini A (2006) Acrylated vegetable oils as photocrosslinkable materials. J Appl Polym Sci 99:3218–3221. doi: 10.1002/app.22322

Pham PD, Monge S, Lapinte V, et al (2013) Various radical polymerizations of glycerol-based monomers. Eur J Lipid Sci Technol 115:28–40. doi: 10.1002/ejlt.201200202

Pohl K, Rodriguez F (1981) Adiabatic polymerization of acrylamide using a persulfate–bisulfite redox couple. J Appl Polym Sci 26:611–618. doi: 10.1002/app.1981.070260220

Poljanšek I, Fabjan E, Burja K, Kukanja D (2013) Emulsion copolymerization of vinyl acetate-ethylene in high pressure reactor-characterization by inline FTIR spectroscopy. Prog Org Coat 76:1798–1804. doi: 10.1016/j.porgcoat.2013.05.019

Ramli RA, Hashim S, Laftah WA (2013) Synthesis, characterization, and morphology study of poly(acrylamide-co-acrylic acid)-grafted-poly(styrene-co-methyl methacrylate) “raspberry”-shape like structure microgels by pre-emulsified semi-batch emulsion polymerization. J Colloid Interface Sci 391:86–94. doi: 10.1016/j.jcis.2012.09.047

Ramos AM, Lobo LS, Bordado JM (1998) Polymers from pine gum components: Radical and coordination homo and copolymerization of pinenes. Macromol Symp 127:43–50. doi: 10.1002/masy.19981270109

Ren S, Trevino E, Dubé MA (2015) Copolymerization of limonene with n-butyl acrylate. Macromol React Eng 9:339–349. doi: 10.1002/mren.201400068

Reuben F, Theodore W, Hampden Z (1973) Process for the production of sucrose esters of fatty acids. US Patent 3,714,144, 30 Jan1973

Reyes-Mercado Y, Vázquez F, Rodríguez-Gómez FJ, Duda Y (2008) Effect of the acrylic acid content on the permeability and water uptake of poly(styrene-co-butyl acrylate) latex films. Colloid Polym Sci 286:603–609. doi: 10.1007/s00396-008-1838-6

Rincón FD, Esposito M, de Araújo PHH, et al (2014) Robust calorimetric estimation of semi-continuous and batch emulsion polymerization systems with covariance estimation. Macromol React Eng 8:456–466. doi: 10.1002/mren.201300151

Rincón FD, Esposito M, de Araújo PHH, et al (2013) Calorimetric estimation employing the unscented kalman filter for a batch emulsion polymerization reactor. Macromol React Eng 7:24–35. doi: 10.1002/mren.201200044

Roberge S, Dubé MA (2016a) Bulk terpolymerization of conjugated linoleic acid with styrene and butyl acrylate. ACS Sustain Chem Eng 4:264–272. doi: 10.1021/acssuschemeng.5b01106

Roberge S, Dubé MA (2016b) Emulsion-based pressure sensitive adhesives from conjugated linoleic acid/styrene/butyl acrylate terpolymers. Int J Adhes Adhes 70:17–25. doi: 10.1016/j.ijadhadh.2016.05.003

Roberge S, Dubé MA (2016c) Infrared process monitoring of conjugated linoleic acid/styrene/butyl acrylate bulk and emulsion terpolymerization. J Appl Polym Sci 133:n/a-n/a. doi: 10.1002/app.43574

Roberts W, Day A (1950) A study of the polymerization of alpha-pinene and beta-pinene with friedel crafts type catalysts. J Am Chem Soc 72:1226–1230. doi: 10.1021/ja01159a044

Roice M, Pillai VNR (2005) Poly(styrene-co-glycerol dimethacrylate): Synthesis, characterization, and application as a resin for gel-phase peptide synthesis. J Polym Sci Part Polym Chem 43:4382–4392. doi: 10.1002/pola.20917

Rybinski W von, Hill K (1998) Alkyl polyglycosides—properties and applications of a new class of surfactants. Angew Chem Int Ed 37:1328–1345. doi: 10.1002/(SICI)1521-3773(19980605)37:103.0.CO;2-9

Salehpour S, Dubé MA (2011) Towards the sustainable production of higher-molecular-weight polyglycerol. Macromol Chem Phys 212:1284–1293. doi: 10.1002/macp.201100064

Schull V, Arnoldi D (1998) Method of producing non-vitrified processing aid low in residual monomers for thermoplastic polymers. US Patent 5,767,231, 16 Jun 1998

Sharma S, Srivastava A (2004) Synthesis and characterization of copolymers of limonene with styrene initiated by azobisisobutyronitrile. Eur Polym J 40:2235–2240. doi: 10.1016/j.eurpolymj.2004.02.028

Sharma S, Srivastava A (2003) Radical copolymerization of limonene with acrylonitrile: Kinetics and mechanism. Polym-Plast Technol Eng 42:485–502. doi: 10.1081/PPT-120017966

Sharma S, Srivastava AK (2007) Azobisisobutyronitrile-initiated free-radical copolymerization of limonene with vinyl acetate: Synthesis and characterization. J Appl Polym Sci 106:2689–2695. doi: 10.1002/app.24205

Silverstein MS (2014) Emulsion-templated porous polymers: A retrospective perspective. Polymer 55:304–320. doi: 10.1016/j.polymer.2013.08.068

Silvestre AJD, Gandini A (2008) Terpenes: Major sources, properties and applications. In: Gandini A (ed) Monomers, Polymers and composites from renewable resources. Elsevier, Amsterdam, pp 17–38

Singh A, Kamal M (2012) Synthesis and characterization of polylimonene: Polymer of an optically active terpene. J Appl Polym Sci 125:1456–1459. doi: 10.1002/app.36250

Stockburger GJ (1981) Process for preparing sorbitan esters. US Patent 4,297,290, 27 Oct 1981

Supanchaiyamat N, Shuttleworth PS, Hunt AJ, et al (2012) Thermosetting resin based on epoxidised linseed oil and bio-derived crosslinker. Green Chem 14:1759–1765. doi: 10.1039/C2GC35154D

Thickett SC, Gilbert RG (2007) Emulsion polymerization: State of the art in kinetics and mechanisms. Polymer 48:6965–6991. doi: 10.1016/j.polymer.2007.09.031

Thomson RAM (1986) A kinetic study of the adiabatic polymerization of acrylamide. J Chem Educ 63:362. doi: 10.1021/ed063p362

Tonoyan AO, Leikin AD, Davtyan SP, et al (1973) Kinetics of the adiabatic polymerization of methyl methacrylate. Polym Sci USSR 15:2080–2085. doi: 10.1016/0032-3950(73)90424-3

Turro NJ, Chow M-F, Chung C-J, Tung C-H (1980) An efficient, high conversion photoinduced emulsion polymerization. Magnetic field effects on polymerization efficiency and polymer molecular weight. J Am Chem Soc 102:7391–7393. doi: 10.1021/ja00544a053

United Nations (2016) The Paris Agreement. http://unfccc.int/paris_agreement/items/9485.php. Accessed 8 Oct 2016

United State Department of Agriculture (2016) Oilseeds: World markets and trade. http://www.fas.usda.gov/data/oilseeds-world-markets-and-trade. Accessed 4 Aug 2016

University of Minnesota (2011) Biological pathways produce isobutyric acid using renewable resources. http://license.umn.edu/technologies/20110077_biological-pathways-produce-isobutyric-acid-using-renewable-resources. Accessed 22 Aug 2016

US Department of Commerce (2014) The NOAA Annual Greehouse Gas Index (AGGI). http://www.esrl.noaa.gov/gmd/aggi/. Accessed 4 Jul 2016

Vendamme R, Schüwer N, Eevers W (2014) Recent synthetic approaches and emerging bio-inspired strategies for the development of sustainable pressure-sensitive adhesives derived from renewable building blocks. J Appl Polym Sci. doi: 10.1002/app.40669

Vicente M, BenAmor S, Gugliotta LM, et al (2001) Control of molecular weight distribution in emulsion polymerization using on-line reaction calorimetry. Ind Eng Chem Res 40:218–227. doi: 10.1021/ie000387e

Vieira RAM, Sayer C, Lima EL, Pinto JC (2002) In-line and in situ monitoring of semi-batch emulsion copolymerizations using near-infrared spectroscopy. J Appl Polym Sci 84:2670–2682. doi: 10.1002/app.10434

Vijitha K, Dhanya K, Francis B, et al (2009) Synthesis and characterization of glycerol dimethacrylate-4-vinyl pyrrole. Asian J Chem 21:6811–6818

Wan T, Zang T, Wang Y, et al (2010) Preparation of water soluble Am–AA–SSS copolymers by inverse microemulsion polymerization. Polym Bull 65:565–576. doi: 10.1007/s00289-009-0234-9

Wang S (2013) Redox-initiated adiabatic emulsion polymerization. Dissertation, Lehigh University

Wang S, Daniels ES, Sudol ED, et al (2016) Isothermal emulsion polymerization of n-butyl methacrylate with KPS and redox initiators: Kinetic study at different surfactant/initiator concentrations and reaction temperature. J Appl Polym Sci 133:43037. doi: 10.1002/app.43037

Wang W, Griffiths RMT, Giles MR, et al (2003) Monitoring dispersion polymerisations of methyl methacrylate in supercritical carbon dioxide. Eur Polym J 39:423–428. doi: 10.1016/S0014-3057(02)00249-5

Wang Y, Li A-L, Liang H, Lu J (2006) Reversible addition–fragmentation chain transfer radical copolymerization of β-pinene and methyl acrylate. Eur Polym J 42:2695–2702. doi: 10.1016/j.eurpolymj.2006.06.015

Wilbon PA, Chu F, Tang C (2013) Progress in renewable polymers from natural terpenes, terpenoids, and rosin. Macromol Rapid Commun 34:8–37. doi: 10.1002/marc.201200513

Williams CK, Hillmyer MA (2008) Polymers from renewable resources: A perspective for a special issue of polymer reviews. Polym Rev 48:1–10. doi: 10.1080/15583720701834133

Wool RP, Bunker SP (2003) Pressure sensitive adhesives from plant oils. US Patent 6,646,033, 11 Nov 2003

Worldwatch Institute (2015) Global Plastic Production Rises, Recycling Lags. http://www.worldwatch.org/global-plastic-production-rises-recycling-lags-0. Accessed 19 Jul 2016

Wu J, Eduard P, Thiyagarajan S, et al (2012) Semicrystalline polyesters based on a novel renewable building block. Macromolecules 45:5069–5080. doi: 10.1021/ma300782h

Xia H, Wang Q, Qiu G (2003) Polymer-Encapsulated Carbon Nanotubes Prepared through Ultrasonically Initiated In Situ Emulsion Polymerization. Chem Mater 15:3879–3886. doi: 10.1021/cm0341890

Xu X, LIN J, CEN P (2006) Advances in the research and development of acrylic acid production from biomass. Chin J Chem Eng 14:419–427. doi: 10.1016/S1004-9541(06)60094-3

Yamamoto D, Matsumoto A (2012) Penultimate unit and solvent effects on 2:1 sequence control during radical copolymerization of n-phenylmaleimide with β-pinene. Macromol Chem Phys 213:2479–2485. doi: 10.1002/macp.201200421

Yao F, Yan G-C, Xu L-Q, et al (2014) Hairy fluorescent nanoparticles from one-pot click chemistry and atom transfer radical emulsion polymerization. Polym Int 63:237–243. doi: 10.1002/pi.4491

Zecha H (1981) Stabilization of colloidal dispersions by polymer adsorption. Acta Polym 32:582–582. doi: 10.1002/actp.1981.010320915

Zhang C, Yan M, Cochran EW, Kessler MR (2015) Biorenewable polymers based on acrylated epoxidized soybean oil and methacrylated vanillin. Mater Today Commun 5:18–22. doi: 10.1016/j.mtcomm.2015.09.003

Zhang H, Grinstaff MW (2014) Recent advances in glycerol polymers: chemistry and biomedical applications. Macromol Rapid Commun 35:1906–1924. doi: 10.1002/marc.201400389

Zhang Y (2014) Copolymerization of Limonene. Dissertation, University of Ottawa

Zhang Y, Dubé MA (2014a) Copolymerization of n-butyl methacrylate and d-limonene. Macromol React Eng 8:805–812. doi: 10.1002/mren.201400023

Zhang Y, Dubé MA (2014b) Copolymerization of 2-ethylhexyl acrylate and d-limonene. Polym Plast Technol Eng 54:499. doi: 10.1080/03602559.2014.961080

Zhang Y, Li T, Jin Z, et al (2007) Synthesis of nanoiron by microemulsion with Span/Tween as mixed surfactants for reduction of nitrate in water. Front Environ Sci Eng China 1:466–470. doi: 10.1007/s11783-007-0074-5

Zhu X, Chen J, Cheng Z, et al (2003) Emulsion polymerization of styrene under pulsed microwave irradiation. J Appl Polym Sci 89:28–35. doi: 10.1002/app.12089

Zondlo M (2002) Final report on the safety assessment of acrylates copolymer and 33 related cosmetic ingredients. Int J Toxicol 21 Suppl 3:1–50. doi: 10.1080/10915810290169800

4. Starch Nanoparticle Incorporation in Latex-based Adhesives

Chapter 4 contains a manuscript published in the European Polymer Journal on July 14, 2018.

Starch Nanoparticle Incorporation in Latex-based Adhesives

Yujie Zhang, Michael F. Cunningham, Niels M.B. Smeets, Marc A. Dubé*,

_____

Y. Zhang, Prof. M.A. Dubé*

Department of Chemical and Biological Engineering,

Centre for Catalysis Research and Innovation,

University of Ottawa, 161 Louis Pasteur Pvt.,

Ottawa, Ontario, K1N 6N5, Canada

Prof. M.F. Cunningham

Department of Chemical Engineering,

Queen's University, 9 University Ave,

Kingston, Ontario, K7L 3N6, Canada

Dr. N.M.B. Smeets

EcoSynthetix Inc.,

3365 Mainway,

Burlington, Ontario, L7M 1A6, Canada

_____

Abstract

Starch nanoparticles (SNPs) are chosen as renewable alternatives to partially replace petroleum-based monomers and produce bio-based latexes for adhesive applications. To maintain adhesive performance, SNPs are modified (i.e., via increasing cross-link density, vinyl functionalization, and adjusting hydrophilic/hydrophobic balance) to facilitate their incorporation into the latex particles. The modified SNPs are then polymerized in a semi-batch emulsion polymerization at 60 °C, and yield low viscosity latexes with up to 17 wt.% SNP loading and 42 wt.% solids. TEM/STEM imaging is performed and reveals the presence of a core-shell particle morphology. This is supported by comparing the adhesive properties of SNP-containing latex films from an *in situ* preparation vs. a blend of acrylic latex with SNPs. The results suggest that the modified SNPs were largely encapsulated into the latex particles rather than in the aqueous phase or at the latex particle/water interface.

Keywords: adhesives, bio-sourced materials, emulsion polymerization, nanoparticles, polymer modification, renewable materials, starch

Introduction

The use of renewable feedstocks in polymer formulations has drawn increasing attention among researchers and industry, as it is an important part of sustainable polymer product development.[1–3] Despite the availability of numerous renewable building blocks, polymer products made from renewable feedstocks often result in significant performance property changes.[3–6] Nevertheless, it is indeed possible to achieve comparable or even better properties when advanced polymer chemistry and engineering techniques are applied.[1,3,7]

Starch is a polysaccharide existing in many plants (e.g., potato, wheat, corn) and is non-toxic, biodegradable, low-cost and abundant.[8–10] Native starch consists of two macromolecules: amylose, which contains mostly linear α-D-(1→4)-glucan units and amylopectin, which is composed of branched α-D-(1→4)-glucan with α-D-(1→6) linkages at the branch points.[11] Depending on the source of starch, the amylose and amylopectin composition varies; for instance, corn starch contains about 0-70 wt.% amylose, while amylose content in potato starch ranges from 12-20 wt.%.[9,12,13] Starch molecules are densely packed in semi-crystalline granules, which may have various sizes (diameter from 1-100 μm), size distribution (e.g., mono-, bi- or tri-modal distribution), and shapes (e.g., spherical, plate).[10,14] To date, starch has been widely used in the food industry, in paper coatings, adhesives and biomedical applications.[8,15]

Recently, developed starch morphologies such as starch nanocrystals and starch nanoparticles (SNPs) have the potential to open pathways towards materials with new

and exciting properties.[9,16–18] SNPs with varying properties, such as shape and crystallinity, can be produced via hydrolysis of native starch using acids or enzymes, as well as physical treatments (e.g., reactive extrusion, ultrasonication and irradiation).[14,16,17] Various modification methods (e.g., cross-linking, hydrophobization, anionic/cationic charging, vinyl functionalization) can be performed on SNP surfaces to tune the hydrophobicity of SNPs, introduce functional groups and alter their behavior.[17,19–21]

SNPs have been applied in composite materials as nano-fillers to improve mechanical and barrier properties,[22] as stabilizers for emulsion systems,[23,24] as drug delivery carriers,[25,26] or as binders in paper.[14] In addition, SNPs can be grafted with vinyl or acrylic monomers (e.g., butadiene, methyl methacrylate), as well as some polymers, to enhance their compatibility with hydrophobic matter.[25,27,28] More recently, SNPs modified with functional groups were used as Pickering stabilizers and/or monomers in emulsion polymerization to make starch-based latexes.[29–32] Pei et al. showed that latexes could be prepared with only up to 9 wt.% SNP loading (based on total polymer mass) and with relatively low solids (6-10 wt.%) due to compatibility issues between the hydrophilic starch and hydrophobic synthetic polymers.[29,30] In our previous work, various grades of SNPs with loadings as high as 50 wt.% (based on total polymer mass) were used to produce stable latexes, but the challenge remains to completely incorporate the SNPs into the latex particles.[32] In the present context, incorporation refers to SNPs that are encapsulated or chemically bound to acrylic polymer as opposed to free SNPs or starch molecules in solution.

SNPs were chosen to replace petroleum-based monomers to produce SNP-containing latexes for adhesive applications. Due to their hydrophilic nature, SNPs tend to reside in the water phase or, less likely, at the particle-water interface. Thus, to maintain the adhesive properties of an acrylic latex film, one would prefer to have the SNPs well incorporated into the latex. In other words, unless the SNPs are encapsulated in the particle cores by acrylic polymer, or at least partially covered with the acrylic polymer, the SNPs will interfere with adhesion to a substrate.[33,34] To achieve this, we modified the SNPs to promote their incorporation into latex particles. We are exploring three potential levers to improve compatibility between the hydrophilic SNPs and the hydrophobic vinyl monomers: i) cross-linking, followed by ii) attachment of vinyl groups to the SNP surfaces, and subsequent iii) polymerization of a "tie-layer" of a moderately hydrophilic monomer to the SNP surfaces. Sodium trimetaphosphate (STMP) was chosen as a non-reversible cross-linker as it is nontoxic and commonly used in the food industry to produce starch phosphates.[35–37] A functionalized sugar-based monomer (FSM), was used as a source of vinyl groups to attach to the SNP surfaces. The FSM provides an additional bio-based component added to the latex formulation. In addition, the FSM shows a very low tendency to homopolymerize but reacts more readily with other vinyl monomers.[38,39] Butyl vinyl ether (BVE) monomer was then added as a "tie-layer" monomer, because it has an appreciable water solubility compared to other hydrophobic monomers, and is prone to copolymerize with other monomers rather than homopolymerize.[40–42] The "tie-layer" monomer is expected to act as a bridge between the SNPs and the other more hydrophobic monomers. The cross-linked and functionalized SNP cores were then

incorporated in a semi-batch emulsion polymerization to produce stable SNP-based latexes for adhesive applications.

Experimental Section

Materials

Experimental grade SNPs and functionalized sugar monomer (FSM) were supplied by EcoSynthetix Inc. (Burlington, ON). Sodium trimetaphosphate (STMP) was used as cross-linker, sodium bicarbonate ($NaHCO_3$) was used as buffer, and 1 M hydrochloric acid (HCl) and sodium hydroxide (NaOH) pellets were used to adjust pH. FSM was used to functionalize the SNPs. Butyl acrylate (BA, 99%), methyl methacrylate (MMA, 99%) and acrylic acid (AA, 99.5%) were used as the main monomers, butyl vinyl ether (BVE) as a "tie-layer" monomer, potassium persulfate (KPS, 99%) as initiator, EF-800 (49-51 wt.% aqueous solution) as surfactant, and hydroquinone (HQ) as inhibitor. All of the chemicals above were purchased from Sigma-Aldrich, with the exception of EF-800, which was provided by Cytec Industries. Distilled deionized water (DDW) was used throughout this project. BA was purified using an inhibitor removal column, and all other chemicals were used as received. Nitrogen gas (GR4.8, Linde Canada) was used to purge the reactor to remove oxygen.

Increase Cross-link Density of the SNPs

All SNP modifications and subsequent polymerizations were conducted in a 500 mL RC1e glass reactor (Mettler-Toledo) equipped with a Hastelloy stirrer set, two semi-batch

feeding pumps, a pH probe and an inlet for nitrogen sparging. To begin, the cross-linking of SNPs with STMP was conducted using an aqueous solution reaction as described in the literature.[37,43,44] SNPs were dispersed in DDW while mixing (300 rpm) and heating to a desired temperature (25-60 ^{o}C). Once the SNPs were fully dispersed and the temperature set point was reached, $NaHCO_3$ was added to the dispersion and the pH of the solution was adjusted to different target values using NaOH and HCl solutions prior to the addition of the STMP cross-linker. After a desired reaction time (0-8 h), the cross-linking reaction was stopped by adjusting the pH of the reaction mixture to 6.5 using the HCl solution. The solution was then cooled to room temperature and characterized. A series of experiments were conducted to tune the cross-linking reaction conditions (Table 4.1).

Table 4.1 SNP cross-linking reaction conditions.

Run	STMP (wt.%)	$NaHCO_3$ (wt.%)	pH
1.1	0.1	1	10
1.2	1	1	10
1.3	0.1	3	10
1.4	1	3	10
1.5	0.1	1	11
1.6	1	1	11
1.7	0.1	3	11
1.8	1	3	11

Functionalization of SNPs

Functionalized sugar-based monomer (FSM) was used to functionalize the cross-linked SNPs. FSM is a proprietary water-soluble macromonomer, and contains glucose (hydroxyl groups) and polymerizable double bonds (maleic acid end groups) in its structure. The

FSM was chemically bound to the SNP hydroxyl groups as an added step in the STMP crosslinking procedure, prior to the final pH adjustment. The FSM was added to the cross-linked SNPs and reacted for an additional hour, and then the pH was adjusted to 6.5. This approach, allowed the FSM to be added directly to the SNP dispersion immediately after the cross-linking reaction with no additional processing required.

Synthesis of SNP-based Latexes

The cross-linked/functionalized SNPs were added to a standard semi-batch emulsion polymerization formulation at a 15 wt.% SNP loading (relative to total polymer weight) and 40 wt.% solids content (Table 4.2). The polymerization process started with the preparation of the cross-linked and functionalized SNPs as per the procedure outlined below (Table 4.2: initial charge). During the heating process, the reactor was purged with nitrogen for 30 min. Next, an initial initiator charge was added to the reactor. In cases where a BVE “tie-layer” was introduced to the formulation, the BVE was added to the initial initiator charge and the reaction held for 30 min. Finally, a monomer pre-emulsion and initiator aqueous solution were fed to the reactor. The monomer pre-emulsion was fed at a constant rate over a period of 210 min, while the initiator solution was fed over a period of 240 min. After semi-batch feeding, the reaction was cooled to 25 °C and the reaction mixture was stored in a polystyrene container for subsequent characterization. Throughout the polymerization, latex samples were taken periodically to measure conversion and particle size; HQ solution (0.1~0.2 g of 1 wt.% solution) was added to each sample to quench the polymerization.

Table 4.2 Standard emulsion polymerization formulation.

Component	Amount (g)	(phm[a)])
Initial Charge		
SNP	21.0	15.0
DDW	151.2	66.0
$NaHCO_3$[b)]	0.4	0.3
Initial Initiator Charge		
KPS	0.4	0.3
DDW	11.6	8.3
Monomer Pre-Emulsion		
EF-800	5.5	3.9
DDW	27.8	19.9
BA	110.9	79.3
MMA	5.4	3.9
AA	2.5	1.8
Initiator Solution		
KPS	0.9	0.6
DDW	20.0	14.3

[a)] parts per hundred parts monomers (including SNP, BA, MMA and AA); [b)] buffer added only for non-modified SNPs

Characterization

A Brookfield viscometer was used with spindle R4 at 100 rpm to determine the viscosity of the SNP solutions and the final latexes at room temperature. Particle size was measured at room temperature using Dynamic Light Scattering (DLS) with a Malvern NanoS Zetasizer at an angle of 173°. One drop of SNP dispersion was diluted in 2 mL of DDW, and then one drop of diluted solution was diluted again in 2 mL of DDW in a 4 mL polystyrene cuvette. After three measurements, average intensity-weighted particle size was reported.

A Bruker AVANCE-300 spectrometer was used to conduct ^{31}P-NMR to confirm the crosslinking of SNPs; 4096 scans were performed per measurement. About 0.02 g dry SNP samples were dispersed in 1.5 g solvent (deuterium oxide:DDW, 10:90 w:w) for analysis. A Bruker AVANCE-400 ^{1}H-NMR spectrometer was used to detect the presence of vinyl groups in the functionalized SNPs; 32 scans were performed per measurement. Approximately 0.02 g dry SNP samples were dispersed in 1.5 g deuterium oxide for analysis.

A standard gravimetric method was used to measure solids content and conversion. Samples were taken periodically, weighed in an aluminium dish, and then dried in a fume hood at room temperature to constant weight. Solids content was calculated with:

$$wt.\%\ solids = \frac{M_{dp}}{M_I} \quad (1)$$

where M_{dp} is the mass of dry polymer, and M_l is the mass of the latex.

Global (overall) conversion (Equation (2)) was calculated based on the total monomer weight.

$$wt.\%\ global\ conversion = \frac{M_p}{M_{tm}} = \frac{M_{dp} - M_i - M_s - M_b - M_w}{M_{tm}} \quad (2)$$

where M_{tm} is total monomer mass, M_p is polymer mass, M_i is the mass of initiator, M_s is the mass of SNPs, M_b is the mass of buffer and M_w is the mass of DDW.

A FEI Tecnai G2 Spirit Twin Transmission Electron Microscope (TEM) and JEM-2100F FETEM (JEOL) were used to assess particle morphology. Two droplets of latex were diluted in 50 mL DDW. One droplet of the diluted sample was placed on a glow-discharged copper grid. The sample was then dried at room temperature and scanned in the TEM or Scanning Transmission Electron Microscope (STEM).

Tack, peel strength and shear strength of latex films were tested in a temperature- and humidity-controlled room (23 ± 1°C and 50% ± 5% RH) following Pressure Sensitive Tape Council standards (PSTC, 2004). Loop tack and 180^o peel strength were measured using an Instron 3000 Universal Tester, along with Bluehill 2 Materials Testing Software. Shear strength was measured using an in-house built shear tester with Labview software. For tack, a 1″ × 6″ strip of film was used to form a teardrop loop, and the narrow point was masked with tape and clamped by the upper grip of the Instron Tester. The film was lowered at a rate of 1 mm/s until an area of 1″ × 1″ contact with the stainless-steel substrate mounted into the lower grip was achieved; the film was then removed from the substrate at a rate of 300 mm/min. The maximum force (N/m) required to remove the

film was reported as loop tack. For peel strength measurements, a 1” × 5” strip of film was adhered to a stainless-steel substrate lengthwise using a 2040 g roll coater. The end of the strip was masked with tape and clamped by the upper grip, while the substrate was inserted into the lower grip. The sample was peeled off the substrate at a rate of 300 mm/min. The average force (N/m) required to peel the strip from the substrate was reported as peel strength. For shear strength measurements, the film (0.5" x 5") was adhered to the substrate covering an area of 0.5” x 0.5”, and placed in the shear tester using a C-clamp with a 500 g weight attached to the loop of the strip. The time required for the film to fall off the testing panel was recorded as an indicator of shear strength.

Results and Discussions

As noted in the introduction, the direct use of unmodified SNPs leads to challenges in latex stability, low SNP incorporation, and poor adhesive performance.[32] Therefore, the SNPs were modified to facilitate their incorporation into the latex particles. Prior to polymerization, the cross-linking density of SNPs were increased using STMP in aqueous solution, and then functionalized using FSM. Next, the modified SNPs were reacted with BVE, a “tie-layer” monomer. As noted earlier, the “tie-layer” monomer acts as a bridge between SNPs and hydrophobic monomers, making the SNPs more hydrophobic and thus more prone to react with hydrophobic monomers.

Increase Cross-link Density of the SNPs

Increasing cross-linking density of the SNPs with STMP was investigated using ^{31}P-NMR spectroscopy (Figure 4.1). Peak identification is shown in Figure 4.1. where the peaks from 4.6 to 2.8 ppm represent phosphate monoester (P_{me}); the peak from 2.8 to 2.1 ppm corresponds to phosphoric acid (PO_4); the peak at 1.1 to -2.5 ppm represents phosphate diester (P_{de}); the peaks between -5.2 to -6.1 ppm correspond to grafted pyrophosphate (PP_g), the external phosphate of sodium tripolyphosphate (STPP) and grafted sodium tripolyphosphate ($STPP_g$); the peak at -6.1 to -7.1 ppm represents pyrophosphate (PP); the peak between -19.9 to -20.7 ppm represents the internal phosphate of STPP and $STPP_g$; and the peak between -21.4 to -21.8 represents STMP. The presence of peaks P_{de} confirmed the occurrence of the cross-linking reaction.[35,37,45,46] Cross-linking of SNPs (Figure 4.2) starts with the opening of STMP by attacking hydroxyl group on SNPs in the presence of NaOH, which can produce STPP and $STPP_g$. The reaction is then followed by the addition of another hydroxyl group on SNPs to $STPP_g$, which may produce P_{me}, P_{de}, PP, PO_4 and PP_g.

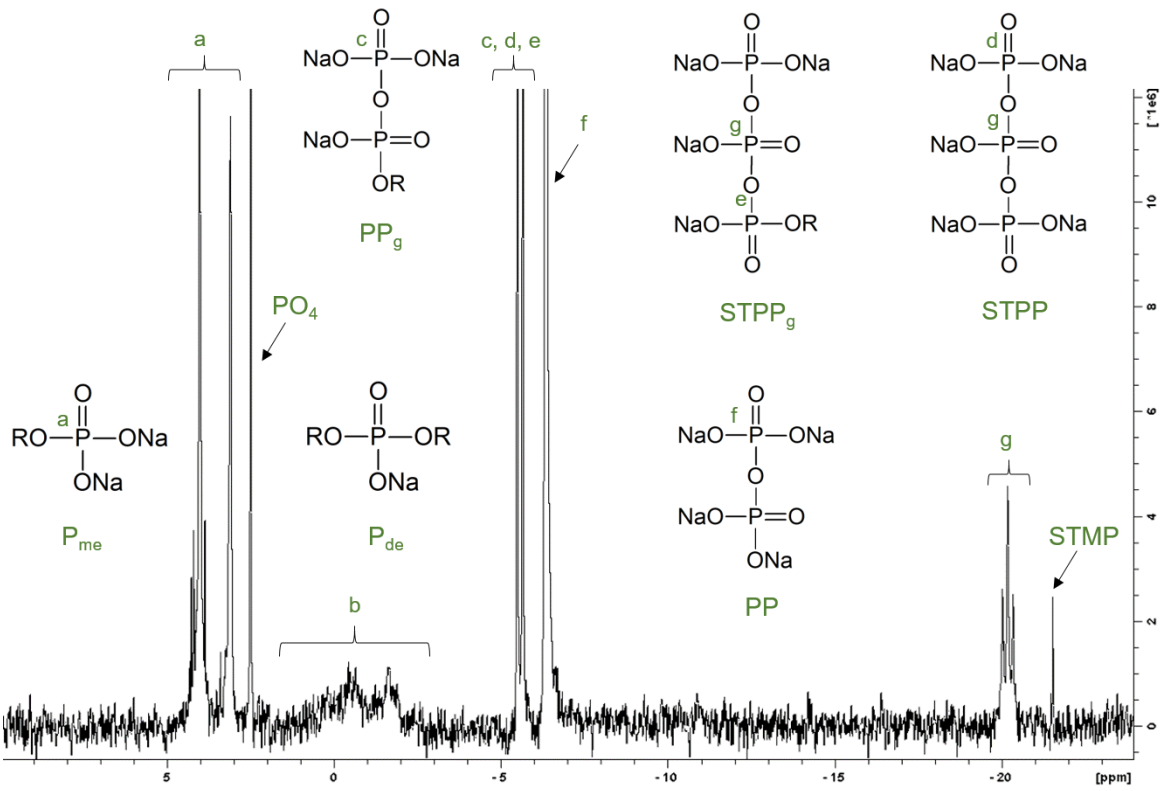

Figure 4.1 An example of a ^{31}P-NMR spectrum of SNPs cross-linked with STMP ([SNP]=15 wt.%, initial pH =11, [STMP] = 1 wt.%, [NaHCO3] = 3 wt.%, reaction time = 3 h).

With increasing reaction time, the STMP peak decreased, while the P_{me}, P_{de} and PP peaks increased, indicating an increase in degree of cross-linking with time (Table 4.3). The ^{31}P-NMR spectra obtained in this work are consistent with Lack's and Sang's study on the cross-linking reaction mechanism of polysaccharides using STMP.[35,46] The literature and our experiments suggest that both intra- and inter-particle cross-linking occurred,[47] which implies that starch hydrogels could be produced at high degrees of cross-linking. However, it can be noted that no starch hydrogels were produced in any runs (Table 4.1).

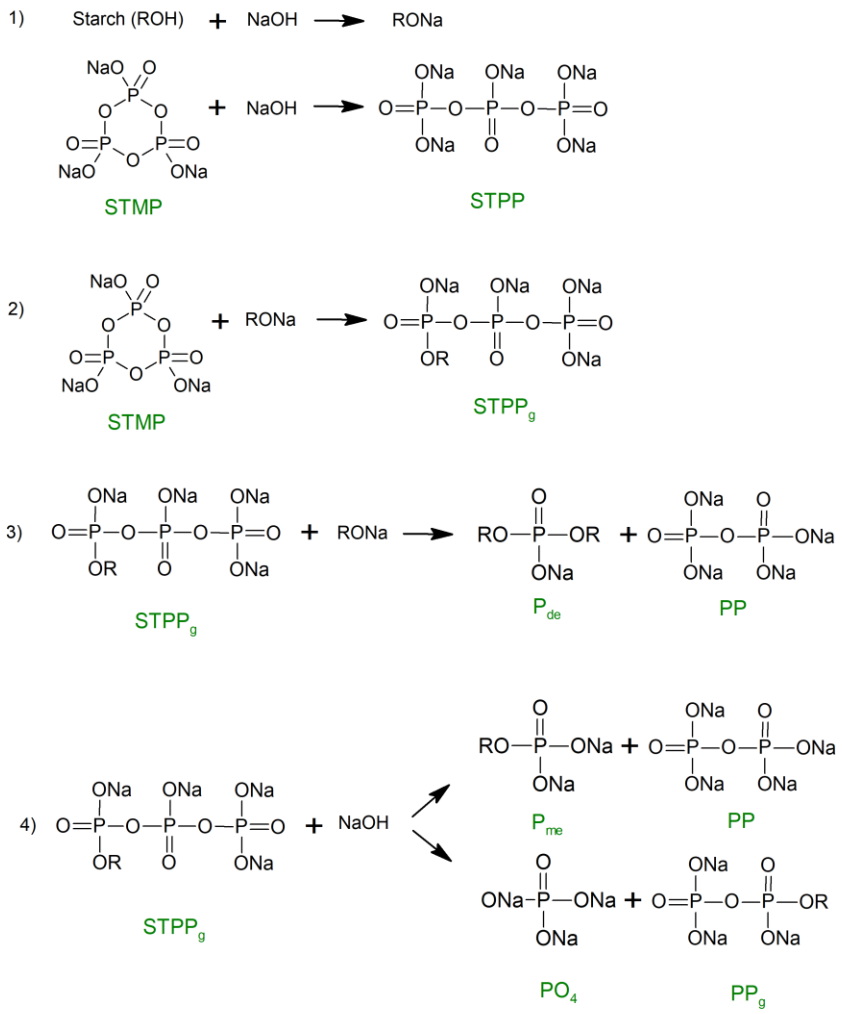

Figure 4.2 Reaction mechanism for the cross-linking of starch using STMP in alkaline condition.

Table 4.3 Relative concentration (% peak area) of selected peaks in ^{31}P-NMR spectrum with different cross-linking time ([SNP] = 15 wt.%, initial pH = 11, [STMP] = 0.1 wt.%, [NaHCO3] = 3 wt.%).

Time (h)	**4.6 ~ 2.1 ppm**	**1.1 ~ -2.5 ppm**	**-6.1 ~ -7.1 ppm**	**-21.6 ~ -21.8 ppm**
	P_{me}	**P_{de}**	**PP**	**STMP**
1	12.11	2.75	42.41	16.75
3	16.65	8.70	52.12	0.76
6	18.20	10.08	52.49	0.50

Functionalization of SNPs

STMP cross-linked SNPs (SNP-STMP) were functionalized with 3 wt.% FSM (relative to SNPs).[48] To confirm the attachment of the FSM, functionalized SNPs were filtered through a membrane with a 30 nm pore size to remove any non-covalently bonded FSM. The retentate was dried and further analyzed with ^{1}H-NMR (Figure 4.3), where the peaks corresponding to the FSM vinyl groups (5.7 ~ 5.9 ppm) and carbon chains (0.6 ~ 1.7 ppm) were observed, confirming the attachment of the FSM. FSM functionalized SNPs are henceforth referred to as SNP-STMP-FSM. To measure the bonding efficiency of the FSM to the SNPs, ^{1}H-NMR spectra of filtered SNP-STMP-FSM were compared with those of unfiltered SNP-STMP-FSM. The peak areas corresponding to FSM vinyl groups (5.7 ~ 5.9 ppm, A_1) and glucose (5.0 ~ 5.5 ppm, A_2) were used to estimate the bonding efficiency with Equation (3):

$$Bonding\ efficiency = \left(\left(\frac{A_{1,filtered}}{A_{2,filtered}} \right) / \left(\frac{A_{1,unfiltered}}{A_{2,unfiltered}} \right) \right) \cdot 100\% \quad (3)$$

For example, a bonding efficiency of 48% was achieved for samples prepared at the reaction conditions used in Run 1.5.

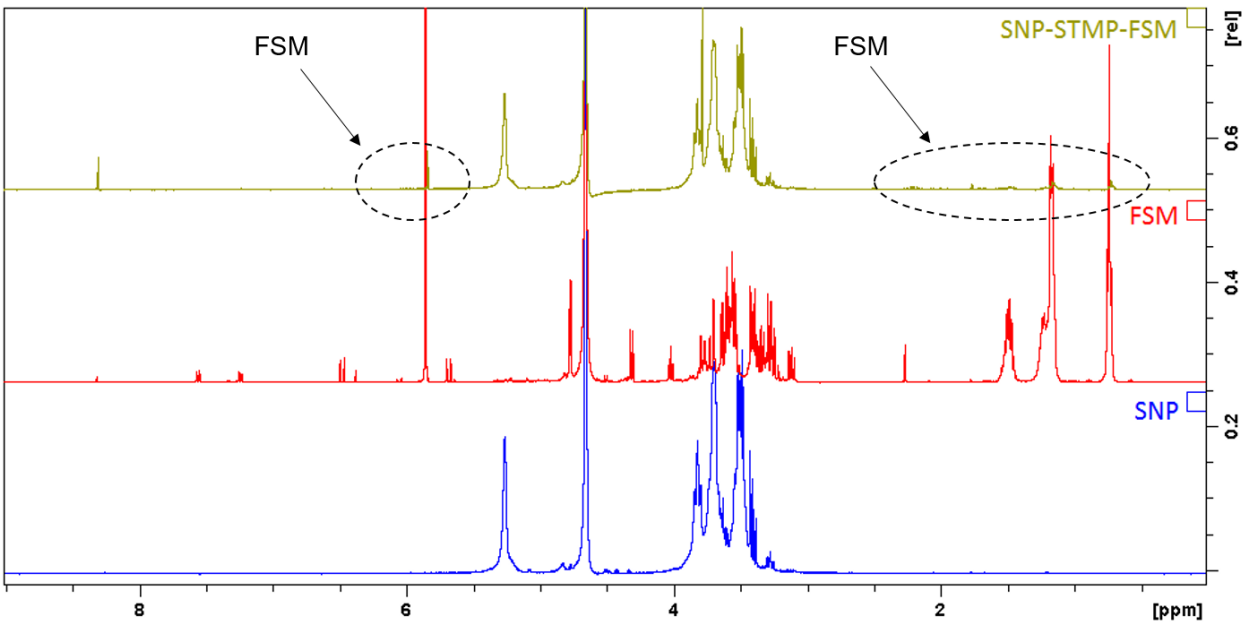

Figure 4.3 ^{1}H-NMR spectrums of filtered SNP-STMP-FSM, FSM and SNP.

Semi-Batch Emulsion Polymerization

Effect of SNP Modification

A series of experiments was conducted (Table 4.4) in order to test for the necessity of each modification procedure and the effect of the components (e.g., STMP, FSM) added during each step. All the polymerizations in Table 4.4 were performed at a 15 wt.% SNP loading and a target of 40 wt.% solids content. Three types of modified SNPs were used: SNP, SNP-STMP and SNP-STMP-FSM. The STMP, FSM and BVE were directly added to the reaction mixture along with the initial initiator charge, and, to be consistent, in the same amounts used in the modification procedure. An additional component, BVE, was introduced as a "tie-layer" monomer. Our previous study on SNPs indicated that the use of a "tie-layer" monomer facilitates the incorporation of SNPs.[32] The appropriate hydrophobicity, water solubility and reactivity of the "tie-layer" monomer is the key to

the process. After a screening study, butyl vinyl ether (BVE) was chosen as the most appropriate "tie-layer" monomer. BVE has a water solubility of 3 g/L at 20 ^{o}C, and will not undergo homopolymerization, but is possible to copolymerize with other vinyl monomers.[40–42]

Table 4.4 Summary of screening experiments to determine roles of STMP, FSM and BVE.

Run	SNP Type	Added to reaction mixture			Result	Viscosity (mPa.s)	Particle Size (nm)
		STMP	FSM	BVE			
2.1	SNP	×	×	×	Coagulated	N/A	N/A
2.2	SNP	√	×	×	Coagulated	N/A	N/A
2.3	SNP	×	√	×	Coagulated	N/A	N/A
2.4	SNP	×	×	√	Stable but viscous	>500	351
2.5	SNP-STMP	×	×	√	Stable	167	275
2.6	SNP-STMP	×	×	×	Stable	216	309
2.7	SNP-STMP-FSM	×	×	√	Stable, low viscosity	110	265

Before the semi-batch reaction (i.e., prior to pre-emulsion and initiator solution feeds), BVE was added to the SNP dispersion along with the initiator. The aqueous solution polymerization was continued for 0.5 h before semi-batch feeding of the pre-emulsion and initiator solutions. Because BVE has a low tendency to homopolymerize and due to its relatively high water solubility, it is believed that BVE preferentially reacts in the water phase with the SNPs.[40,41] At 15 wt.% SNP loading and 40 wt.% solids, without the

addition of BVE, we were unable to produce stable latexes (Runs 2.1-2.3, Table 4.4), however, with the addition of BVE (Run 2.4, Table 4.4), the run was successful with no visible grit (brown or white), but with a high viscosity (>500 mPa.s). Normally, the presence of visible grit is an indicator that SNPs were not fully incorporated in the latex particles and that a significant amount remained in the aqueous phase. This result indicated that the addition of BVE promoted latex stability. It is suspected that the low reactivity and high solubility of BVE also served to consume initiator radicals and reduce the amount of secondary particle nucleation.

When STMP cross-linked SNPs (SNP-STMP) were used in Runs 2.5 and 2.6, stable latexes were produced. However, brown grit was visible in Run 2.6 where no BVE was added. This suggests that cross-linking of SNPs using STMP promotes latex stability and a lower latex viscosity, perhaps due in part to their negative charge and/or an increase in SNP density. Furthermore, it was noticed that the addition of BVE resulted in lower latex viscosity and particle size (Table 4.4).

In Run 2.7, the application of functionalized, cross-linked SNPs (SNP-STMP-FSM) yielded the lowest viscosity (110 mPa.s) latex without visible grit. Both Runs 2.5 and 2.7 gave stable latexes with a relatively low viscosity, however, adhesive testing results (discussed below) suggest that vinyl functionalization of SNPs with a suitable vinyl monomer facilitates the incorporation of SNPs into the latex. In any case, as the addition of BVE proved important for reduction of the latex viscosity, it was henceforth added to the polymerization formulation.

In most cases, particle size increased with reaction time (Figure 4.4). No significant differences in overall conversion (Figure 4.5) between all controlled experiments were observed. The brief inhibition period at the beginning of the reactions was likely due to the presence of inhibitor in the MMA and AA.

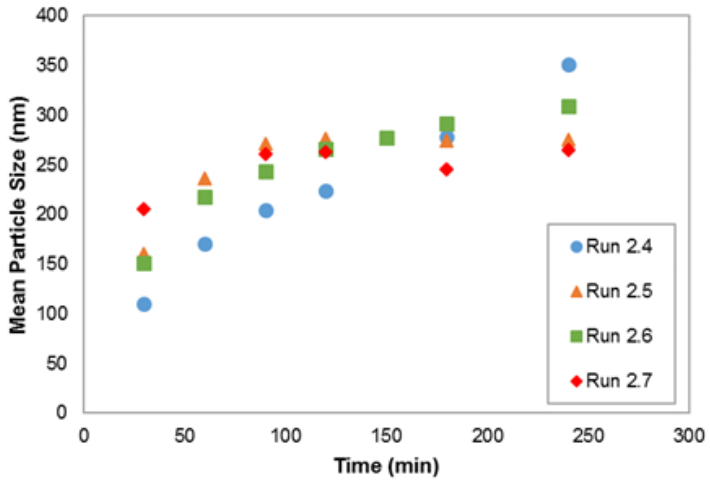

Figure 4.4 Mean particle size vs. time for Runs 2.4 to 2.7.

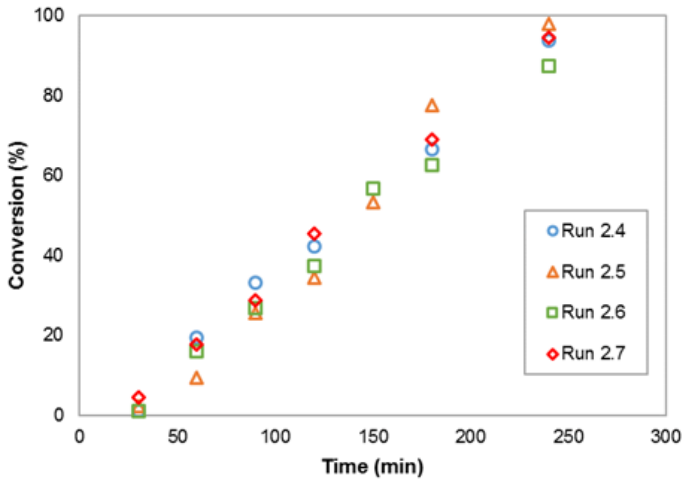

Figure 4.5 Global conversion for Runs 2.4 to 2.7.

Effect of Cross-linking Reaction Time

Experiments were conducted to verify the effect of the extent of cross-linking of the SNPs (Table 4.5). The SNP-STMP prepared in Runs 1.1 and 1.5 (Table 4.1) were used. 200 g samples were taken at cross-linking reaction times of 1, 3 and 6 h. Samples collected from Run 1.1 were used directly in the polymerization, whereas the samples from Run 1.5 were functionalized with FSM at the same cross-linking conditions for an additional 1 h to prepare SNP-STMP-FSM. All runs underwent the same polymerization conditions and had the same formulation, except that BVE was used for the SNP-STMP-FSM runs (Table 4.5).

Table 4.5 Polymerizations with different cross-linking reaction times.

Run	SNP Type	Cross-linking time (h)	Tie-layer monomer	Results	Viscosity (mPa.s)	Particle size (nm)
1.1-1	SNP-STMP	1	×	Some coagulum	N/A	N/A
1.1-3	SNP-STMP	3	×	Stable	371	352
1.1-6	SNP-STMP	6	×	Stable	288	318
1.5-1	SNP-STMP-FSM	1	√	Stable	98	391
1.5-3	SNP-STMP-FSM	3	√	Stable	132	416
1.5-6	SNP-STMP-FSM	6	√	Stable	111	359

Except for Run 1.1-1 (Table 4.5), where a small amount of coagulum was formed, all runs produced stable latexes. The SNP-STMP latexes (Runs 1.1-3 and -6) had much higher

viscosities compared with the SNP-STMP-FSM latexes (Runs 1.5-1, -3 and -6). This supports our earlier findings that vinyl functionalization coupled with the addition of BVE, promote latex stability and lower viscosity. The particle sizes in all the runs were greater than 300 nm, with no clear trends observed in particle size between samples with different cross-linking times. The global conversions for all the runs showed similar trends (Figure 4.6).

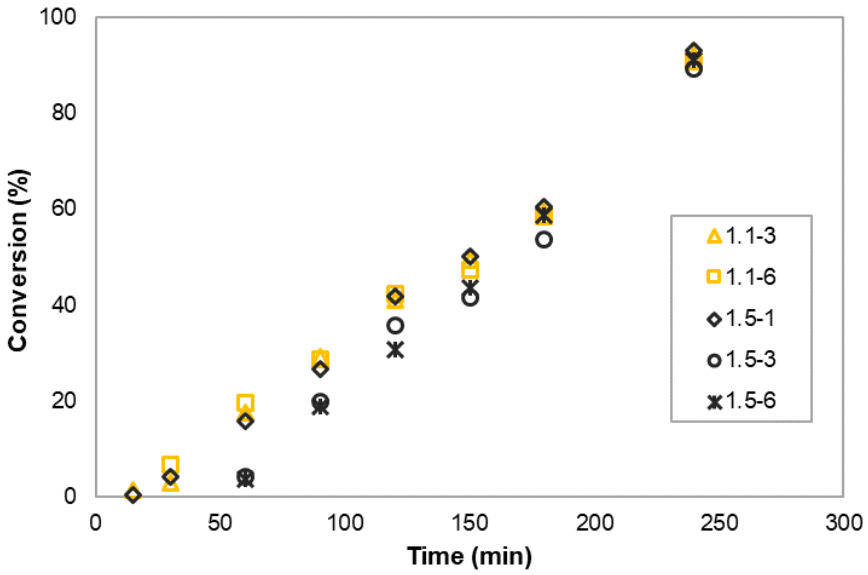

Figure 4.6 Global conversion for runs with different cross-linking reaction times.

In general, latex particle size increased with reaction time, reached a maximum and remained stable to the end of the reaction (Figure 4.7). However, one exception was observed. For Runs 1.5-1, where the SNPs were only cross-linked for 1 h, the particle size decreased after 60 min. A similar particle size decrease was noted in Run 2.7 (Figure 4.4), where the SNPs were also cross-linked for only 1 h. Non-crosslinked SNPs may swell in

aqueous solution at low concentrations, but with increased polymerization, deswelling of these SNPs is likely and this would lower their particle size.[49,50] Thus, the decreased latex particle size in the cases above, suggests insufficient cross-linking of the SNPs occurred.

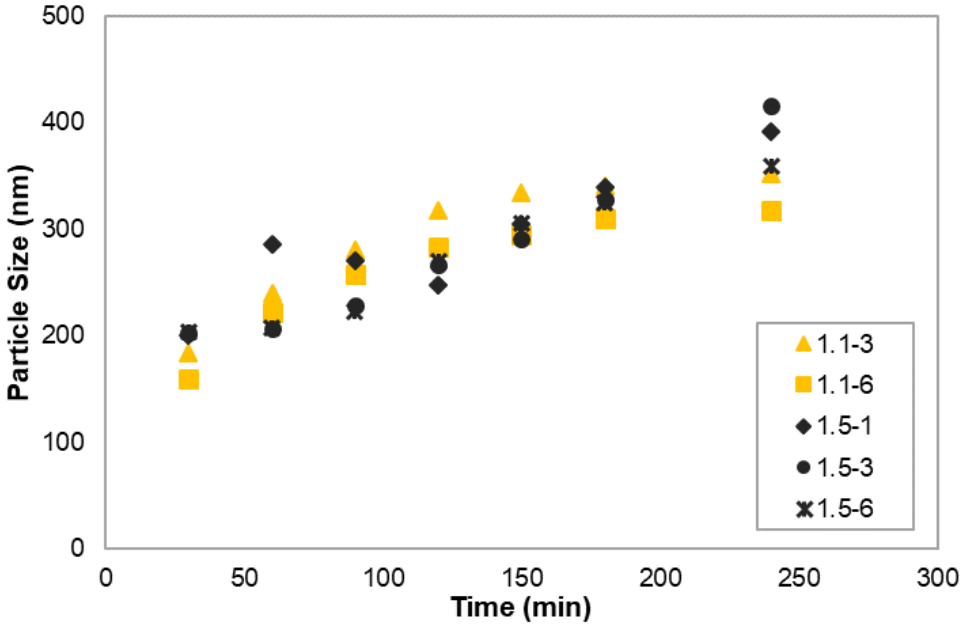

Figure 4.7 Mean latex particle size for runs with different cross-linking reaction times.

Adhesive Properties

Adhesive property is usually evaluated by tack, peel strength and shear strength.[33,51] Tack is the force that allows an adhesive to detach from a substrate upon contact under light or no pressure. Peel strength is defined as the force needed to peel away a strip of adhesives coated film with standard dimensions from a substrate at a standard peel rate and angle. Shear strength is the measurement of shear deformation under constant shear stress, and is related to the internal or cohesive strength of the adhesive. To obtain

adhesives with superior properties, polymer composition, glass transition temperature (T_g), molecular weight and the polymer microstructure should be finely tuned.

To investigate the effect of SNP-STMP-FSM on adhesive properties, the SNP-STMP-FSM based films (Run 2.7) were compared to base case acrylic films and films using blends of the base case acrylic latex and SNP (Figure 4.8-4.10). The acrylic base case latex was prepared using the same monomer composition as Run 2.7, and a similar particle size (251 nm) was achieved. At the same solids content as Run 2.7 (40 wt. %), we were unable to prepare coherent films due to low viscosity; this was only achieved at a solids content of 49 wt.%. Blends were prepared at room temperature (cold blend) and at the reaction temperature (60 ^{o}C, hot blend) to have the same starch concentration and solids content as Run 2.7. As shown in Figure 4.8 and 4.9, films from Run 2.7 showed much higher peel strength and slightly higher tack compared with the acrylic base case latex. Both cold and hot blend films gave relatively low peel strength and tack. However, the shear strength of Run 2.7 was slightly lower than that of the acrylic base case and both of those were significantly lower than that of the blended films (Figure 4.10). Given that starch has a higher T_g, a lower tack and peel strength, and a higher shear strength were expected for the case of the blended films.[51,52] The comparative increases in peel strength and tack and decrease in shear strength in Run 2.7 suggests that SNP-STMP-FSM may be encapsulated by acrylic polymers instead of mainly residing in the aqueous phase, as would be the case for the blended films, or on the surface of the particles. This would imply a core-shell morphology (or encapsulation of SNPs), where the shell would govern the adhesive properties, in most cases.[53,54] However, the shear strength of the films

from Run 2.7 was lower than that for the acrylic base case, indicating that the acrylic polymer on the surface of the latex particles in Run 2.7 may be poorly bonded to the SNP cores.

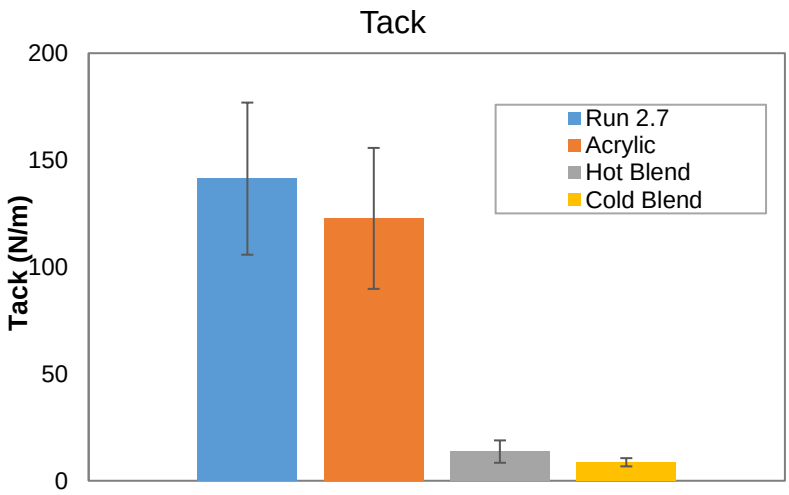

Figure 4.8 Tack comparison between Run 2.7 (SNP-STMP-FSM with BVE), acrylic base case and blended films.

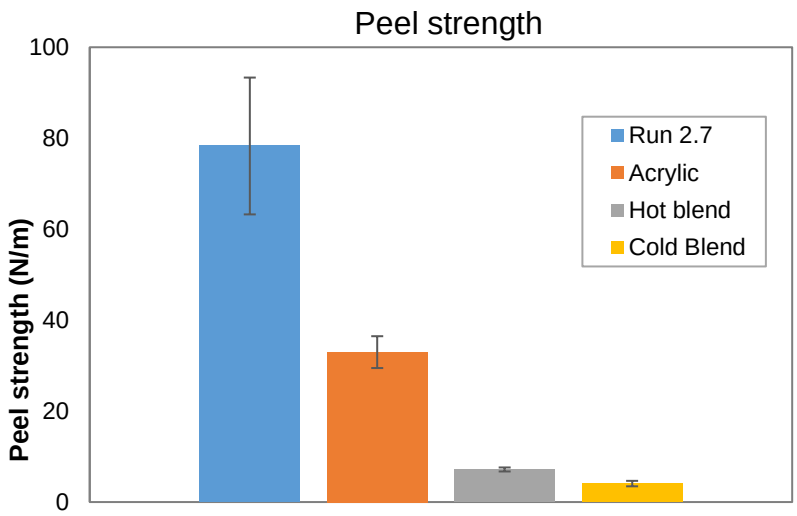

Figure 4.9 Peel strength comparison between Run 2.7 (SNP-STMP-FSM with BVE), acrylic base case and blended films.

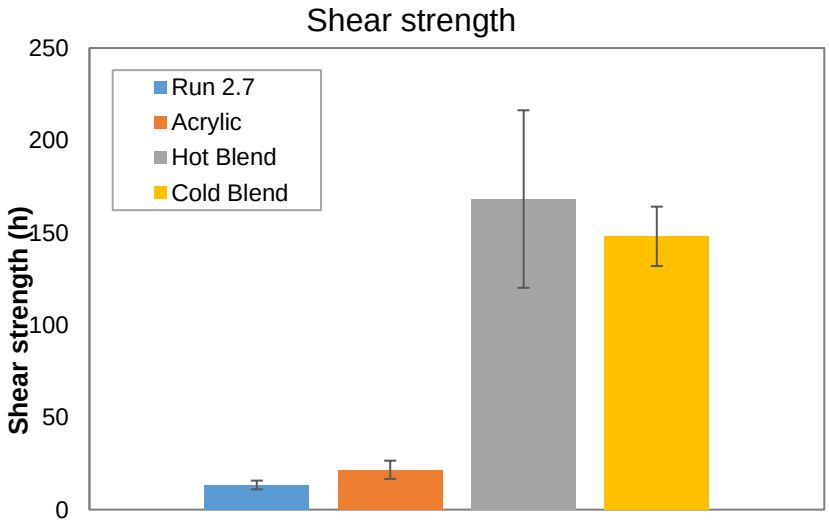

Figure 4.10 Shear strength comparison between Run 2.7 (SNP-STMP-FSM with BVE), acrylic base and blended films.

Adhesive properties of stable latexes prepared in Runs 2.5 to 2.7 (Table 4.4) are shown in Figure 4.11-4.13. Comparing Runs 2.5 and 2.6, it is noted that the addition of BVE provided no significant differences in adhesive properties. Adhesive films produced from the latex prepared using SNP-STMP-FSM (Run 2.7) gave higher tack and peel strength, but lower shear strength compared to the films prepared using SNP-STMP (Runs 2.5 and 2.6). This is another indication that FSM functionalization is essential to incorporate SNPs into the latex. Without vinyl functionalization, it is possible to graft to SNPs via hydrogen abstraction, however, the efficiency is not high enough to encapsulate SNPs.[25,27,28,32] Moreover, the vinyl groups are needed to bind the "tie-layer" monomer (i.e., BVE) to the SNPs to make them hydrophobic. Because SNP-STMP-FSM particles are hydrophilic, the SNPs will tend to be located at the surface of the latex particles or in the water phase. As the reactivity of the FSM (FSM has maleic acid end groups) and BVE are similar, and BVE has an appreciable water solubility, copolymers of maleic acid and BVE in the aqueous solution can be produced.[40] Thus, when BVE was added to the SNP-STMP-FSM dispersion, it likely reacted with the vinyl groups on the FSM and, as a result, increased the hydrophobicity of the SNPs. This increased hydrophobicity enhanced the likelihood of the SNPs copolymerizing with the hydrophobic acrylic monomers.

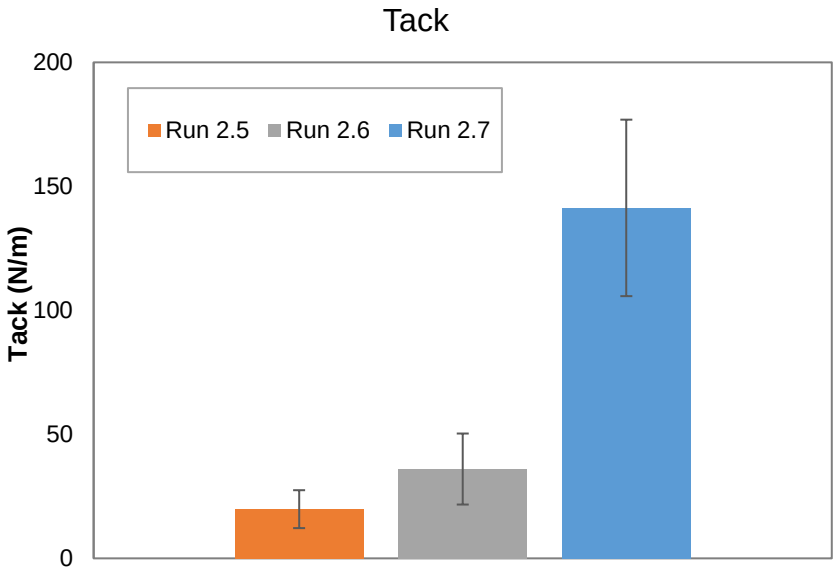

Figure 4.11 Tack for Runs 2.5 (SNP-STMP with BVE), 2.6 (SNP-STMP), and 2.7 (SNP-STMP-FSM with BVE).

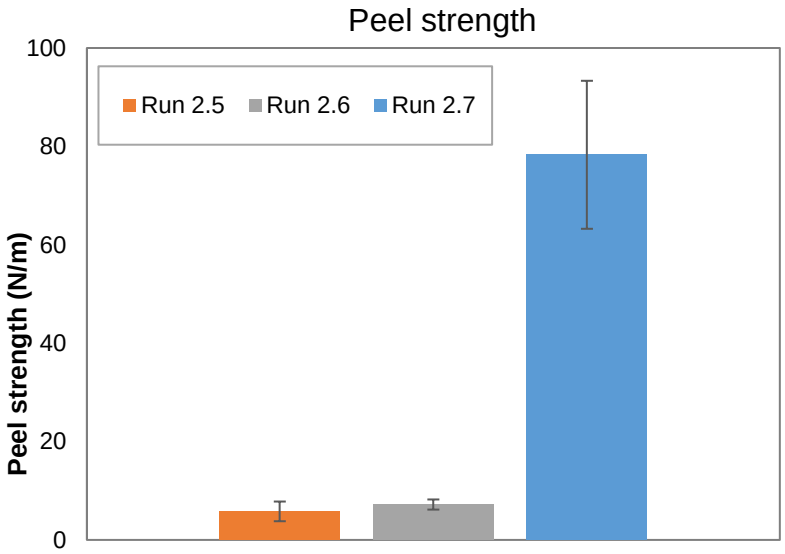

Figure 4.12 Peel strength for Runs 2.5 (SNP-STMP with BVE), 2.6 (SNP-STMP), and 2.7 (SNP-STMP-FSM with BVE).

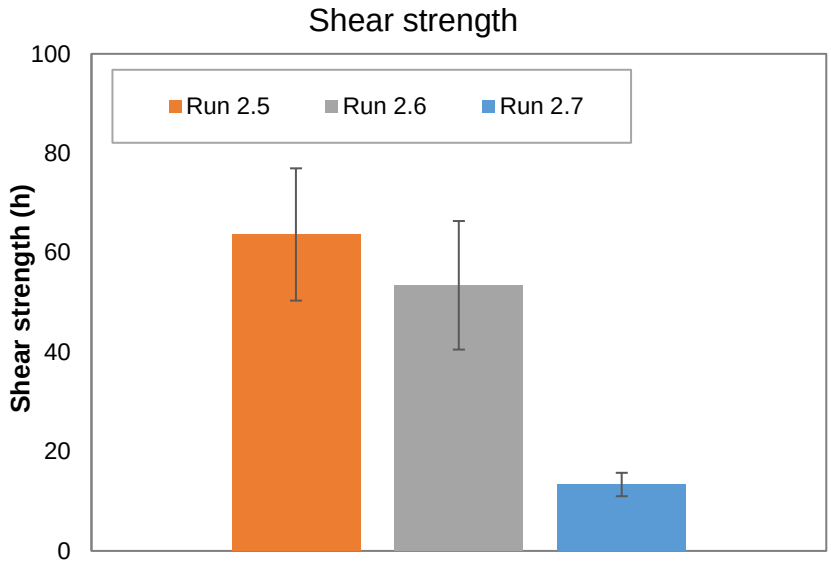

Figure 4.13 Shear strength for Runs 2.5 (SNP-STMP with BVE), 2.6 (SNP-STMP), and 2.7 (SNP-STMP-FSM with BVE).

The adhesive properties of films prepared using stable latexes with SNP-STMP and SNP-STMP-FSM and different cross-linking reaction times were tested (Figure 4.14-4.16). For most cases with STMP cross-linked SNPs, increased cross-linking time led to higher tack (Figure 4.14). Tack results for the SNP-STMP based films were generally lower than that of the SNP-STMP-FSM at the same cross-linking times, suggesting that SNP-STMP-FSM were better incorporated into the acrylic polymers compared to the SNP-STMP; i.e., more acrylic polymers were located on the particle surface, which improved tack.[51]

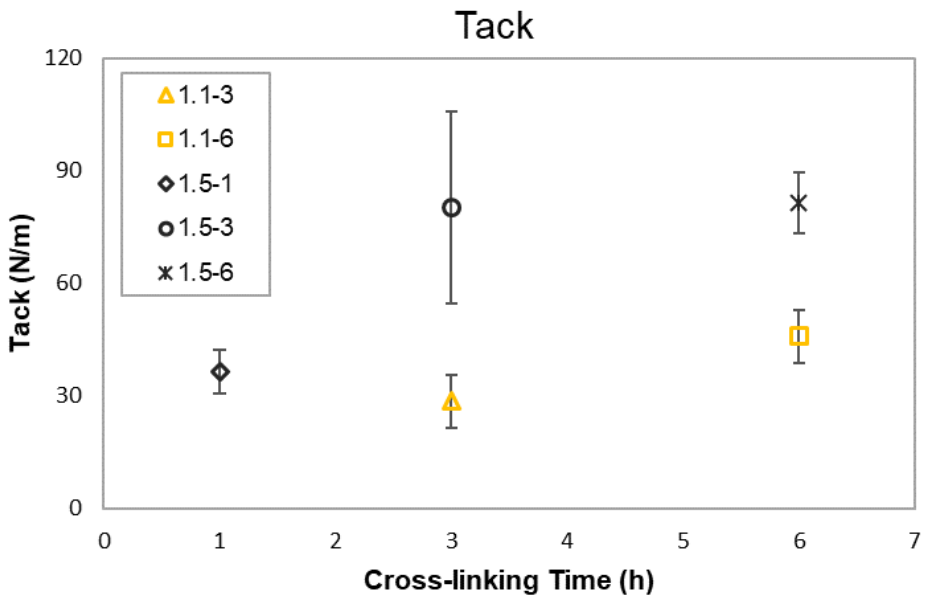

Figure 4.14 Tack for runs with different cross-linking reaction times.

For latexes using SNP-STMP (Runs 1.1-3 and -6), peel strength increased with cross-linking time (Figure 4.15). For the latexes using SNP-STMP-FSM (Runs 1.5-1, -3 and -6), peel strength went through a maximum for Run 1.5-3 (14.98 N/m). Similar to tack, the SNP-STMP-FSM based films exhibited higher peel strength except for the sample with 6 h cross-linking time. These results are consistent with the argument made above regarding the presence of a more cross-linked starch core as opposed to the starch comprising the shell polymer. For shear strength measurements (Figure 4.16), Runs 1.1-3 and -6, gave decreasing shear strength with increased cross-linking time. For Runs 1.5-1, -3 and -6, shear strength decreased from 1 h to 3 h cross-linking time and remained unchanged thereafter. Films with SNP-STMP showed relatively higher shear strength compared with that using SNP-STMP-FSM. The reduced shear strength with increasingly cross-linked

cores suggests that the cores (SNPs) were perhaps not well bonded to the purely acrylic shell polymers. Using a pre-emulsion feed containing a balance of chain transfer agent and cross-linker should theoretically assist in addressing this issue, thereby improving adhesive properties.[55,56]

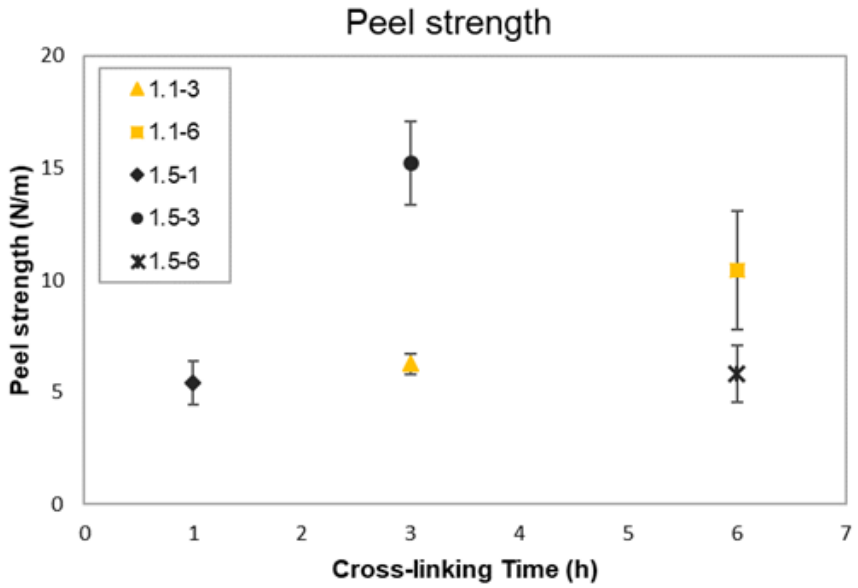

Figure 4.15 Peel strength for runs with different cross-linking reaction times.

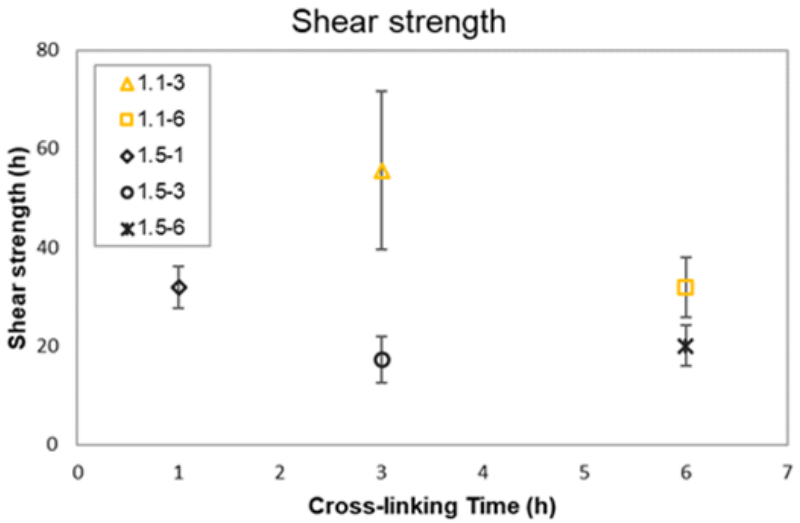

Figure 4.16 Shear strength for runs with different cross-linking reaction times.

Latex Particle Morphology

Particle imaging (TEM) was performed to examine the latex particle morphology. TEM imaging of SNP-STMP-FSM containing latex was first attempted using samples obtained from Run 1.5-3. In the TEM images, free SNPs are observed as small black particles; see for example, the blended pure acrylic latex with SNPs in Figure 4.17a. As shown in Figure 4.17b (Run 1.5-3), the latex particles were narrowly dispersed (which concurs with DLS measurements for the same latex) and no free SNPs were visible. This indicated that the latex particles in Run 1.5-3 were mainly composed of SNP-STMP-FSM and acrylic polymers, and suggests that the SNPs were largely encapsulated in the latex particles. However, a core-shell morphology was not clearly evident due to the low contrast in the TEM image. To improve the image contrast, STEM was used on the same sample grid (Figure 4.17c). In Figure 4.17c, a core-shell structure with a range of shell thicknesses can be observed for most particles. It was still difficult to observe thin-shelled particles, but if one zooms in to the image, the heat produced via the electron beam caused the shell to expand. This suggests that the low T_g acrylic polymer was the main component of the shell (Figure 4.17d). At the same time, the shell expansion also posed challenges for the estimation of particle size and shell thickness. A measurement was performed on the initial images taken using STEM (prior to shell expansion), yielded an average particle size of 485 nm and core diameter to total diameter ratios ranging from 0.75 to 0.90. According to the mass balance:

$$m_c/m_s = \left(\rho_c \cdot {d_c}^3\right) \Big/ \left(\rho_s \cdot \left((d_c + 2\delta)^3 - {d_c}^3\right)\right) \quad (4)$$

where m_c is the mass of the core (SNPs), m_s is the mass of the shell (acrylic polymers), ρ corresponds to the density, d_c represents radius of the core, and δ represents the shell thickness.

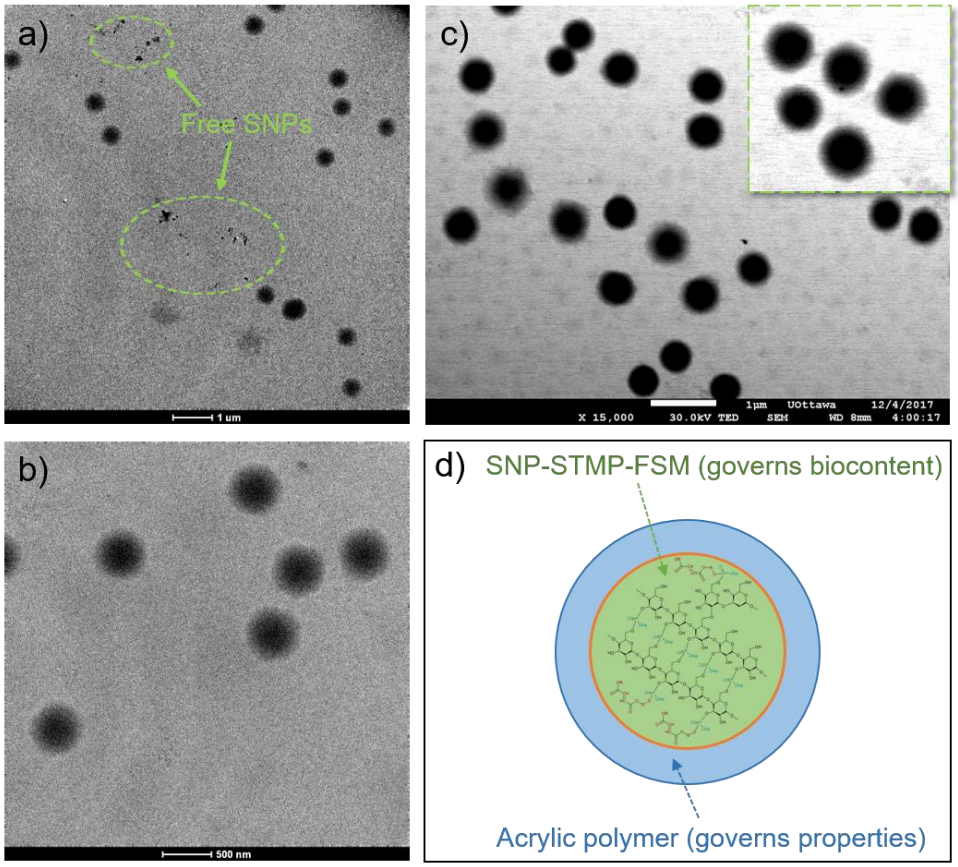

Figure 4.17 a) TEM image of hot blend; b) TEM image of Run 1.5-3 sample; c) STEM image of Run 1.5-3 sample; d) core-shell structure scheme.

Based on the average particle core diameter measured, to achieve complete encapsulation of all the SNPs at a 17 wt.% loading, a minimum particle core diameter/total diameter ratio of 0.71 would be expected. A ratio below 0.71 would

indicate that some SNPs would not be encapsulated or at least only partially encapsulated. A ratio greater than 0.71 would indicate that all SNPs are fully encapsulated, and that excess acrylic polymer is present as latex particles with no SNPs. Thus, the TEM results coupled with the mass balance calculation strongly supports significant encapsulation of the modified SNPs.

To further support the existence of a core-shell morphology and to calculate the shell thickness, latex with an alternative formulation to yield a higher T_g acrylic polymer was prepared: MMA/BA/AA (66/32/2) vs. BA/MMA/AA (93/5/2). The same SNP modification procedure and polymerization formulation as Run 1.5-3 was used. A stable, MMA-rich latex with a low viscosity of 77.5 mPa.s and an average particle size of 262 nm was produced. The TEM image of the MMA-rich latex confirmed the presence of a core-shell structure (Figure 4.18). A simple mass balance analysis was performed on the core-shell particles from the images and the results were averaged. The particle size was in the range of 200-260 nm with shell thicknesses ranging from 5 to 20 nm; these gave a core diameter/total diameter ratio between 0.90 and 0.98. As discussed above, this suggests complete SNP encapsulation with the presence of pure methacrylic latex particles.

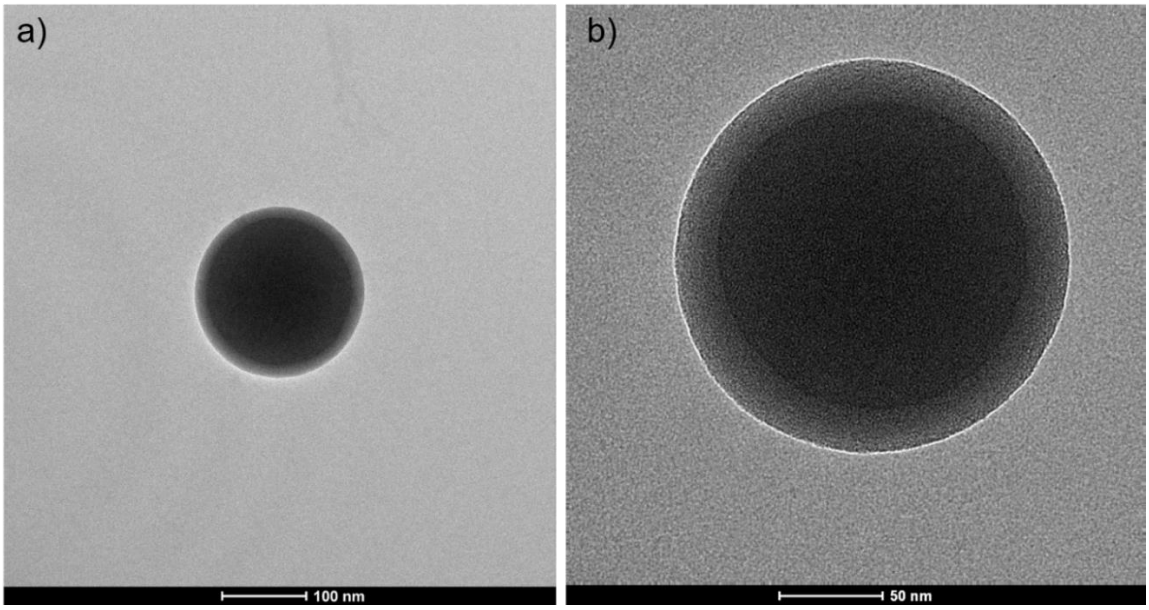

Figure 4.18 TEM image of an MMA rich latex particle.

In summary, TEM imaging results confirmed the presence of a core-shell morphology, which correlates well with our findings in the adhesive properties study, where better tack and peel strength was achieved in SNP-STMP-FSM containing latexes as a result of an SNP core/acrylic polymer shell morphology.

Conclusions

To enable the encapsulation of SNPs in the development of bio-based latexes for adhesive applications, SNPs were modified by cross-linking, functionalizing with a vinyl group and tuning their hydrophobicity through the addition of BVE. ^{31}P-NMR and ^{1}H-NMR spectra confirmed the successful cross-linking reaction and vinyl functionalization.

Stable and low viscosity latexes were successfully produced at up to 17 wt.% SNP loading and 42 wt.% solids with a semi-batch emulsion polymerization protocol. A series of experiments demonstrated the necessity of each modification procedure and the effect of the components (e.g., STMP, FSM) added during each part of the process. Films prepared with SNP-containing latexes were tested for their tack, peel strength and shear strength. By comparing adhesive properties of SNP-STMP-FSM containing films with base case acrylic films and films using blends of the base case acrylic latex with SNPs, increases in tack and peel strength, and decreased shear strength were observed, which supported the presence of a core-shell (SNP core/acrylic polymer shell) latex particle morphology. TEM and STEM images also supported the presence of the core-shell morphology and mass balance calculations suggested a significant degree of encapsulation of the SNPs in the latex particles. Furthermore, the mass balance calculations suggest that the SNP loading can be increased to achieve a higher bio-content.

Acknowledgements

Financial support for this work through the Natural Sciences and Engineering Research Council (NSERC) of Canada and EcoSynthetix Inc. (Burlington, ON) is gratefully acknowledged.

References

[1] Y. Zhang, M.A. Dubé, Green emulsion polymerization technology, in: W. Pauer (Ed.), Advances in Polymer Science: Polymer Reaction Engineering of Dispersed Systens, Springer, Berlin, Heidelberg, 2017: pp. 1–36.

[2] M.A. Dubé, S. Salehpour, Applying the principles of green chemistry to polymer production technology, Macromol. React. Eng. 8 (2014) 7–28.

[3] M.N. Belgacem, A. Gandini, Monomers, Polymers and Composites from Renewable Resources, Elsevier, Oxford, UK, 2008.

[4] A. Gandini, T.M. Lacerda, From Monomers to Polymers from Renewable Resources: Recent Advances, Prog. Polym. Sci. 48 (2015) 1–39.

[5] Y. Zhang, M.A. Dubé, Copolymerization of n-butyl methacrylate and d-limonene, Macromol. React. Eng. 8 (2014) 805–812.

[6] N. Hernandez, R.C. Williams, E.W. Cochran, The Battle for the "Green" Polymer. Different Approaches for Biopolymer Synthesis: Bioadvantaged vs. Bioreplacement, Org. Biomol. Chem. 12 (2014) 2834–2849.

[7] B.H. Shanks, P.L. Keeling, Bioprivileged Molecules: Creating Value from Biomass, Green Chem. 19 (2017) 3177–3185.

[8] A.J.F. Carvalho, Starch: major sources, properties and applications as thermoplastic materials, in: A. Gandini (Ed.), Monomers, Polymers and Composites from Renewable Resources, Elsevier, Amsterdam, 2008: pp. 321–342.

[9] R.F. Tester, J. Karkalas, X. Qi, Starch—composition, fine structure and architecture, J. Cereal Sci. 39 (2004) 151–165.

[10] T. Vasanthan, J. Li, D. Bressler, R. Hoover, Starch as Gelling Agent, in: Starch-Based Polymeric Materials and Nanocomposites, CRC Press, 2012: pp. 33–68.

[11] J. Ahmed, Starch-based polymeric materials and nanocomposites chemistry, processing, and applications, Boca Raton: CRC Press, 2012, Boca Raton, 2012.

[12] R. Hoover, The impact of heat-moisture treatment on molecular structures and properties of starches isolated from different botanical sources, Crit. Rev. Food Sci. Nutr. 50 (2010) 835–847.

[13] R.A. Talja, M. Peura, R. Serimaa, K. Jouppila, Effect of amylose content on physical and mechanical properties of potato-starch-based edible films, Biomacromolecules. 9 (2008) 658–663.

[14] H.-Y. Kim, S.S. Park, S.-T. Lim, Preparation, characterization and utilization of starch nanoparticles, Colloids Surf. B Biointerfaces. 126 (2015) 607–620.

[15] L. Chen, X. Li, L. Li, S. Guo, Acetylated starch-based biodegradable materials with potential biomedical applications as drug delivery systems, Curr. Appl. Phys. 7, Supplement 1 (2007) e90–e93.

[16] D. Le Corre, J. Bras, A. Dufresne, Starch nanoparticles: A review, Biomacromolecules. 11 (2010) 1139–1153.

[17] N.M.B. Smeets, S. Imbrogno, S. Bloembergen, Carbohydrate functionalized hybrid latex particles, Carbohydr. Polym. 173 (2017) 233–252.

[18] K.S. Sandhu, V. Nain, Starch Nanoparticles: Their Preparation and Applications, in: Plant Biotechnology: Recent Advancements and Developments, Springer, Singapore, 2017: pp. 213–232.

[19] H. Namazi, F. Fathi, A. Heydari, Nanoparticles Based on Modified Polysaccharides, IntechOpen, (2012).

[20] N. Lin, J. Huang, P.R. Chang, D.P. Anderson, J. Yu, Preparation, modification, and application of starch nanocrystals in nanomaterials: A review, J. Nanomater. 2011 (2010) e573687.

[21] R. Hui, C. Qi-he, F. Ming-liang, X. Qiong, H. Guo-qing, Preparation and properties of octenyl succinic anhydride modified potato starch, Food Chem. 114 (2009) 81–86.

[22] A. Sorrentino, G. Gorrasi, V. Vittoria, Potential perspectives of bio-nanocomposites for food packaging applications, Trends Food Sci. Technol. 18 (2007) 84–95.

[23] S.B. Haaj, W. Thielemans, A. Magnin, S. Boufi, Starch nanocrystal stabilized pickering emulsion polymerization for nanocomposites with improved performance, ACS Appl. Mater. Interfaces. 6 (2014) 8263–8273.

[24] C. Li, P. Sun, C. Yang, Emulsion stabilized by starch nanocrystals, Starch - Stärke. 64 (2012) 497–502.

[25] I. Echeverria, I. Silva, I. Goñi, M. Gurruchaga, Ethyl methacrylate grafted on two starches as polymeric matrices for drug delivery, J. Appl. Polym. Sci. 96 (2005) 523–536.

[26] E.S. Dragan, D.F.A. Loghin, A.-I. Cocarta, M. Doroftei, Multi-stimuli-responsive semi-IPN cryogels with native and anionic potato starch entrapped in poly(N,N-dimethylaminoethyl methacrylate) matrix and their potential in drug delivery, React. Funct. Polym. 105 (2016) 66–77.

[27] M.-C. Li, X. Ge, U.R. Cho, Emulsion grafting vinyl monomers onto starch for reinforcement of styrene-butadiene rubber, Macromol. Res. 21 (2013) 519–528.

[28] J.-H. Hwang, H. Ryu, U.-R. Cho, A Study on Starch-acrylic Graft Copolymerization by Emulsion Polymerization, Elastomers Compos. 43 (2008) 221–229.

[29] X. Pei, K. Zhai, Y. Tan, K. Xu, C. Lu, P. Wang, T. Wang, C. Chen, Y. Tao, L. Dai, H. Li, Synthesis of monodisperse starch-polystyrene core-shell nanoparticles via seeded emulsion polymerization without stabilizer, Polymer. 108 (2017) 78–86.

[30] X. Pei, Y. Tan, K. Xu, C. Liu, C. Lu, P. Wang, Pickering polymerization of styrene stabilized by starch-based nanospheres, Polym. Chem. 7 (2016) 3325–3333.

[31] H. Lange, Emulsion polymerization of vinyl acetate with renewable raw materials as protective colloids, MASc Thesis, KTH, 2011.

[32] S. Cummings, The Incorporation of vinyl modified regenerated starch nanoparticles in emulsion polymerizations, PhD Thesis, University of Ottawa, 2017.

[33] I. Benedek, Pressure-sensitive Adhesives And Applications, Marcel Dekker Inc, Hoboken, 2004.

[34] S. Tobing, A. Klein, L. h. Sperling, B. Petrasko, Effect of network morphology on adhesive performance in emulsion blends of acrylic pressure sensitive adhesives, J. Appl. Polym. Sci. 81 (2001) 2109–2117.

[35] S. Lack, V. Dulong, L. Picton, D.L. Cerf, E. Condamine, High-resolution nuclear magnetic resonance spectroscopy studies of polysaccharides crosslinked by sodium trimetaphosphate: a proposal for the reaction mechanism, Carbohydr. Res. 342 (2007) 943–953.

[36] F. Gao, D. Li, C. Bi, Z. Mao, B. Adhikari, Preparation and characterization of starch crosslinked with sodium trimetaphosphate and hydrolyzed by enzymes, Carbohydr. Polym. 103 (2014) 310–318.

[37] K. Woo, P.A. Seib, Cross-linking of wheat starch and hydroxypropylated wheat starch in alkaline slurry with sodium trimetaphosphate, Carbohydr. Polym. 33 (1997) 263–271.

[38] A.M. North, D. Postlethwaite, The copolymerization of methylmethacrylate and maleic anhydride, Polymer. 5 (1964) 237–245.

[39] S. Bloembergen, I.J. McLennan, R. Narayan, Sugar based vinyl monomers and copolymers useful in repulpable adhesives and other applications, US5872199 A, 1999.

[40] P.L. Dubin, U.P. Strauss, Hydrophobic bonding in alternating copolymers of maleic acid and alkyl vinyl ethers, J. Phys. Chem. 74 (1970) 2842–2847.

[41] H. Braun, Y. Yagci, O. Nuyken, Copolymerization of butyl vinyl ether and methyl methacrylate by combination of radical and radical promoted cationic mechanisms, Eur. Polym. J. 38 (2002) 151–156.

[42] J.C. Bevington, T.N. Huckerby, A.D. Jenkins, The copolymerization activity of some vinyl ethers, J. Macromol. Sci. Part A. 36 (1999) 1907–1922.

[43] J. Rajas, E. Azevedo, Funcationalization and crosslinking of microcrystalline cellulose in aqueous media: A safe and economic approach, Int. J. Pharm. Sci. Rev. Resear. 8 (2011) 28.

[44] M. Gui-Jie, W. Peng, M. Xiang-Sheng, Z. Xing, Z. Tong, Crosslinking of corn starch with sodium trimetaphosphate in solid state by microwave irradiation, J. Appl. Polym. Sci. 102 (2006) 5854–5860.

[45] S. Lim, P.A. Seib, Preparation and pasting properties of wheat and corn starch phosphates, Cereal Chem. 70 (1993) 137–144.

[46] Y. Sang, O. Prakash, P.A. Seib, Characterization of phosphorylated cross-linked resistant starch by 31P nuclear magnetic resonance (31P NMR) spectroscopy, Carbohydr. Polym. 67 (2007) 201–212.

[47] V.M. Acquarone, M.A. Rao, Influence of sucrose on the rheology and granule size of cross-linked waxy maize starch dispersions heated at two temperatures, Carbohydr. Polym. 51 (2003) 451–458.

[48] N. Pokeržnik, M. Krajnc, Synthesis of a glucose-based surfmer and its copolymerization with n-butyl acrylate for emulsion pressure sensitive adhesives, Eur. Polym. J. 68 (2015) 558–572.

[49] B.H. Tan, K.C. Tam, Y.C. Lam, C.B. Tan, Osmotic compressibility of soft colloidal systems, Langmuir. 21 (2005) 4283–4290.

[50] A.M. Matser, P.A.M. Steeneken, Rheological properties of highly cross-linked waxy maize starch in aqueous suspensions of skim milk components. Effects of the concentration of starch and skim milk components, Carbohydr. Polym. 32 (1997) 297–305.

[51] R. Jovanović, M.A. Dubé, Emulsion-based pressure-sensitive adhesives: A review, J. Macromol. Sci. Part C. 44 (2004) 1–51.

[52] D. Satas, Handbook of Pressure Sensitive Adhesive Technology, 2nd ed.., Van Nostrand Reinhold, New York, 1989.

[53] J. Garrett, P.A. Lovell, A.J. Shea, R.D. Viney, Water-borne pressure-sensitive adhesives: Effects of acrylic acid and particle structure, Macromol. Symp. 151 (2000) 487–496.

[54] A. Pizzi, K.L. Mittal, Handbook of Adhesive Technology, 2nd ed., MDekker, New York, 2003.

[55] L. Qie, M.A. Dubé, Manipulation of chain transfer agent and cross-linker concentration to modify latex micro-structure for pressure-sensitive adhesives, Eur. Polym. J. 46 (2010) 1225–1236.

[56] L. Qie, M.A. Dubé, Manipulating latex polymer microstructure using chain transfer agent and cross-linker to modify PSA performance and viscoelasticity, Macromol. React. Eng. 5 (2011) 117–128.

5. Increasing Starch Nanoparticle Content in Emulsion Polymer Latexes

Chapter 5 contains a manuscript published in the Industrial & Engineering Chemistry Research on March 13, 2019.

Increasing Starch Nanoparticle Content in Emulsion Polymer Latexes

Yujie Zhang, Michael F. Cunningham, Niels M.B. Smeets, Marc A. Dubé*,

_____

Y. Zhang, Prof. M.A. Dubé*

Department of Chemical and Biological Engineering,

Centre for Catalysis Research and Innovation,

University of Ottawa, 161 Louis Pasteur Pvt.,

Ottawa, Ontario, K1N 6N5, Canada

Prof. M.F. Cunningham

Department of Chemical Engineering,

Queen's University, 9 University Ave,

Kingston, Ontario, K7L 3N6, Canada

Dr. N.M.B. Smeets

EcoSynthetix Inc.,

3365 Mainway,

Burlington, Ontario, L7M 1A6, Canada

_____

Abstract

Starch nanoparticles (SNPs) were used to partially replace petroleum-based polymers in a bio-based latex adhesive application. Modification of SNPs (i.e., increasing cross-link density, functionalizing using a sugar-based monomer, and tuning SNP hydrophobicity) was performed prior to their incorporation in a semi-batch emulsion polymerization to produce stable SNP-based latexes. SNP loadings and latex solids content were varied to study their effect on latex stability and properties (e.g., viscosity, particle size, adhesive properties, particle morphology). Stable and low viscosity latexes with up to 45 wt.% SNP loadings and 55 wt.% latex solids were achieved. STEM images confirmed the presence of the core-shell morphology, where SNPs were located in the particle cores and provided bio-content, while the acrylic polymers were present as the shell and governed the application properties. Pushing the limits of SNP loading and latex solids was shown to come at a cost to adhesive and other properties.

Keywords: starch nanoparticles, emulsion polymerization, bio-sourced materials, adhesives, polymer modification

Introduction

Synthetic polymers have contributed tremendously to our increased standard of living given their versatility and high resource efficiency. Nevertheless, significant environmental impact has resulted from the production process, as well as the waste management of the products at the end of their useful lifetime.[1,2] Limits to our fossil resources and their increasing cost have encouraged the development of more sustainable alternatives: polymers that are derived from renewable resources (e.g., starch, cellulose, lignin).[3,4] Renewable resources are abundant and offer a variety of building blocks to tailor material types and applications.[5] However, in most cases, it is essential to apply polymer chemistry (e.g., functionalization, hydrolysis, cross-linking) and engineering techniques (e.g., apply real-time analysis, tune particle morphology) to obtain materials with comparable or improved properties.[4–6]

Starch is considered as one of the most promising renewable alternatives and has drawn increasing attention in recent years. Since 2000, the number of publications related to starch has nearly tripled, especially in the field of polymer science, where starch related citations have increased exponentially.[7] As one of the largest biopolymer markets, it is estimated that the global industrial starch market size will grow to 103.5 billion USD in 2023 as a result of the multiple functionalities of starch and starch derivatives in a wide range of applications (e.g., food additives, paper making, textiles).[8]

Native starch is produced by many plants such as corn, potatoes and wheat. It is a polymeric carbohydrate that consists of two macromolecules: linear amylose and

branched amylopectin. In general, starch contains 20 to 25 % amylose depending on the type of plant.[9,10] Starch molecules arrange themselves in semi-crystalline granules and each plant has its unique granular shape, size and crystalline structure.[10,11] Modified starch with various morphologies, for instance, starch nanoparticles (SNPs) and starch nanocrystals, have been developed, which offer novel properties for applications such as in drug delivery and paper binders.[12–16]

SNPs with particle sizes ranging from 20 nm to 6 μm can be produced through chemical pathways (e.g., reactive extrusion, emulsion precipitation) or physical treatments (e.g., microfluidization, ultrasonication).[17–20] To explore more exciting possibilities of SNP-based materials, further modification of SNPs has proven necessary.[21,22] There are generally two types of approaches to modify SNPs: via small molecule chemistry and via polymerization. Small molecule chemistry approaches are normally achieved by introducing various moieties, e.g., esters, ethers and anhydrides.[23–25] Modification of SNPs through polymerization involves “grafting from” and “grafting to” techniques, and can be performed using free radical polymerization, living/controlled radical polymerization, ring-opening polymerization, etc.[22,26–28]

Modification of SNPs can not only introduce new functionalities, but also allow us to tune the hydrophobicity of SNPs to improve their compatibility with hydrophobic materials. This has made it possible to incorporate SNPs into polymeric materials in many ways: as stabilizers for emulsion systems,[20,29,30] as nano-fillers in composite materials,[11,31] or as macromers to polymerize with other organic chemicals (normally, in emulsion

systems).[32–35] However, in many cases, only low amounts of SNPs can be incorporated into the reaction formulation. An increase in SNP loading inevitably leads to stability issues, limited incorporation and deterioration of properties.[30,34,36]

Recently, we successfully produced SNP-based latexes with good adhesive properties by encapsulating SNPs into the latex particles.[35] SNPs were modified using a non-toxic cross-linker, a vinyl functionalized sugar-based monomer and a "tie-layer" monomer, to tune their hydrophobicity. These modified SNPs were subsequently polymerized in a semi-batch emulsion polymerization and a core-shell (SNP core/acrylic polymer shell) morphology was achieved at 17 wt.% SNP loading and 42 wt.% solids. In this work, SNP loading and latex solids were varied to investigate their effect on latex stability and other properties (e.g., viscosity, particle size, adhesive properties, particle morphology). Our objective is to propose a formulation with an optimum SNP loading and solids content while achieving significant encapsulation/incorporation and maintaining polymer properties. Strategies to further increase the SNP loading and latex solids are discussed.

Materials and Methods

Materials

Experimental grade SNPs and functionalized sugar monomer (FSM) were supplied by EcoSynthetix Inc. (Burlington, ON). Butyl acrylate (BA, 99%), methyl methacrylate (MMA, 99%), acrylic acid (AA, 99.5%), butyl vinyl ether (BVE), sodium trimetaphosphate (STMP), sodium bicarbonate ($NaHCO_3$), hydrochloric acid (HCl, 1M), sodium hydroxide (NaOH), potassium persulfate (KPS, 99%), tetrahydrofuran (THF, 99%) and hydroquinone (HQ),

were purchased from Sigma-Aldrich. EF-800 (49-51 wt.% aqueous solution) was provided by Cytec Industries. Distilled deionized water (DDW) was used throughout this work. BA and MMA were purified by passing through an inhibitor removal column and stored at 4 °C; all other chemicals were used as received. Nitrogen gas (GR4.8, Linde Canada) was used to purge the reactor to remove oxygen.

Modification of SNPs

Experimental grade SNPs were modified following a three-step procedure discussed previously.[35] First, STMP, a non-toxic cross-linker, was used to increase the cross-link density of SNPs. 60 g starch was dispersed with 340 g DDW at 60 °C in a 500 mL RC1e glass reaction calorimeter (Mettler-Toledo) equipped with a Hastelloy stirrer set and a pH probe. After the SNPs were fully dispersed and the solution temperature was constant, 1.8 g $NaHCO_3$ was added to the solution; the solution pH was adjusted to 11 using NaOH and HCL solutions. 0.6 g of STMP was then added to the solution and reacted for 1 h. After cross-linking the SNPs for 1 h, vinyl functionalization was performed by adding 6 g FSM aqueous solution (30 wt.%). After reacting for another hour, the reaction was stopped by adjusting pH of the solution to 6.5; the solution was cooled to room temperature and characterized. The last step of the modification was to introduce a “tie-layer” monomer BVE, a step which was performed at the beginning of the polymerization and discussed next.

Semi-batch Emulsion Polymerization

Polymerization of modified SNPs was conducted in the same RC1e reactor as above, equipped with two semi-batch feed pumps and an inlet for nitrogen sparging. A standard semi-batch emulsion polymerization formulation was used (Table 5.1). A designated amount of SNP solution was added to the reactor, dispersed at 300 rpm and purged with nitrogen while heating to 60 °C for 30 min. Then, the initial initiator charge and BVE were introduced to the solution and reacted for 30 min to perform the final SNP modification step. Afterwards, the semi-batch polymerization was begun by feeding a monomer pre-emulsion at a constant rate for 210 min along with an initiator solution for 240 min. After completion of the semi-batch feeds, the reaction was continued for another 30 min and eventually cooled to 25 °C. Latex samples were taken periodically during polymerization to measure conversion and particle size; HQ solution (0.1~0.2 g of 1 wt.% solution) was added to each sample to quench the polymerization. A series of formulations were designed and tested at various SNP loadings and solids contents (Table 5.2).

Table 5.1 Typical emulsion polymerization formulation (25 wt.% SNP loading and 40 wt.% solids content).

Solution	**Component**	**Weight (g)**
SNP solution	SNP	35.11
	DDW	152.72
Initial charge	KPS	0.57
	DDW	14.48

	BVE	4.70
Monomer pre-emulsion	EF-800	9.63
	DDW	43.06
	BA	172.24
	MMA	9.24
	AA	3.71
Initiator solution	KPS	1.72
	DDW	40.76

Table 5.2 Experimental design for emulsion polymerizations at various SNP loadings and solids contents and summary of results.

Runs	**SNP Loading* (wt.%)**	**Solids (wt.%)**	**Conversion (wt.%)**	**Viscosity (mPa.s)**	**Z-Average Particle Size (nm)**	**Result**
1	15	40	93	65	367	Stable, low viscosity
2	25	40	91	68	419	Stable, low viscosity
3	35	40	92	74	429	Stable, low viscosity
4	45	40	92	75	453	Stable, low viscosity
5	55	40	50	88	412	Low conversion
6	60	40	N/A	N/A	N/A	Failed
7	15	50	92	169	490	Stable
8	20	50	91	219	498	Stable
9	25	50	90	340	565	Stable

10	25	55	90	>500	604	Stable, high viscosity

*SNP loading = total mass SNP/total mass of solids

Analytical Methods

Cross-linking of SNPs was confirmed by ^{31}P-NMR using a Bruker AVANCE-300 spectrometer. Sample solutions contain ~0.02 g dry SNP samples and 1.5 g solvent (D_2O: DDW, 10:90 w:w). A Bruker AVANCE-400 ^{1}H-NMR spectrometer was used to verify the vinyl functionalization of SNPs by carrying out 32 scans. Solution of modified SNPs were filtered using a membrane with pore size of 30 nm to remove free FSM in the solution. About 0.02 g dried retentate samples were dispersed in 1.5 g D_2O for analysis.

Dynamic Light Scattering (DLS) with a Malvern NanoS Zetasizer at an angle of 173^{o} was used to measure particle size at room temperature. One drop of sample was diluted in 2 mL of DDW in a 4 mL polystyrene cuvette. Three measurements were performed, and average intensity-weighted particle size was reported. To measure solids content and conversion, a gravimetric method was used.[35] Viscosity of the final latex was determined using a Brookfield viscometer with spindle R4 at 100 rpm. To assess latex particle morphology, Scanning Transmission Electron Microscope (STEM) was performed using a JEM-2100F FETEM (JEOL). Two droplets of latex were first diluted in 50 mL DDW, then one droplet of the diluted sample was dropped on a glow-discharged copper grid. The sample was then dried at room temperature and scanned. All images were taken at 10,000X magnification and under an operating voltage of 20 kV.

THF and water barrier properties were tested using a hydrophobic and a hydrophilic membrane, respectively. Dry polymer samples were weighed and sealed in a hydrophilic or hydrophobic membrane pouch, and then swelled in 20 mL DDW or THF in a glass jar. The glass jar was sealed and kept in a wrist shaker for 24 h at room temperature. The swollen samples were then dried at room temperature and weighed. The weight percentage of the dried sample relative to the original sample was reported. Peel strength, shear strength and tack of latex films were tested by applying Pressure Sensitive Tape Council standards (PSTC, 2004) in a temperature- and humidity-controlled room (23 ± 1°C and 50% ± 5% RH).[35]

Results and Discussion

Our goal was to achieve the highest possible SNP incorporation into the latex polymer while maintaining performance properties, in this case, adhesion properties of the latex films. An additional goal was to increase the latex solids content. As noted earlier, to facilitate SNP incorporation in emulsion latexes, we modified the SNPs by increasing their cross-link density using STMP, adding vinyl functionalization using a sugar-based monomer, and tuning their hydrophobicity with a "tie-layer" monomer, BVE. The modified SNPs were then polymerized via semi-batch emulsion polymerization at various SNP loadings and overall solids contents.

Modification of SNPs

SNPs were first cross-linked in solution using 1 wt.% STMP (relative to SNPs) at pH 11 and 60 °C for 1 h. After the cross-linking reaction, ^{31}P-NMR spectroscopy confirmed an

increase in SNP cross-link density (Figure 5.1). In Figure 5.1, the peak spanning 1.5 to -3.5 ppm corresponds to the phosphate diester, which shows that SNP cross-linking with STMP has occurred, although it cannot provide a quantitative measure.[35,37,38] Both intra- and inter-particle cross-linking were observed, however, there was no sign of the formation of hydrogel.

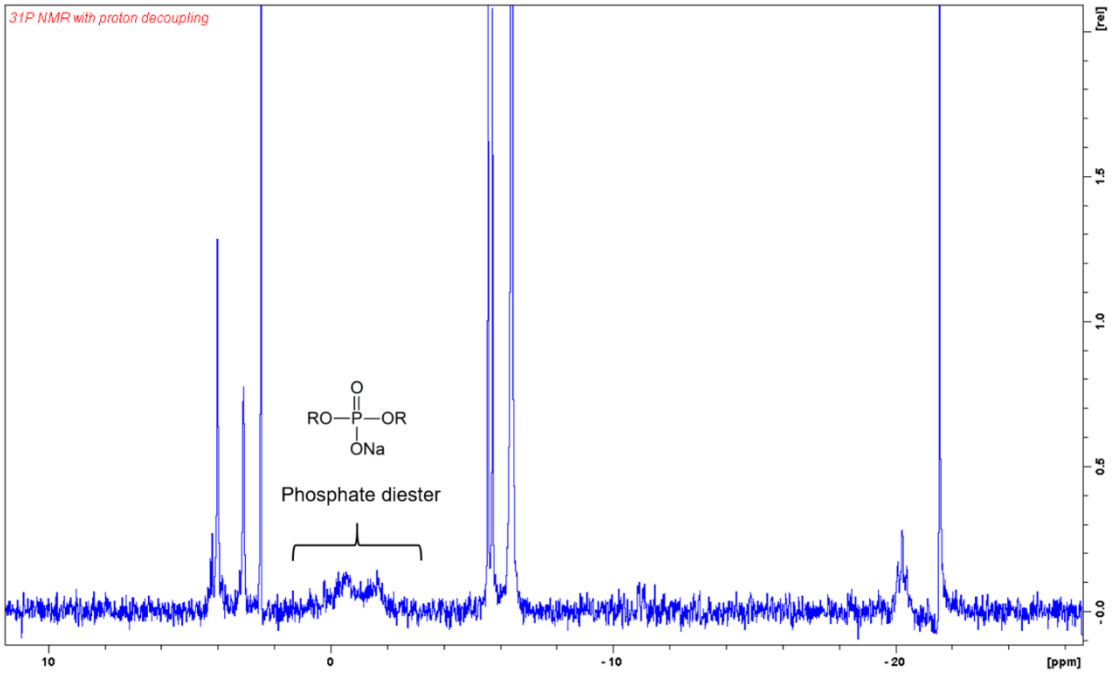

Figure 5.1 Typical ^{31}P-NMR spectrum of cross-linked SNPs ([SNP] = 15 wt.%, [STMP] = 1 wt.%, initial pH = 11, reaction time = 1 h).

Vinyl functionalization was then performed using 3 wt.% of FSM (relative to SNPs) for one hour. Filtered, functionalized SNPs were analyzed with ^{1}H-NMR spectroscopy to verify the attachment of the FSM and measure bonding efficiency, which represents the percentage of FSM attached to SNPs (Figure 5.2). In Figure 5.2, the peak spanning 5.7 to 5.9 ppm represents the vinyl groups, and the peaks spanning 0.6 to 1.7 ppm correspond to carbon

chains. This indicates that the FSM attached to the SNP surfaces. Bonding efficiency was calculated to be 42.9% using a method developed previously.[35]

The final modification step involved the copolymerization of the vinyl-functionalized SNPs with BVE ("tie-layer" monomer), thereby tuning the SNPs' hydrophobicity.[34,35] We have previously shown that the addition of BVE not only lowers latex viscosity, but also facilitates the incorporation of SNPs.[35] The final modified SNPs were characterized using ^{1}H-NMR spectroscopy, where peaks corresponding to BVE copolymer (5.5 to 7.0 ppm) were identified (Figure 5.2).

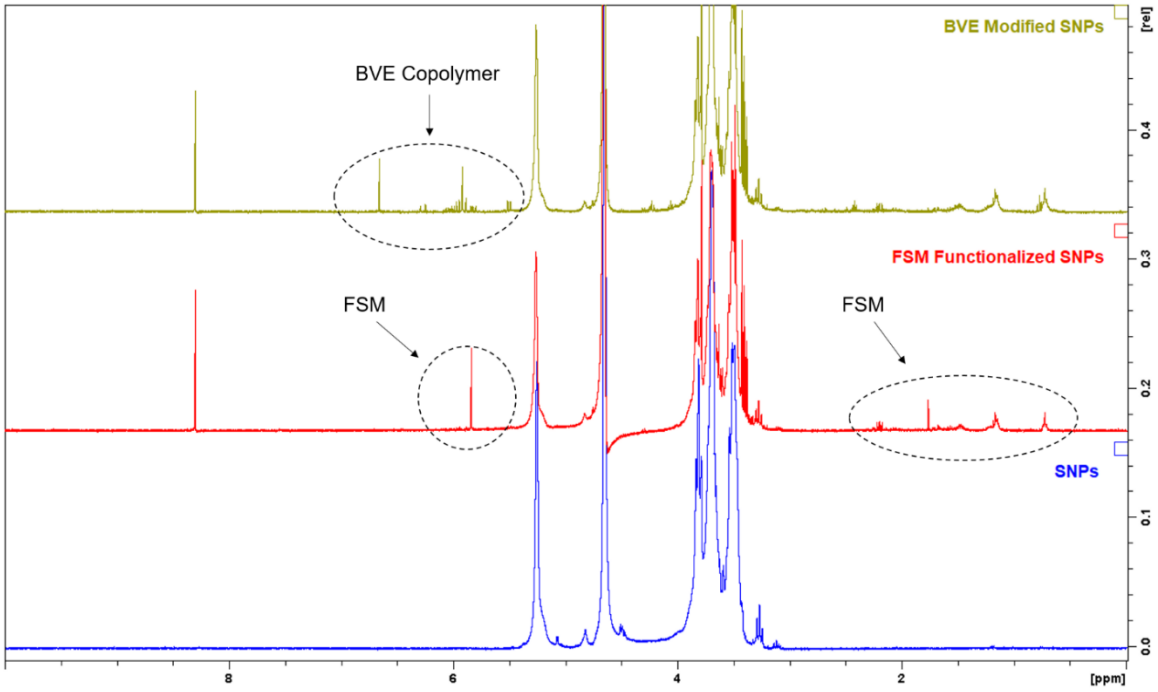

Figure 5.2 ^{1}H-NMR spectra of SNP, FSM-functionalized SNPs (filtered), and BVE-modified SNPs.

Semi-batch emulsion polymerization

The modified SNPs were used in semi-batch emulsion polymerizations at various SNP loadings and latex solids contents (Table 5.2). In all runs, surfactant concentration in the pre-emulsion, as well as the initiator concentration in the feed (relative to acrylic monomers), were kept constant. Latex solids contents at 40, 50 and 55 wt.% were tested, while SNP loadings were varied from 15 to 60 wt.% (based on total mass of solids). The typical overall monomer conversion profile includes a brief inhibition period during the first 30 min, likely resulting from inhibitor in the AA and BVE (Figure 5.3).

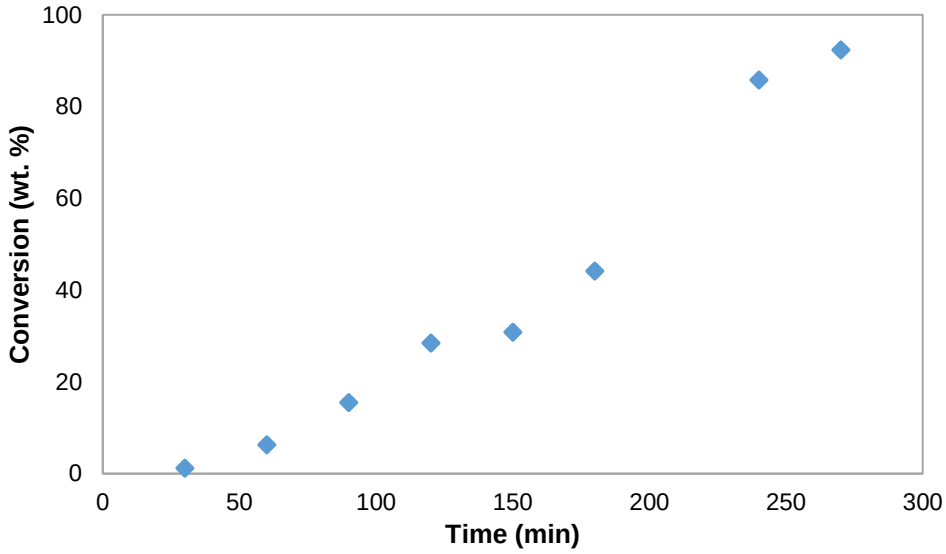

Figure 5.3 Typical overall monomer conversion vs. time trend (Run 4).

At 40 wt.% latex solids content, SNP loadings were varied from 15 to 60 wt.% (Runs 1 to 6). Stable and low viscosity (< 100 mPa.s) latexes were achieved for runs with SNP loadings of 15 to 45 wt.%. When the SNP loading was increased to 55 wt.%, a stable and low viscosity latex was produced, however, conversion was limited to only 50 wt.% at the end of the designed reaction time. Because the concentration of SNPs (32 wt. %) was high,

the viscosity of the SNP solution increased, and this made it difficult to properly mix the reaction mixture. Also, as the number of SNP particles increased, more initiator-derived radicals were likely consumed in hydrogen abstraction reactions rather than by reaction with the acrylic monomer; this would lower the polymerization rate and monomer conversion.[13,34,39] When SNP loading was further increased to 60 wt.%, phase separation of the latex was observed, which correlates with the increased consumption of initiator-derived radicals by the SNPs.

For the stable runs (Runs 1-4), the final latex particle size increased with SNP loading (Figure 5.4). In general, during polymerization, particle size increased with reaction time, while polydispersity index underwent a steady decrease to a constant value of ~0.1 by the end of the polymerization (Figure 5.4). One additional observation was that with increasing SNP loading, the time required during the polymerization to achieve stable latex particles was extended (Figure 5.5). Prior to polymerization, the SNP solutions yielded a bimodal particle size distribution (Figure 5.6).[14,40,41] During the early, unstable stages of the polymerization, a bimodal particle size distribution was still observed. Once stable latex particles were formed, a single distribution of particle sizes was observed. For example, at 15 wt.% SNP loading (Run 1), the transition from a bimodal to unimodal distribution first occurred for the sample taken at a reaction time of 30 min, while at 55 wt.% SNP loading, this transition was observed at 240 min. At the beginning of the polymerization, the reaction mixture was composed of individual SNPs as well as SNP agglomerates, hence the bimodal particle size distribution. During the monomer pre-emulsion and initiator feed stages, the SNPs (individual and agglomerates) acted as latex

particle seeds as polymer chain growth emanated from the vinyl groups on the SNP surfaces. The particles emanating from individual SNPs were highly unstable, so those particles tended to coagulate quickly with other SNPs to reduce the oil-water interfacial area. Those particles were then stabilized by surfactant and generated stable latex particles. It was at this point that the unimodal particle size distribution was noted. In the case of high acrylic monomer concentrations, pure acrylic latex particles may have formed through normal nucleation mechanisms; these particles might be smaller compared with the SNP-based particles, but were on the same order of magnitude of the particles nucleated from SNPs and formed part of the same distribution. This proposed mechanism is supported by the STEM images discussed later. When the SNP loading was increased, the available acrylic monomer per particle decreased, and as a result, the formation of stable latex particles, indicated by the unimodal particle size distribution, was delayed (Figure 5.5).

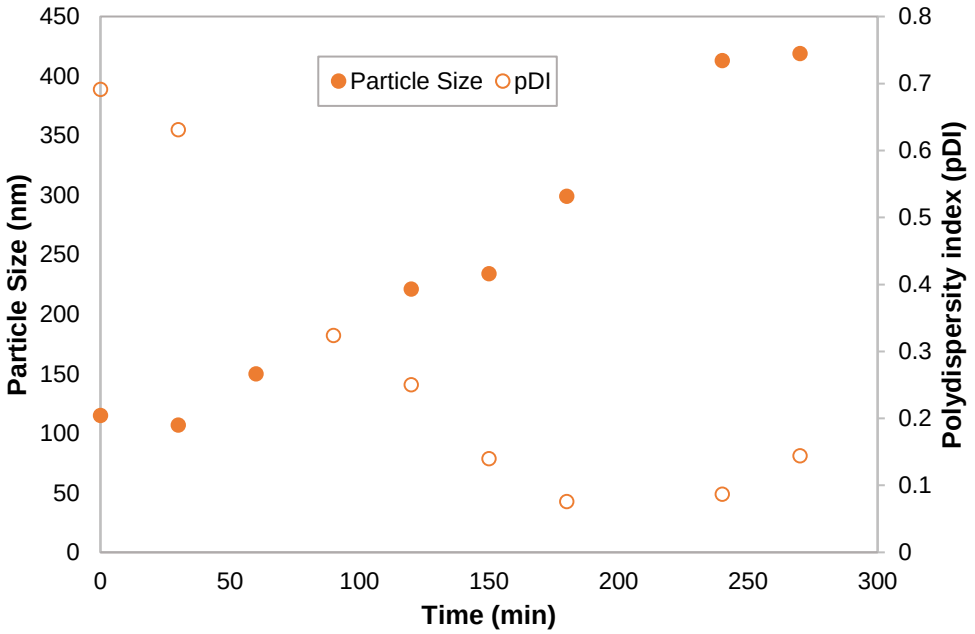

Figure 5.4 Typical particle size and polydispersity index trend with time (Run 2).

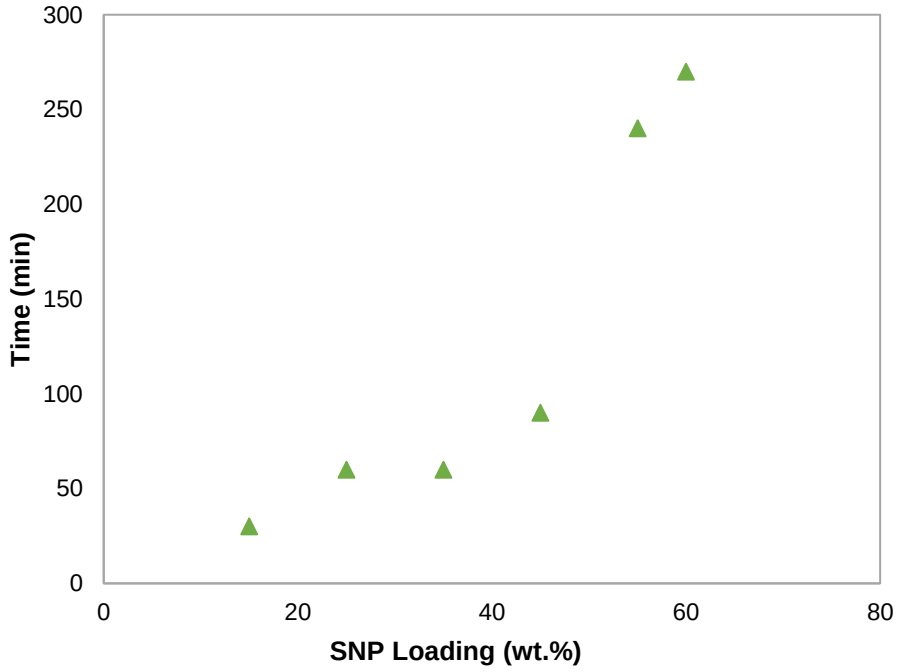

Figure 5.5 Stable latex particle formation time at various SNP loadings.

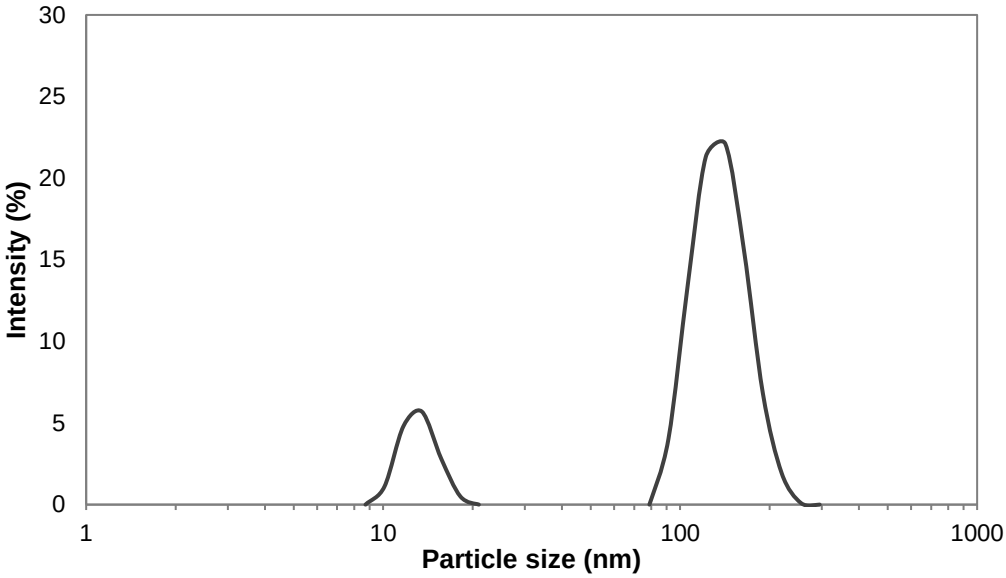

Figure 5.6 Typical particle size distribution of SNPs.

Similar to the observations at 40 wt.% solids, at 50 wt.% solids content, with the increase of SNP loading from 15 to 25 wt.% (Runs 7 to 9), both latex viscosity and particle size increased. Comparing Runs 2 (40 wt.% solids), 9 (50 wt.% solids) and 10 (55 wt.% solids) at the same SNP loading, latex viscosity increased dramatically with solids content, and latex particle size also increased. In summary, stable SNP-based latexes were produced with up to 45 wt.% SNP loading and up to 55 wt.% latex solids. At each latex solids content, there is a limit to the achievable SNP loading. Latex stability limits are reached because of the lower polymerization rate and increased viscosity due to the presence of the SNPs.

Latex particle morphology was studied with STEM imaging (Figure 5.7). In general, core-shell particle morphologies were observed in latexes with SNP loadings of 15 to 45 wt.% (Runs 1 to 4); free SNPs were not observed, in all cases. This proved that significant encapsulation of SNPs was achieved in latexes with up to 45 wt.% SNP loadings at 40 wt.%

solids content. At a 15 wt.% SNP loading, some pure acrylic particles (particles with no dark core, Figure 5.7a) were observed and those pure acrylic particles were smaller compared with the core/shell latex particles. Fewer pure acrylic polymer particles were observed for latexes at a 25 wt.% SNP loading (Figure 5.7b), while at 35 and 45 wt.% SNP loadings (Figure 5.7c and 5.7d), no pure acrylic polymer particles were observed. The latex particle sizes measured from STEM images concurred with that from DLS measurements: at lower SNP loadings, there were more smaller particles, while the population of larger particles grew with SNP loading (Figure 5.8). Furthermore, the average ratio of particle shell thickness to overall particle diameter decreased with increasing SNP loading. At low SNP loadings, more acrylic monomer was available so that both pure acrylic polymer particles and core/shell particles were observed. At the same time, when SNP concentration was lower, smaller particles were formed and on average, the ratio of shell thickness to particle diameter was higher. However, when SNP loading was further increased, less or no pure acrylic latex particles were noticed, the acrylic polymer shell thickness decreased, and particle size, as well the core diameter, increased.

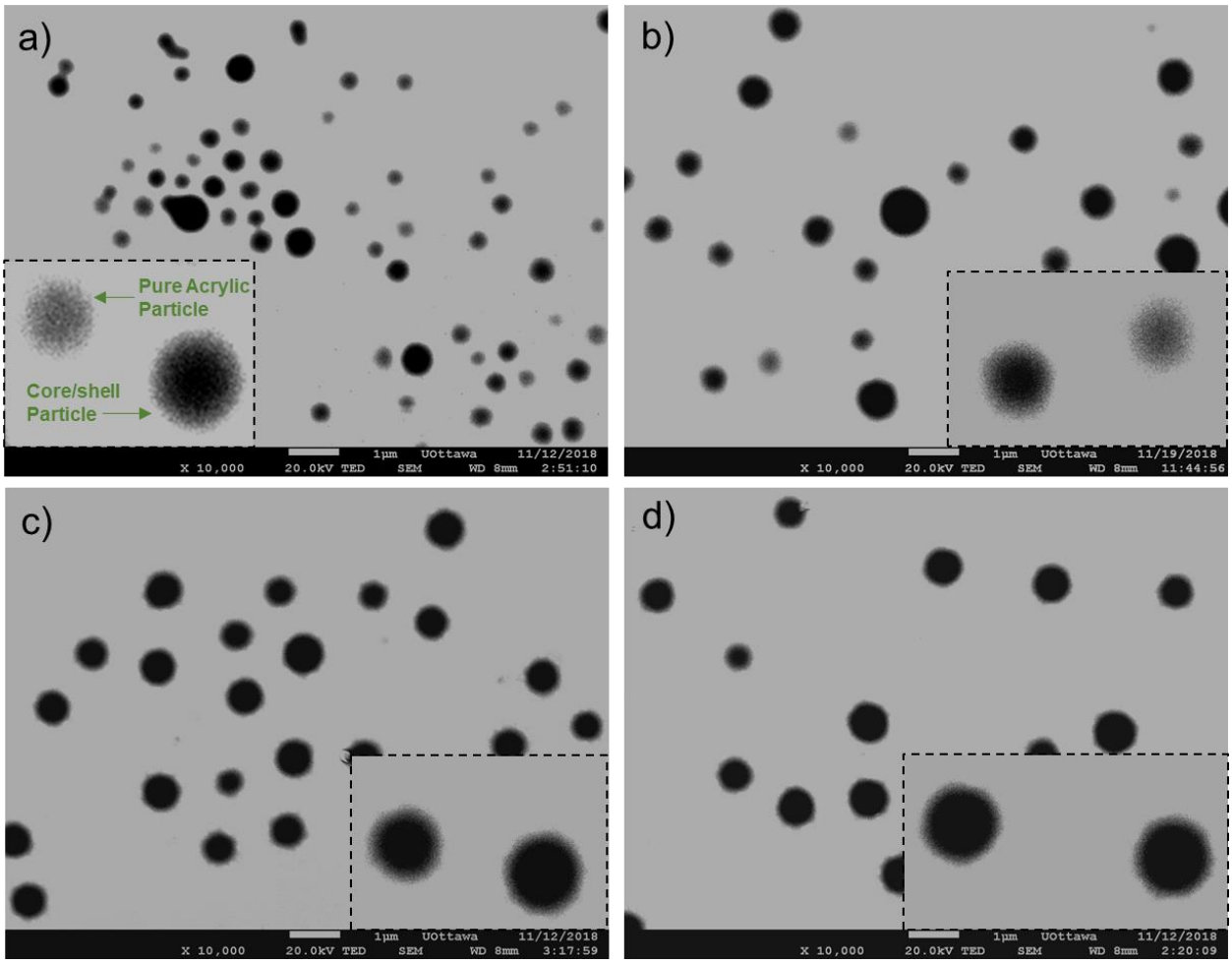

Figure 5.7 Latex particles morphology changes with SNP loadings: a) 15 wt.% SNP loading (Run 1); b) 25 wt.% SNP loading (Run 2); c) 35 wt.% SNP loading (Run 3); d) 45 wt.% SNP loading (Run 4).

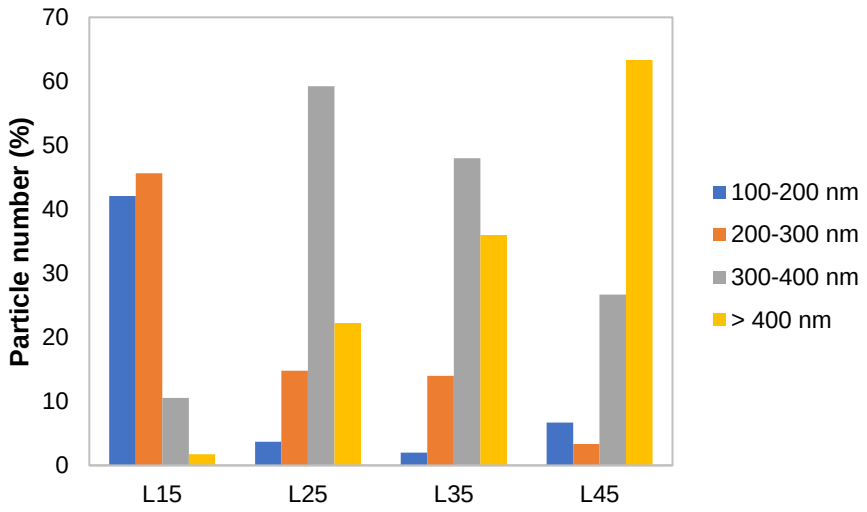

Figure 5.8 Particle size distribution at various SNP loadings.

Adhesive properties (i.e., shear strength, peel strength and tack) of the latexes with different SNP loadings were compared (Figure 5.9-5.11). Tack indicates "stickiness" of the adhesives when it first comes into contact with the substrate and depends on the interfacial and bulk properties of the materials. Peel strength measures the force required to peel away an adhesive strip from the substrate and is related to the film viscoelastic and surface properties. Shear strength represents the adhesive resistance to shearing forces and refers to cohesive strength.[42,43]

Due to the low viscosity of the latexes at 40 wt.% solids contents (Runs 1 to 4), it was not possible to cast consistent adhesive films for adhesive testing. Testable adhesive films were prepared using latexes from Runs 7 to 9. All adhesive properties decreased with increased SNP loading (Figure 5.9-5.11). As discussed above, when increasing SNP loading, the amount of acrylic monomer available per particle was decreased. This would reduce the thickness of the acrylic polymer shell relative to the total particle diameter and

eventually result in incomplete coverage of the SNP surfaces. This would be a likely cause of reduced adhesive properties. In a previous study, we demonstrated that at 15 wt.% SNP loading and 42 wt.% solids content, tack and peel strength increased compared to an acrylic base case formulation.[35] Thus, pushing the limits of SNP loadings, while maintaining latex stability, may come at a cost to adhesive and likely other properties. Nevertheless, it is possible to take corrective action to compensate for these property changes by adjusting the SNP cross-linking density and/or the microstructure of the acrylic shell polymers.[35,43]

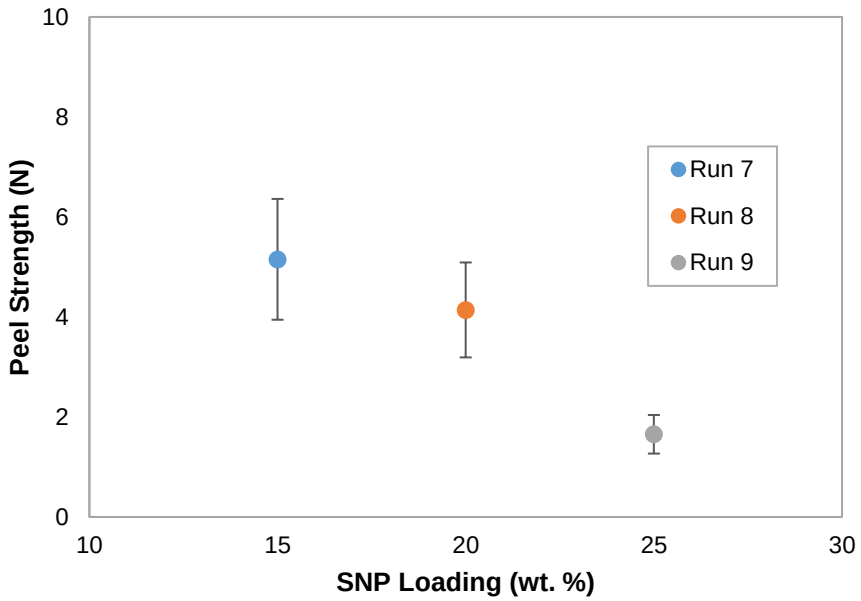

Figure 5.9 The effect of SNP loading on peel strength.

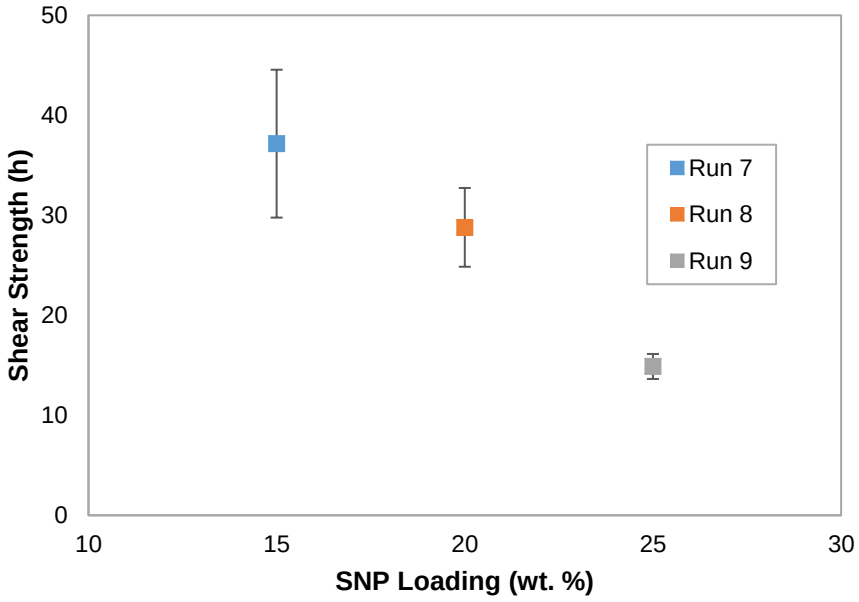

Figure 5.10 The effect of SNP loading on shear strength.

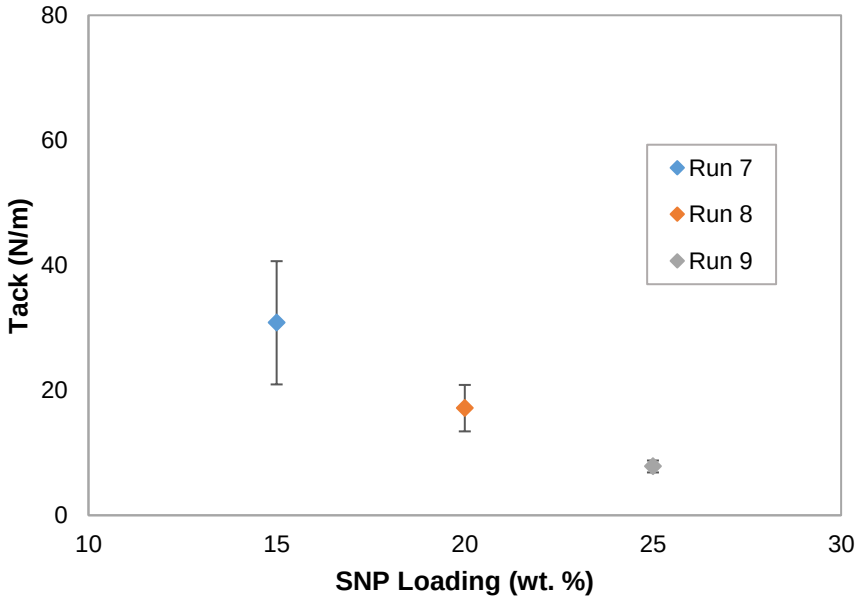

Figure 5.11 The effect of SNP loading on tack.

Barrier properties of the dried latex/SNPs samples to THF and water were tested (Table 5.3), where pure acrylic latex and modified SNPs were used as reference materials. The dried latex/SNP films became more resistant to THF and less so to water with increasing SNP content (Table 5.3). Significant change in the water barrier property was only noticed when SNP loadings reached 45 wt.%. This may be an indication that SNP particles may not have been completely covered by acrylic polymer or that the acrylic polymer shell thickness was low, so once latex particles were swollen in water, SNPs may have leached out while shaking.

Table 5.3 THF and water resistance properties at different SNP loadings.

Sample	SNP Loading (wt.%)	THF Insoluble (wt.%)	Water Insoluble (wt.%)
Acrylic latex	0	60	98
Run 1	15	69	95
Run 2	25	72	88
Run 3	35	72	82
Run 4	45	75	56
Run 5	55	91	20
SNPs	100	98	0

Conclusion

Bio-sourced latexes with up to 45 wt.% SNP loadings and 55 wt.% latex solids contents have been produced via semi-batch emulsion polymerization. To facilitate the

incorporation of SNPs into latex particles, SNPs were modified by increasing cross-link density, attaching vinyl functional groups and introducing a “tie-layer” monomer. Emulsion formulations with various SNP loadings and latex solids contents were applied to investigate their effect on latex stability and properties. With the increase of SNP loading or latex solids content, latex viscosity and particle size increased. Furthermore, the time required to form stable latex particles extended when SNP loading was increased, as a result of decreased acrylic monomer concentration. STEM images confirmed the presence of core/shell (SNPs core/acrylic polymer shell) particle morphologies for latexes with up to 45 wt.% SNP loadings at 40 wt.% solids content, and acrylic shell thickness (relative to total particle diameter) decreased when SNP loading was increased. Adhesive property tests from this and our previous study indicate that although it is possible to obtain SNP-based latexes with good adhesive properties, pushing the limits of SNP loading will inevitably influence the latex adhesive properties. However, one can adjust the SNP cross-link density and/or the microstructure of the acrylic shell polymer to fine tune the adhesive properties of SNP-based latexes.[35,43] Nevertheless, significant amounts of SNPs (up to 45 wt.%) have been encapsulated in latex particles to achieve a core/shell particle morphology and a low viscosity (<100 mPa.s) latex. This overcomes two typical challenges when introducing SNPs into emulsion formulations.[13,32,34,36,44]

Acknowledgments

Financial support for this work through the Natural Sciences and Engineering Research Council (NSERC) of Canada and EcoSynthetix Inc. (Burlington, ON) is gratefully acknowledged.

References

(1) Ojeda, T. Polymers and the Environment. Polym. Sci. 2013.

(2) Duval, C. Plastic Waste and the Environment. In *Environmental Impact of Polymers*; Wiley-Blackwell, 2014; pp 13–25.

(3) Asher, S. A. *Technology and Applications of Polymers Derived from Biomass*; Elsevier, 2018.

(4) Zhang, Y.; Dubé, M. A. Green Emulsion Polymerization Technology. In *Advances in Polymer Science*; Advances in Polymer Science; Springer, Berlin, Heidelberg, 2017; pp 1–36.

(5) Belgacem, M. N.; Gandini, A. *Monomers, Polymers and Composites from Renewable Resources*; Elsevier: Oxford, UK, 2008; Vol. first.

(6) Shanks, B. H.; Keeling, P. L. Bioprivileged Molecules: Creating Value from Biomass. Green Chem. 2017, 19, 3177–3185.

(7) Web of Science http://apps.webofknowledge.com (accessed Oct 16, 2018).

(8) Global Industrial Starch Market | Size | Share | Trend | Research | Statics | Growth | Value | Analysis | Industrial Starch Market Industry Competitiveness https://www.mordorintelligence.com/industry-reports/industrial-starches-market (accessed Oct 16, 2018).

(9) Carvalho, A. J. F. Chapter 15 - Starch: Major Sources, Properties and Applications as Thermoplastic Materials. In *Monomers, Polymers and Composites from Renewable Resources*; Gandini, A., Ed.; Elsevier: Amsterdam, 2008; pp 321–342.

(10) Regina, A.; Li, Z.; Morell, M. K.; Jobling, S. A. Chapter 2 - Genetically Modified Starch: State of Art and Perspectives. In *Starch Polymers*; Halley, P. J., Avérous, L., Eds.; Elsevier: Amsterdam, 2014; pp 13–29.

(11) Ahmed, J. *Starch-Based Polymeric Materials and Nanocomposites Chemistry, Processing, and Applications*; Boca Raton: CRC Press, 2012.

(12) Dragan, E. S.; Loghin, D. F. A.; Cocarta, A.-I.; Doroftei, M. Multi-Stimuli-Responsive Semi-IPN Cryogels with Native and Anionic Potato Starch Entrapped in poly(N,N-

Dimethylaminoethyl Methacrylate) Matrix and Their Potential in Drug Delivery. React. Funct. Polym. 2016, 105, 66–77.

(13) Cummings, S.; Cunningham, M.; Dubé, M. A. The Use of Amylose-rich Starch Nanoparticles in Emulsion Polymerization. J. Appl. Polym. Sci. 135, 46485.

(14) Cummings, S. The Incorporation of Vinyl Modified Regenerated Starch Nanoparticles in Emulsion Polymerizations. Ph.D. Thesis, University of Ottawa, 2017.

(15) Haaj, S. B.; Thielemans, W.; Magnin, A.; Boufi, S. Starch Nanocrystal Stabilized Pickering Emulsion Polymerization for Nanocomposites with Improved Performance. ACS Appl. Mater. Interfaces 2014, 6, 8263–8273.

(16) Sanchez de la Concha, B. B.; Agama-Acevedo, E.; Nuñez-Santiago, M. C.; Bello-Perez, L. A.; Garcia, H. S.; Alvarez-Ramirez, J. Acid Hydrolysis of Waxy Starches with Different Granule Size for Nanocrystal Production. J. Cereal Sci. 2018, 79, 193–200.

(17) Saari, H.; Fuentes, C.; Sjöö, M.; Rayner, M.; Wahlgren, M. Production of Starch Nanoparticles by Dissolution and Non-Solvent Precipitation for Use in Food-Grade Pickering Emulsions. Carbohydr. Polym. 2017, 157, 558–566.

(18) Liu, D.; Wu, Q.; Chen, H.; Chang, P. R. Transitional Properties of Starch Colloid with Particle Size Reduction from Micro- to Nanometer. J. Colloid Interface Sci. 2009, 339, 117–124.

(19) Song, D.; Thio, Y. S.; Deng, Y. Starch Nanoparticle Formation via Reactive Extrusion and Related Mechanism Study. Carbohydr. Polym. 2011, 85, 208–214.

(20) Haaj, S. B.; Magnin, A.; Boufi, S. Starch Nanoparticles Produced via Ultrasonication as a Sustainable Stabilizer in Pickering Emulsion Polymerization. RSC Adv 2014, 4, 42638–42646.

(21) Smeets, N. M. B.; Imbrogno, S.; Bloembergen, S. Carbohydrate Functionalized Hybrid Latex Particles. Carbohydr. Polym. 2017, 173, 233–252.

(22) Meimoun, J.; Wiatz, V.; Saint-Loup, R.; Parcq, J.; Favrelle, A.; Bonnet, F.; Zinck, P. Modification of Starch by Graft Copolymerization. Starch - Stärke 2018, 70, 1600351.

(23) Ačkar, Đ.; Babić, J.; Jozinović, A.; Miličević, B.; Jokić, S.; Miličević, R.; Rajič, M.; Šubarić, D. Starch Modification by Organic Acids and Their Derivatives: A Review. Mol. Basel Switz. 2015, 20, 19554–19570.

(24) Namazi, H.; Fathi, F.; Heydari, A. Nanoparticles Based on Modified Polysaccharides. 2012.

(25) Lin, N.; Huang, J.; Chang, P. R.; Anderson, D. P.; Yu, J. Preparation, Modification, and Application of Starch Nanocrystals in Nanomaterials: A Review. J. Nanomater. 2010, e573687.

(26) Fan, Y.; Cao, H.; van Mastrigt, F.; Pei, Y.; Picchioni, F. Copper-Mediated Homogeneous Living Radical Polymerization of Acrylamide with Waxy Potato Starch-Based Macroinitiator. Carbohydr. Polym. 2018, 192, 61–68.

(27) Carlmark, A.; Larsson, E.; Malmström, E. Grafting of Cellulose by Ring-Opening Polymerisation – A Review. Eur. Polym. J. 2012, 48, 1646–1659.

(28) Noordergraaf, I.-W.; Fourie, T.; Raffa, P.; Noordergraaf, I.-W.; Fourie, T. K.; Raffa, P. Free-Radical Graft Polymerization onto Starch as a Tool to Tune Properties in Relation to Potential Applications. A Review. Processes 2018, 6, 31.

(29) Pei, X.; Tan, Y.; Xu, K.; Liu, C.; Lu, C.; Wang, P. Pickering Polymerization of Styrene Stabilized by Starch-Based Nanospheres. Polym. Chem. 2016, 7, 3325–3333.

(30) Cheng, L.; Guo, H.; Gu, Z.; Li, Z.; Hong, Y. Effects of Compound Emulsifiers on Properties of Wood Adhesive with High Starch Content. Int. J. Adhes. Adhes. 2017, 72, 92–97.

(31) Sorrentino, A.; Gorrasi, G.; Vittoria, V. Potential Perspectives of Bio-Nanocomposites for Food Packaging Applications. Trends Food Sci. Technol. 2007, 18, 84–95.

(32) Pei, X.; Zhai, K.; Liang, X.; Deng, Y.; Xu, K.; Tan, Y.; Yao, X.; Wang, P. Fabrication of Shape-Tunable Macroparticles by Seeded Polymerization of Styrene Using Non-Cross-Linked Starch-Based Seed. J. Colloid Interface Sci. 2018, 512, 600–608.

(33) Baruch-Teblum, E.; Mastai, Y.; Landfester, K. Miniemulsion Polymerization of Cyclodextrin Nanospheres for Water Purification from Organic Pollutants. Eur. Polym. J. 2010, 46, 1671–1678.

(34) Cummings, S.; Trevino, E.; Zhang, Y.; Cunningham, M.; Dubé, M. A. Incorporation of Modified Regenerated Starch Nanoparticles in Emulsion Polymer Latexes. Starch - Stärke 2018, 71, 1800192.

(35) Zhang, Y.; Cunningham, M. F.; Smeets, N. M. B.; Dubé, M. A. Starch Nanoparticle Incorporation in Latex-Based Adhesives. Eur. Polym. J. 2018, 106, 128–138.

(36) Kumar, M. N. S.; Siddaramaiah. Studies on Cornstarch-Filled Poly(styrene-Co-Butyl Acrylate) Latex-Reinforced Polyester Nonwoven Fabric Composites. J. Reinf. Plast. Compos. 2005, 24, 1985–1994.

(37) Lack, S.; Dulong, V.; Picton, L.; Cerf, D. L.; Condamine, E. High-Resolution Nuclear Magnetic Resonance Spectroscopy Studies of Polysaccharides Crosslinked by Sodium Trimetaphosphate: A Proposal for the Reaction Mechanism. Carbohydr. Res. 2007, 342, 943–953.

(38) Sang, Y.; Prakash, O.; Seib, P. A. Characterization of Phosphorylated Cross-Linked Resistant Starch by ^{31}P Nuclear Magnetic Resonance (^{31}P NMR) Spectroscopy. Carbohydr. Polym. 2007, 67, 201–212.

(39) Li, M.-C.; Ge, X.; Cho, U. R. Emulsion Grafting Vinyl Monomers onto Starch for Reinforcement of Styrene-Butadiene Rubber. Macromol. Res. 2013, 21, 519–528.

(40) Le Corre, D.; Angellier-Coussy, H. Preparation and Application of Starch Nanoparticles for Nanocomposites: A Review. React. Funct. Polym. 2014, 85, 97–120.

(41) Akhavan, A.; Ataeevarjovi, E. The Effect of Gamma Irradiation and Surfactants on the Size Distribution of Nanoparticles Based on Soluble Starch. Radiat. Phys. Chem. 2012, 81, 913–914.

(42) Benedek, I. *Pressure-Sensitive Adhesives And Applications*; Marcel Dekker Inc: Hoboken, 2004.

(43) Jovanović, R.; Dubé, M. A. Emulsion-Based Pressure-Sensitive Adhesives: A Review. J. Macromol. Sci. Part C 2004, 44, 1–51.

(44) Zia-ud-Din; Chen, L.; Ullah, I.; Wang, P. K.; Javaid, A. B.; Hu, C.; Zhang, M.; Ahamd, I.; Xiong, H.; Wang, Z. Synthesis and Characterization of Starch-G-Poly(vinyl Acetate-Co-Butyl Acrylate) Bio-Based Adhesive for Wood Application. Int. J. Biol. Macromol. 2018, 114, 1186–1193.

6. Modification of Adhesive and Latex Properties for Starch Nanoparticle-based Pressure Sensitive Adhesives

Chapter 6 contains a manuscript accepted by Macromolecular Reaction Engineering on July 29, 2019.

Modification of Adhesive and Latex Properties for Starch Nanoparticle-based Pressure Sensitive Adhesives

Yujie Zhang, Michael F. Cunningham, Marc A. Dubé *

Yujie Zhang, Prof. Marc A. Dubé

Department of Chemical and Biological Engineering, Centre for Catalysis Research and Innovation, University of Ottawa, 161 Louis Pasteur Pvt., Ottawa, Ontario, K1N 6N5, Canada

Prof. Michael F. Cunningham

Department of Chemical Engineering, Queen's University, 99 University Ave, Kingston

Abstract

Starch nanoparticle (SNP)-based pressure sensitive adhesives (PSAs) with core-shell particle morphology (starch nanoparticle core/acrylic polymer shell) are produced via seeded, semi-batch emulsion polymerization at 15 wt% SNP loading (relative to total polymer weight) and 40 wt% latex solids. Crosslinker and chain transfer agent (CTA) are introduced to the acrylic shell polymer formulation at a range of concentrations according to a 3^2 factorial design to tailor the latex and adhesive properties of SNP-based latexes. The crosslinker and CTA show no significant effect on polymerization kinetics, particle size and viscosity. Latex gel content is predicted using an empirical model, which is a function of crosslinker and CTA concentration. Both the gel content and glass transition temperature strongly affect the adhesive properties (tack, peel strength and shear strength) of the SNP-based latex films. 3D response surfaces for the adhesive properties are constructed to facilitate the design of SNP-based PSAs with desired properties.

Keywords: starch, adhesives, emulsion polymerization, core-shell polymers, microstructure

Introduction

Pressure sensitive adhesives (PSAs) are viscoelastic polymers able to stick to most surfaces with light contact at room temperature.[1,2] Generally, there are no chemical reactions or physical changes involved in the adhesion process. PSAs can be produced from solution polymerization, emulsion polymerization and hot melt processes. However, emulsion-based PSAs are considered a more sustainable approach because of the use of water as a dispersing medium rather than a potentially toxic solvent.[3]

PSA performance is evaluated by tack, peel strength and shear strength. Those properties can be finely tuned by varying polymer composition, and hence, the glass transition temperature (T_g), and the polymer microstructure (e.g., molecular weight, gel content). One essential feature of PSAs is that their Tg should be 25 to 45 ℃ lower than the usage temperature.[2] Acrylate monomers with long alkyl chain lengths tend to enhance tack, while those with short alkyl chain lengths improve cohesive strength, a property expressed by shear strength.[1] Monomers with polar groups may exhibit strong cohesion due to hydrogen bonding. To improve the shear strength of PSAs, crosslinkers and fillers can be added.[4] An interesting conundrum arises in latex-based PSAs wherein, increasing the shear strength of a PSA typically leads to a reduction in peel strength and tack.[5] Significant experimental effort has been made to overcome this conundrum.[6,7]

Commercial PSAs are dominated by acrylic polymers, styrenic block copolymers and natural rubbers, which are mainly derived from petroleum resources.[8] Given the associated environmental concerns and the depletion of petroleum resources,

development of more sustainable PSAs has become necessary.[8–10] One direct approach is to replace petroleum-based monomers with those obtained from natural resources (e.g., starch, vegetable oils, cellulose, lignin). Thus, we introduced starch nanoparticles (SNP) into conventional emulsion formulations to produce a core-shell (starch core/acrylic polymer shell) latex particles for PSA applications.[11,12] It was shown that the straightforward addition of SNPs in a blend with an acrylic latex yielded poor tack and peel strength results (but good shear strength results), due to the poor interaction between the SNPs and stainless steel substrate used for adhesive testing. Thus, we developed an approach to produce core-shell (SNP core/acrylic polymer shell) latex particles for PSA applications thereby avoiding direct contact between the SNPs and the stainless steel substrate.[11] However, the challenge remains to achieve SNP-based latexes with a wider range of adhesive properties thereby expanding their applicability. For instance, we were able to achieve stable SNP-based latexes (15 wt% SNP loading, 40 wt% solids) with better peel strength and tack compared with that of their pure acrylic counterparts, but their shear strength was lower. As the acrylic polymers on the shell contributed mostly to the adhesive properties of these latexes, this offers many possibilities to further tailor the adhesive properties of SNP-based latexes by controlling the microstructure of the shell polymer.[13–17]

The addition of crosslinker and/or chain transfer agent (CTA) is an effective approach to carefully manipulate polymer microstructure.[18–22] The use of crosslinker should increase gel content, and thus enhance cohesive strength. On the other hand, CTA decreases molecular weight, and hence, improves the flexibility and mobility of the polymer chains,

which results in better adhesion. In general, crosslinker and CTA are used individually.[16,23] Nevertheless, studies have shown that the combined use of crosslinker and CTA can yield unique polymer microstructures and facilitate polymer property optimization.[15,18,19,24] Those studies were mainly performed on conventional emulsion polymerization formulations targeting pure acrylic latex particles.

In this work, we report the combined use of crosslinker and CTA to tailor the acrylic shell polymer microstructure to achieve SNP-based core-shell latex particles with a range of properties. A series of SNP-based latexes with 15 wt% SNP loading (relative to total polymer weight) and 40 wt% solids was produced via seeded, semi-batch emulsion polymerization. A factorial design methodology was applied to various concentrations and combinations of crosslinker and CTA to investigate their effect on particle size, viscosity, gel content, T_g, viscoelastic properties, latex morphology and adhesive properties.

Materials and Methods

Materials

Experimental grade SNPs and functionalized sugar monomer (FSM) were provided by EcoSynthetix Inc. (Burlington, ON). Sodium trimetaphosphate (STMP), sodium bicarbonate ($NaHCO_3$), hydrochloric acid (HCl, 1M), sodium hydroxide (NaOH), butyl acrylate (BA, 99%), methyl methacrylate (MMA, 99%), acrylic acid (AA, 99.5%), butyl vinyl ether (BVE), 1-dodecanethiol (NDM, 98 %), allyl methacrylate (AMA, 98%), potassium

persulfate (KPS, 99%) and tetrahydrofuran (THF, 99%) were purchased from Sigma-Aldrich. EF-800 (49-51 wt% aqueous solution) was provided by Cytec Industries. BA was purified by passing through an inhibitor removal column and stored at 4 ℃; all other chemicals were used as received. Distilled deionized water (DDW) was used throughout this work. Nitrogen gas (GR4.8, Linde Canada) was used to purge the reactor to remove oxygen.

Modification of SNPs

To achieve the encapsulation of SNPs, experimental grade SNPs were modified in a glass RC1e reactor (500 mL, Mettler-Toledo) based on a procedure developed previously.[11,12] SNPs were first crosslinked with 1 wt% STMP and 3 wt% NaHCO3 at pH 10.5 ± 0.1 for two hours at 60 ℃. Then, 3 wt% FSM was added and allowed to react for another two hours, at 60 ℃, before the pH was adjusted to 4.5 ± 0.1. A "tie-layer" monomer, BVE, was introduced prior to semi-batch emulsion polymerization according to the procedure below.

Semi-batch Emulsion Polymerization

Modified SNPs were encapsulated into the acrylic polymer shell (BA/MMA/AA, 93/5/2, wt%) using a standard semi-batch emulsion polymerization formulation (Table 6.1).[11,12] All latexes had 15 wt% SNP loading (relative to total polymer weight) and 40 wt% latex solids. Polymerization was performed at 60 ℃ under nitrogen atmosphere. FSM-modified SNPs were reacted with BVE, the "tie-layer" monomer, for 30 min in aqueous solution,

followed by the semi-batch feeding of monomer pre-emulsion and initiator solution (Table 6.1).

Table 6.1 Typical semi-batch emulsion polymerization formulation (0.4 phm CTA and 0.4 phm crosslinker).

Component	**Amount (g)**	**Amount (wt% based on final latex)**
SNP solution		
SNP	21.2	4.2
DDW	150.7	29.8
Initial charge		
BVE	4.7	0.9
KPS	0.4	0.1
DDW	11.7	2.3
Monomer pre-emulsion		
DDW	48.8	9.6
EF-800	9.7	1.9
BA	194.0	38.4
MMA	10.3	2.0
AA	4.5	0.9
NDM	0.8	0.2
AMA	0.8	0.2
Initiator feed solution		
DDW	46.1	9.1
KPS	2.0	0.4

During polymerization, samples were taken periodically to measure conversion and particle size. A series of experiments was performed with various amounts of AMA, crosslinker, and NDM, the CTA (Table 6.2). A 3^2 factorial design at various crosslinker and CTA concentrations (Run 1 – 9) was conducted, including the base case (Run 1) without crosslinker and CTA. Additional runs (Run 10 and 11) were conducted to confirm the proposed model. The concentrations of NDM and AMA ranged from 0 to 0.4 phm (relative to total acrylic monomer), and both were added in the monomer pre-emulsion.

Table 6.2 Experimental design and summary of results.

Run	AMA (phm)	NDM (phm)	Viscosity (mPa.s)	Particle Size (nm)	Gel Content (wt%)
1	0	0	95	304	63
2	0	0.4	107	297	32
3	0.4	0	110	334	99
4	0.2	0	97	307	98
5	0	0.2	104	280	35
6	0.2	0.2	112	293	64
7	0.4	0.4	107	287	68
8	0.4	0.2	112	280	83
9	0.2	0.4	125	295	34
10	0.1	0	109	291	89
11	0.3	0.2	100	298	78

Analytical methods

Solids content and conversion were measured using a gravimetric method.[11] To measure particle size, dynamic light scattering (DLS) with a Malvern NanoS Zetasizer at an angle of 173^{o} was used. Samples were prepared by diluting one drop of latex in 2 mL of DDW in a 4 mL polystyrene cuvette at ambient temperature. For each sample, three measurements were carried out; an average intensity-weighted particle size and polydispersity index were reported. Viscosity of the final latex was determined at room temperature using a Brookfield viscometer (spindle R4, 100 rpm). Latex particle morphology was observed using a scanning transmission electron microscope (STEM), a JEM-2100F FETEM (JEOL).[11,12]

Adhesive properties (i.e., 180^{o} peel strength, shear strength and loo tack) were tested following Pressure Sensitive Tape Council standards (PSTC, 2004) in a temperature- and humidity-controlled room (23 ± 1°C and 50% ± 5% RH).[25] Latex films were cast using Melinex 462 polyester films (Tekra). For the shear strength test, a contact area of 0.5 inch × 0.5 inch was used to minimize the test time. The gel content of the dried latex sample was measured using a poly(vinylidene fluoride) (PVDF) membrane with a pore size of 5 µm; purchased from EMD Millipore. Polymer samples were weighed (~ 0.02 g) and sealed in a membrane pouch, and then swelled in 30 mL THF in a glass jar. The glass jar was sealed for 24 h at room temperature and then kept in a wrist shaker for another two hours. The swollen samples were then dried at room temperature and weighed. The weight percentage of the dried sample relative to the original sample was reported. Replicates measurements were performed for selected samples to estimate the error.

The T_g of selected latex samples was measured using a Model Q1000 (TA Instruments) differential scanning calorimeter (DSC). About 8 mg of dried latex was weighed and sealed in a standard aluminum sample pan. The sample was first heated to 120 ℃ and held isothermally for 3 min, then cooled to -80 ℃ with a cooling rate of 10 ℃/min. Then the sample was held isothermally for 3 min at -80 ℃, before heated to 120 ℃ with a heating rate of 10 ℃/min. The average T_g was calculated using the T_g estimated from both heating and cooling cycles.

An RDA III rheometer (TA Instruments) with 25 mm parallel plate geometry was used to perform dynamic mechanical analysis (DMA). Around 10 g of latex was dried on silicon release paper in a petri dish for 3 weeks. The dried samples were then cut into 25 mm diameter circles at a thickness of 1.7 ± 0.2 mm. Frequency sweeps at 23 ℃ were performed over a frequency range of about 0.01 Hz - 80 with a strain of 1 %.

Results and discussion

Polymerization process

Stable and low viscosity latexes were achieved at various concentrations of crosslinker and CTA by conducting semi-batch emulsion polymerization using modified SNPs as seed (Table 6.1). No significant differences in polymerization kinetics were noticed in all runs (Figure 6.1). Particle size generally increased with reaction time (Figure 6.2). A unimodal particle size distribution (polydispersity below 0.15) was observed beyond the first sample for all runs, indicating that stable latex particles were formed in the first 30 min.

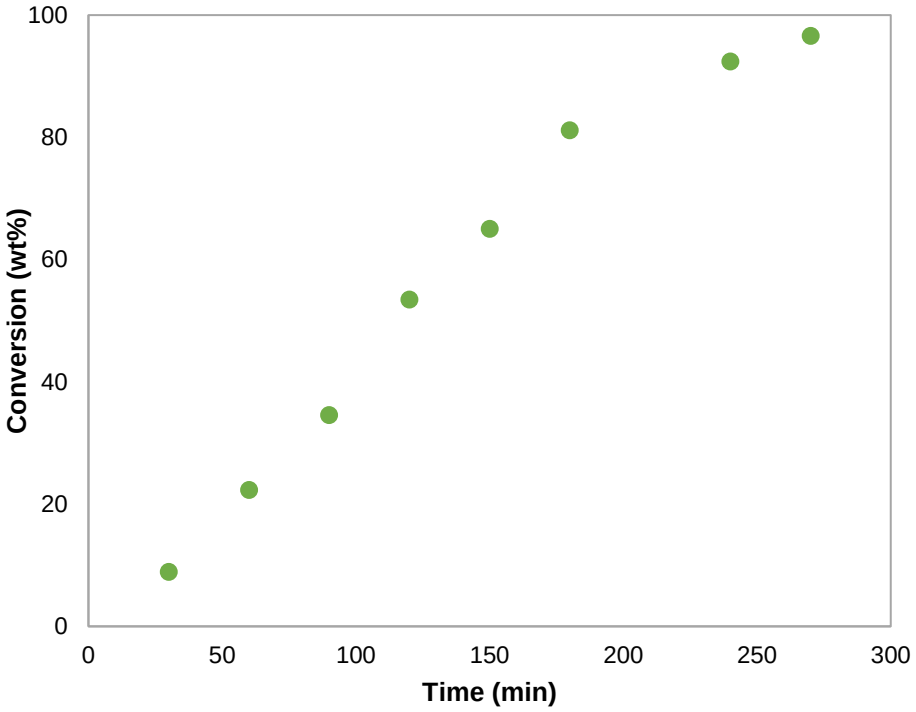

Figure 6.1 Typical overall conversion trend (Run 3).

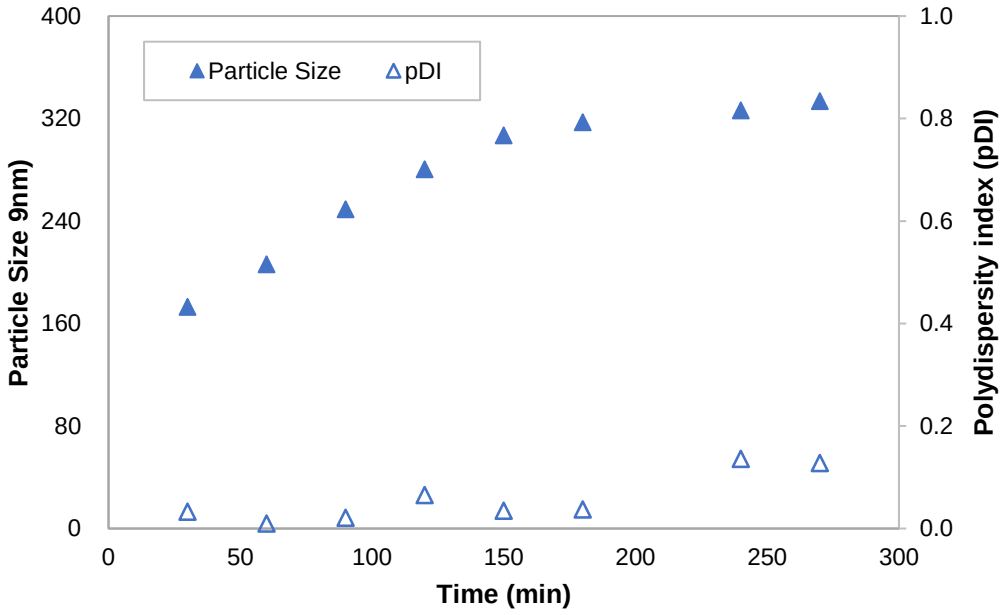

Figure 6.2 Typical particle size trend (Run 3).

In the case of Run 3 (0.4 phm AMA) and 4 (0.2 phm AMA), where only crosslinker was used, a small amount of brown grit (< 7.3 wt% relative to SNPs) was observed. To eliminate grit formation, AMA was then reduced to 0.1 phm (Run 10), however, there was still grit visible, albeit at a low level (< 2.5 wt% relative to SNPs). Further characterization indicated that brown grit was composed of both SNPs and acrylic polymers and resulted from the crosslinking of unstable particles.[26] For all runs including CTA, no grit was observed due to the reduction in crosslinking caused by the presence of CTA.

Gel content

The gel content of all dried latex samples was measured with an estimated error of 5%. It is possible to manipulate gel content over a wide range by changing the concentrations of AMA and NDM (Table 6.2). As expected, the addition of AMA increased the gel content, while introducing CTA reduced the gel content. Significant changes in gel content were observed when up to 0.2 phm AMA or NDM were used individually, the further addition of crosslinker or CTA only changed the gel content slightly. Based on the factorial design (Run 1 to 9, Table 6.2), an empirical model was developed using Minitab. A stepwise regression was used to simplify the model while maintaining its statistical significance (α = 0.05):

$$Gel\ content = 71.51 + 103.2\ AMA - 131.3\ NDM \quad (6.1)$$

From the model (Equation 6.1), it is seen that gel content increases with increasing crosslinker and decreasing CTA concentrations. Using equation 1 with 0.3 phm AMA and 0.2 phm NDM, a gel content of 76.2 wt% was predicted. These conditions were run (Run

11,Table 6.2) and the predicted gel content correlated well with the experimentally measured value of 78.2 wt%.

Glass transition temperature

The T_g of the dried latex samples were measured by DSC. Given the expected core-shell morphology of the latex particles, it was expected that two T_g values would be observed: one corresponding to the acrylic shell polymers ($T_{g,a}$), the other to the SNP cores ($T_{g,s}$). However, due to the low concentration of SNPs (15 wt%), the glass transition of the SNPs is not as obvious as that of the acrylic polymers in many cases (Figure 6.3). As the same SNP cores were applied to all latexes, while the microstructures of acrylic shell polymers were varied, the T_g of the acrylic polymers were of main interest. In general, the T_g of the acrylic polymers ranged from -51 to -43 ℃. With increasing gel content, the T_g increased slightly (Figure 6.4). This was expected as higher gel contents imply a more constrained polymer chain movement, and as a result, a higher T_g.[27]

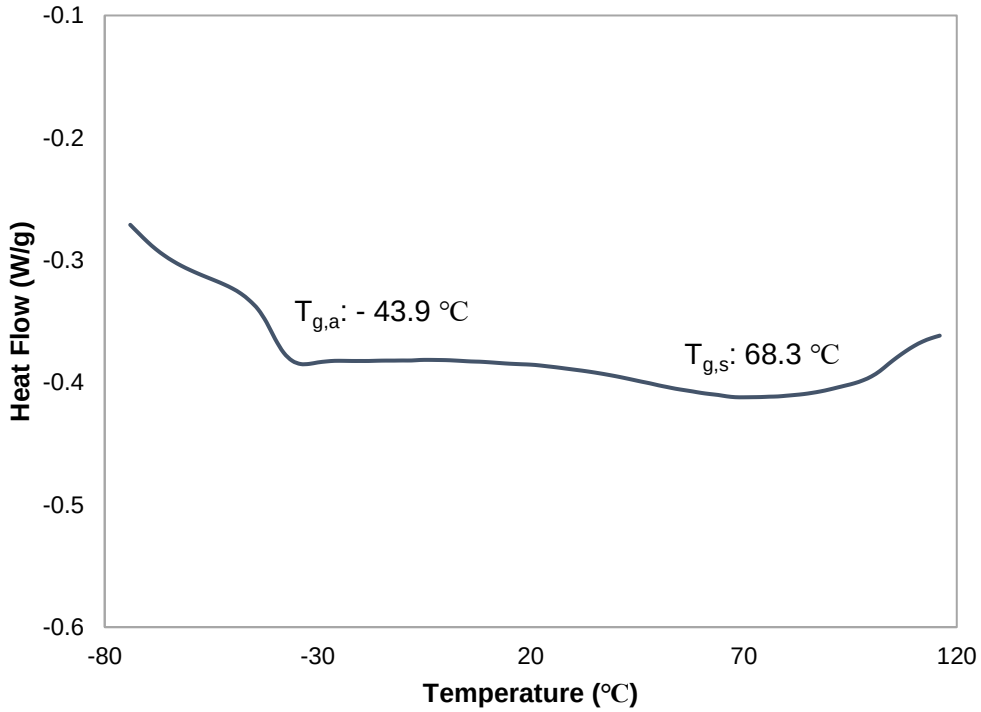

Figure 6.3 Typical DSC curves for SNP-based latexes (Run 8).

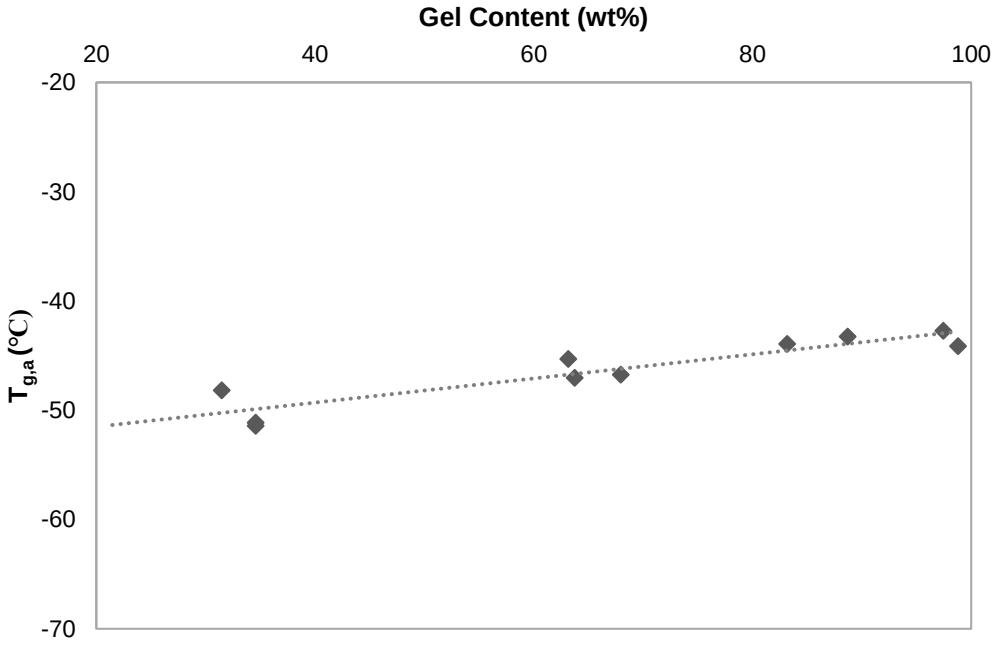

Figure 6.4 Correlation of gel content with Tg for acrylic shell polymers.

Latex morphology

STEM images were obtained for selected samples to confirm the effect of NDM and AMA on the core-shell latex particle morphology. In Figure 6.5, the STEM images of Run 2 (0.4 phm NDM, gel content of 31.5 wt%) and Run 3 (0.4 phm AMA, gel content of 98.8 wt%) are shown. Core-shell particles, as well as pure acrylic particles, were observed with no sign of free SNP particles, which implies that a considerable number of SNPs were encapsulated into latex particles. This was as expected from previous mass balance calculations that suggest the presence of more than enough acrylic polymer to ensure coverage of all SNPs.[11,12] The average size of the core-shell particles is much larger compared with that of the pure acrylic particles. For example, as seen in Figure 6.5b, the average size of core-shell latex particles was calculated to be 404 nm, while the average size of the pure acrylic latex particles was 117 nm. This observation is consistent with our previous studies.[11,12] There was no distinct difference in the latex particle morphologies of Run 2 (Figure 6.5a) and Run 3 (Figure 6.5b) even though the shell polymer microstructure differed greatly. This was expected, as the STEM images were taken when samples were dried. However, the average swelling of the particles in each latex should differ due to the significant difference in gel content of each latex.[16]

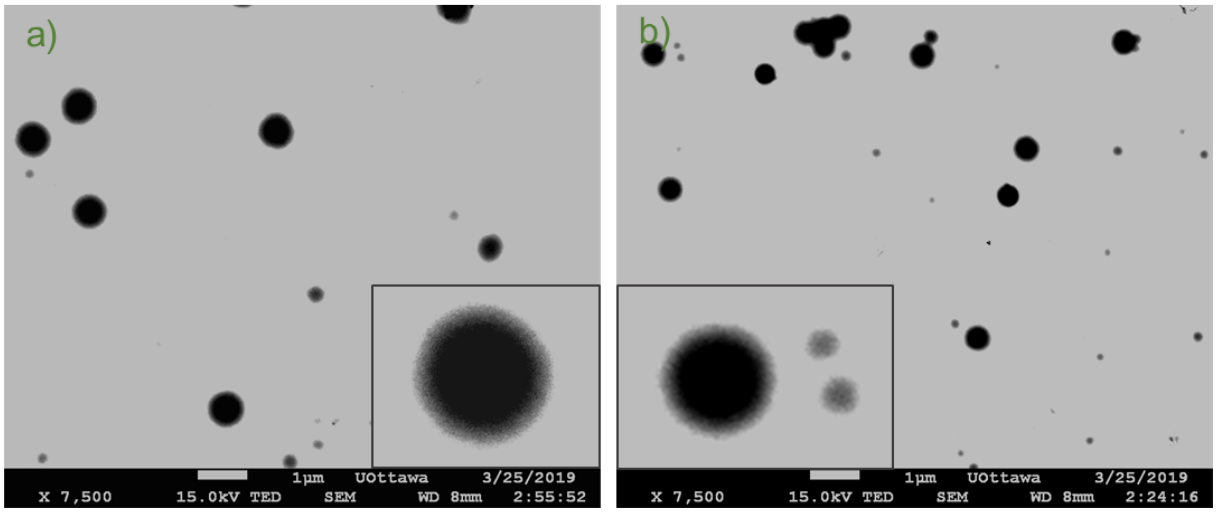

Figure 6.5 STEM images of a) Run 2 (0.4 phm NDM) and Run 3 (0.4 phm AMA).

Adhesive properties

Peel strength, tack and shear strength of SNP-based latexes with various amounts of CTA and crosslinker were tested. Peel strength is the force to peel the adhesive away from the substrate at a standard angle and rate. Tack is a measurement of the force required to detach the adhesive from a substrate when in contact with light or no pressure. Shear strength measures the shear deformation of the adhesive under constant shear stress.

Latex films generated using various CTA and crosslinker compositions (Table 6.2) yielded a range of adhesive properties. At 0.4 phm crosslinker, when CTA was increased from 0 to 0.4 phm, peel strength and tack improved (Figure 6.6-6.7), while the shear strength was reduced significantly (Figure 6.8). Note that the shear strength of Run 3 (0.4 phm crosslinker, Figure 6.8) was measured to be over two months. With the addition of CTA, the latex gel content decreased (Table 6.2) and the chain flexibility and mobility of the acrylic shell polymers were improved; this explains the increases in peel strength and tack, as well as the decrease in shear strength.[28] Cohesive failure in both tack and peel

strength tests was observed in samples from Runs 2 (0.4 phm CTA), 5 (0.2 phm CTA) and 9 (0.2 phm crosslinker, 0.4 phm CTA). This was due to the decreased polymer chain size and reduction in chain entanglements, with the addition of CTA. All other tests exhibited adhesive failure.

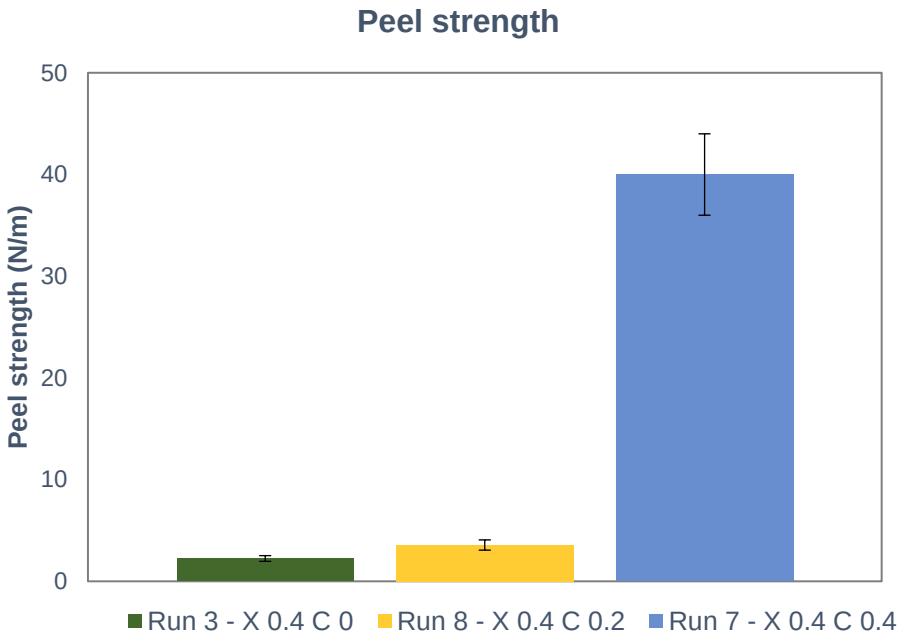

Figure 6.6 Effect of CTA on peel strength at 0.4 phm crosslinker (X = crosslinker concentration, C = CTA concentration).

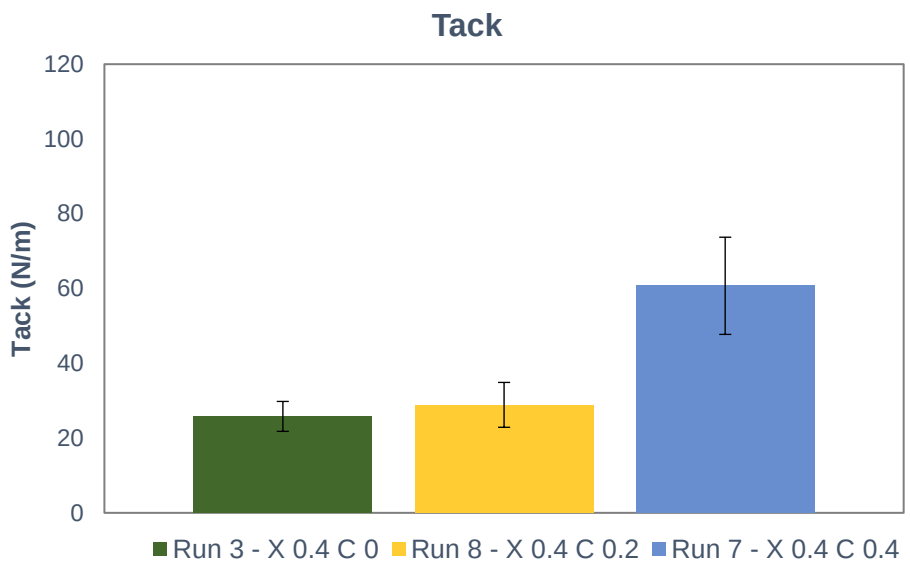

Figure 6.7 Effect of CTA on tack at 0.4 phm crosslinker (X = crosslinker concentration, C = CTA concentration).

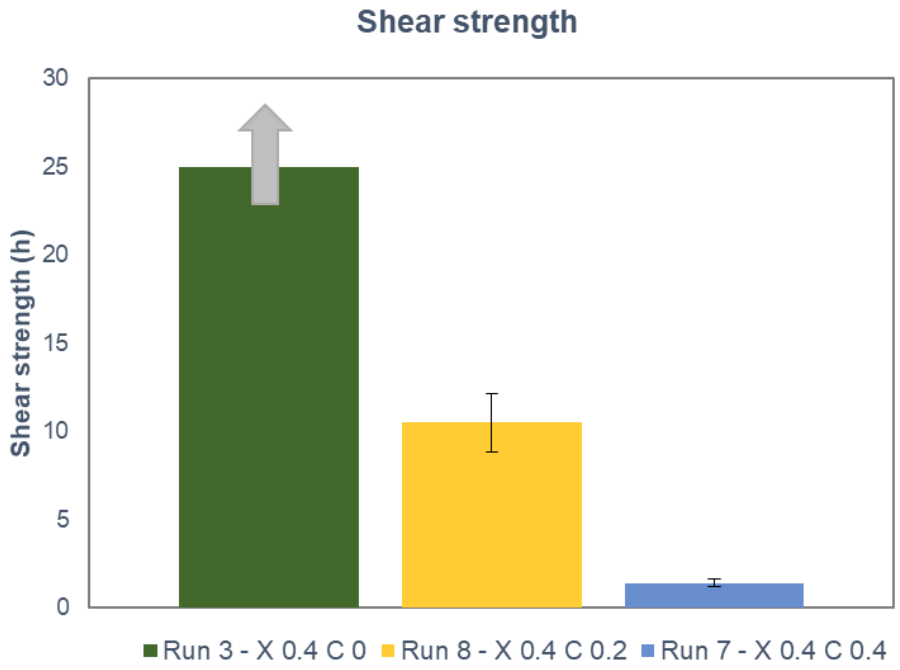

Figure 6.8 Effect of CTA on shear strength at 0.4 phm crosslinker (X = crosslinker concentration, C = CTA concentration). Run 3 time exceeds the scale of the graph (> 2 months).

The effect of crosslinker on adhesive properties at the same CTA concentration (0.2 phm) is shown in Figure 6.9-6.11. With the increase in crosslinker concentration in the acrylic shell formulation, the peel strength showed a maximum, tack decreased, and the shear strength increased. Peel strength increases to a maximum when a loose network structure and appropriate gel content are obtained.[1,19] However, further increases in gel content restrain the movement of acrylic polymer chains, leading to a lower peel strength. At the same time, an increased gel content leads to a reduction in tack and improved shear strength.

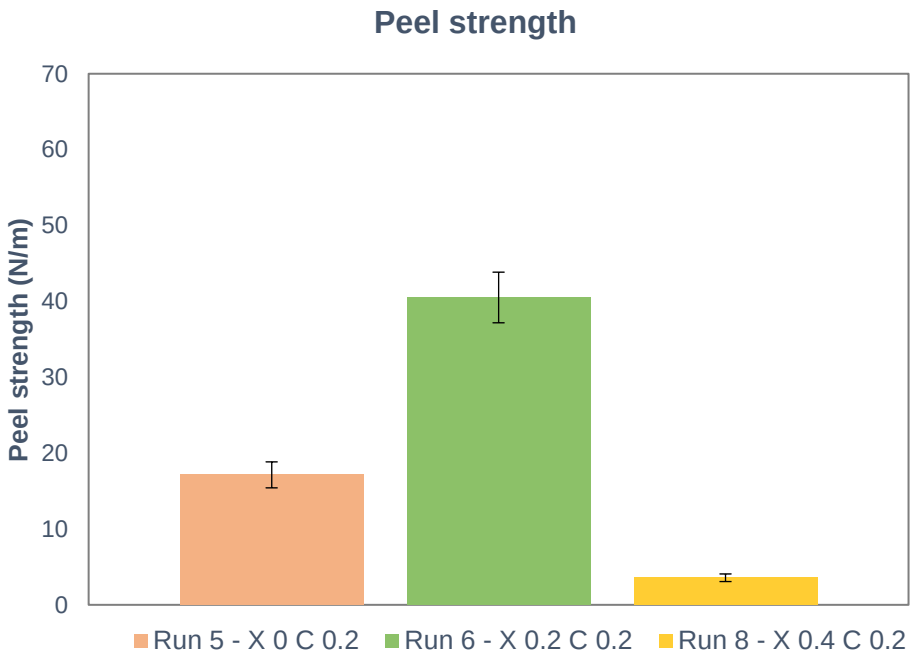

Figure 6.9 Effect of crosslinker on peel strength at 0.2 phm CTA (X = crosslinker concentration, C = CTA concentration).

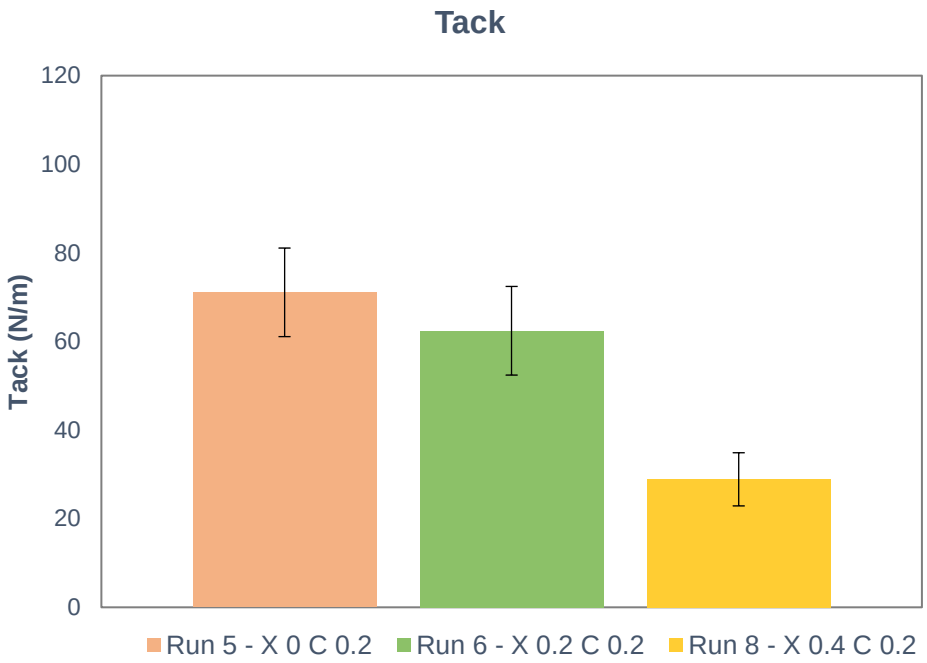

Figure 6.10 Effect of crosslinker on tack at 0.2 phm CTA (X = crosslinker concentration, C = CTA concentration).

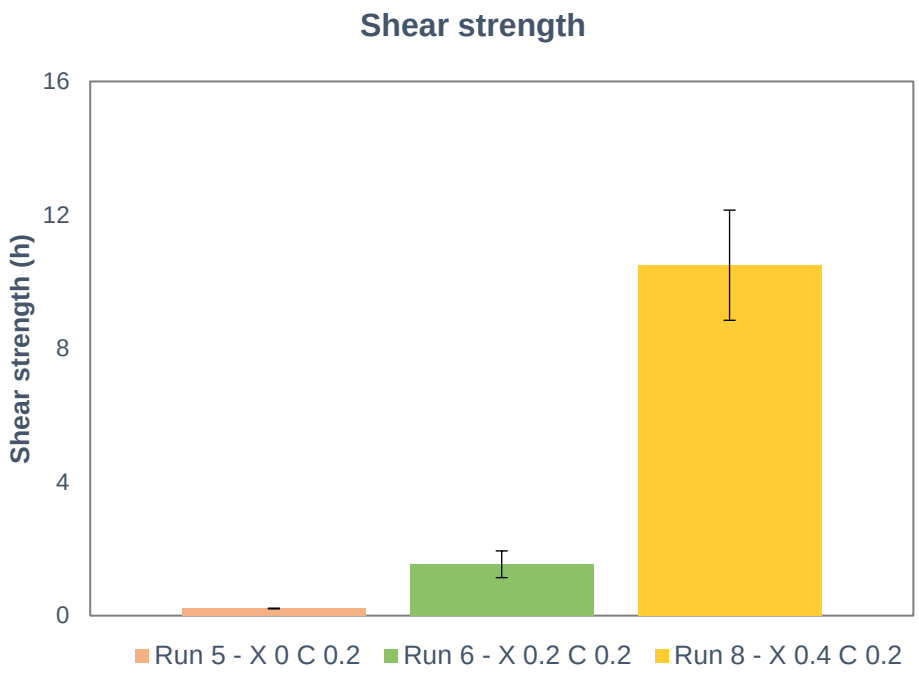

Figure 6.11 Effect of crosslinker on shear strength at 0.2 phm CTA (X = crosslinker concentration, C = CTA concentration).

To better visualize the effect of CTA and crosslinker on adhesive properties, 3D response surfaces for peel strength (Figure 6.12), tack (Figure 6.13) and shear strength (Figure 6.14) were constructed using all of the adhesive property results. The response surfaces are strictly empirical fits to the collected data. Peel strength achieved a maximum in most cases when increasing CTA or crosslinker (Figure 6.12). Tack generally increased with increasing CTA and decreasing crosslinker (Figure 6.13). However, as CTA and crosslinker concentrations were maximized, a near inversion of this trend is evident. Shear strength increased with the addition of crosslinker and decreased with the addition of CTA in all cases (Figure 6.14). Nevertheless, at very high CTA concentrations, the effect of crosslinker on shear strength was negated.

As shown by Qie and Dubé,[18,19] one can achieve a range of latexes with similar gel contents but vastly different microstructure. For example, by varying the molecular weight between crosslinks (i.e., loose vs. tight network), the molecular weight distribution, and the degree of branching, a range of microstructures and gel contents can be achieved. Run 1 (base case, no CTA or crosslinker used) and Run 6 (0.2 phm crosslinker and 0.2 phm CTA) showed similar gel contents, 63.2 wt.% and 63.7 wt.%, respectively (Table 6.2). However, Run 6 yielded higher peel strength and tack, and lower shear strength compared with Run 1 (Figure 6.12-6.14). This suggests that the acrylic shell polymer microstructure was significantly different in these two cases: Run 6 may have a looser network, and/or broader molecular weight distribution, and/or higher degree of branching than Run 1.[1] Thus, to achieve SNP-based latexes with different adhesive properties, one requires an appropriate acrylic shell polymer microstructure (i.e., gel content, molecular weight and distribution, degree of branching). 3D response surfaces can be a useful tool to guide one in the design of latexes with desired properties by manipulating CTA and crosslinker concentration. In our case, SNP-based latexes can be tailored to achieve the desired adhesive performance.

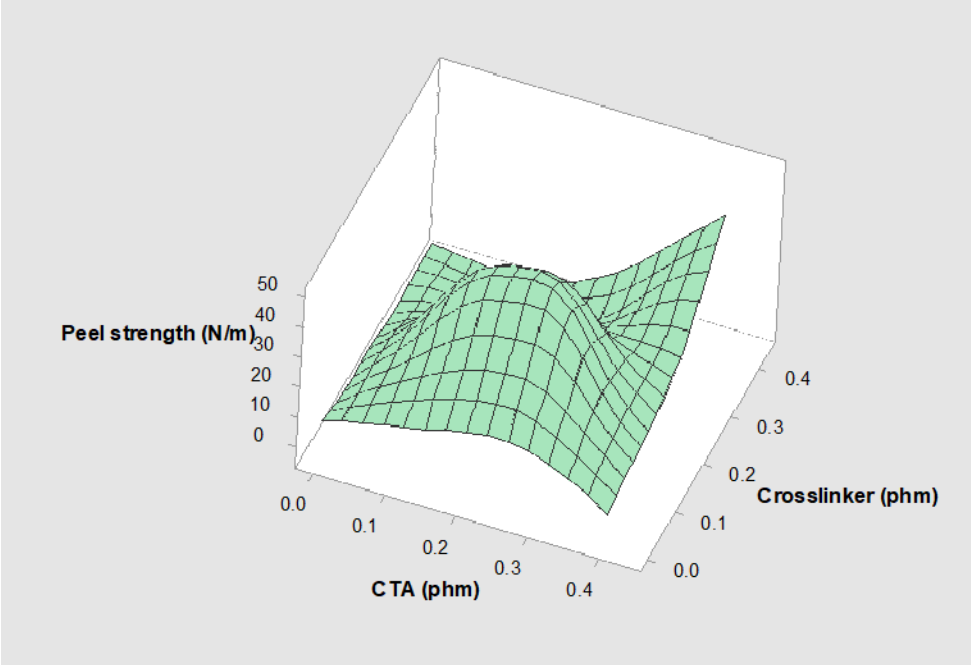

Figure 6.12 3D response surface of peel strength.

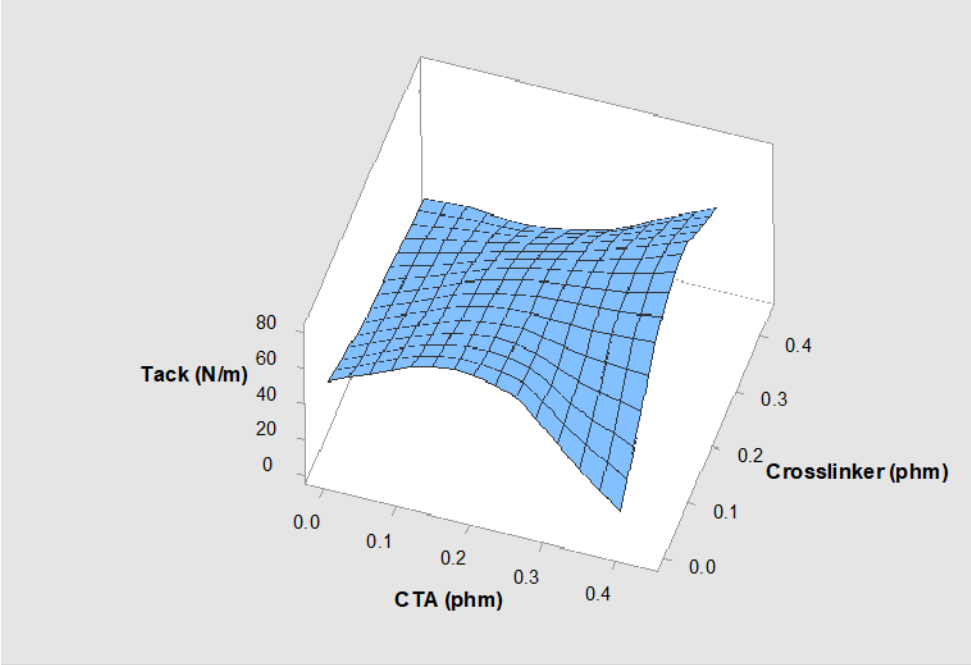

Figure 6.13 3D response surface of tack.

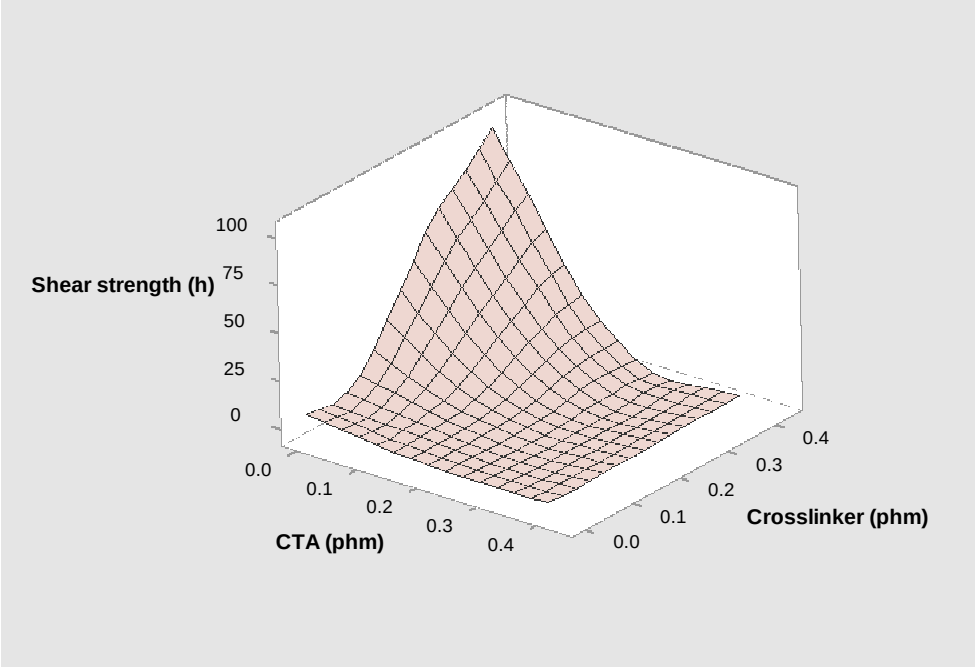

Figure 6.14 3D response surface of shear strength.

Viscoelastic properties

DMA was used to measure the storage modulus (G'), loss modulus (G") and tan δ at 23 ℃ for all latexes. G' measures the elastic deformation of a material and is an indication of the "stiffness" of the adhesive. G" represents the viscous portion of a material and is a measurement of the flexibility of the adhesive. Tan δ is the ratio of storage modulus G' to the loss modulus G".[29] PSA performance is related to the viscoelastic properties of the polymer. For instance, the removal of the adhesive from the substrate takes place under high frequency conditions (about 100 Hz), thus G' and G" at ~100 Hz provide a measure of the debonding strength.[30] On the other hand, the bonding process often occurs at low frequencies (0.01 to 1 Hz), thus G' at low frequency reflects bonding efficiency.[29,30]

In Figure 6.15-6.17, G', G" and tan δ of latexes with different CTA and crosslinker concentrations (Run 6-8) are shown. In all cases, G' was larger than G" (tan δ <1), which suggests that the elastic portion of the polymer dominated the properties. At a frequency of 1 Hz, the G' of all samples was lower than 1×10^5 Pa (Figure 6.15), indicating that all samples met the criterion to wet the substrate according to Dahlquist's theory.[31] When more CTA was added to the acrylic shell formulation, G' was lower at all frequencies (Figure 6.15), indicating better tack and reduced shear strength, which correlates with our adhesive testing results.[1,29] When more crosslinker was added to the formulation, the opposite trend was observed. The loss modulus, G", behaved similarly at low frequencies (<1 Hz, Figure 6.16). However, at higher frequencies, G" increased with crosslinker concentration and decreased with CTA concentration, demonstrating that debonding strength was improved when crosslinker was added, and was reduced when CTA was added. Based on the values of G' and G", the latexes produced from Run 6 to 8 can be used as commercial PSA tapes.[30]

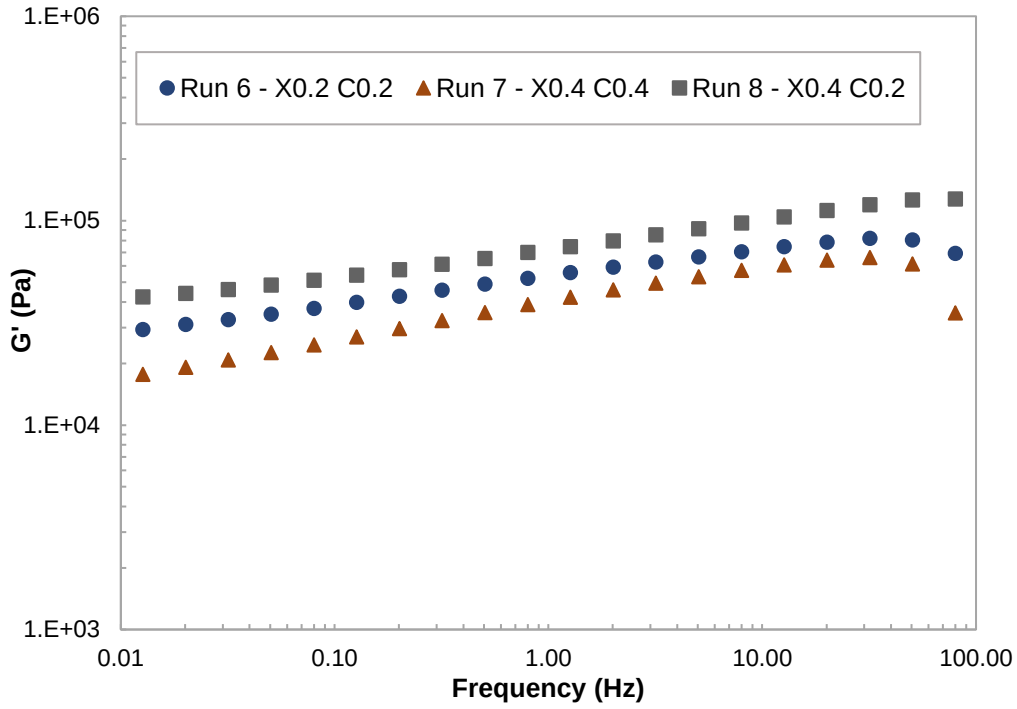

Figure 6.15 Storage modulus G' vs. frequency at 23 ℃ for Run 6 to 8.

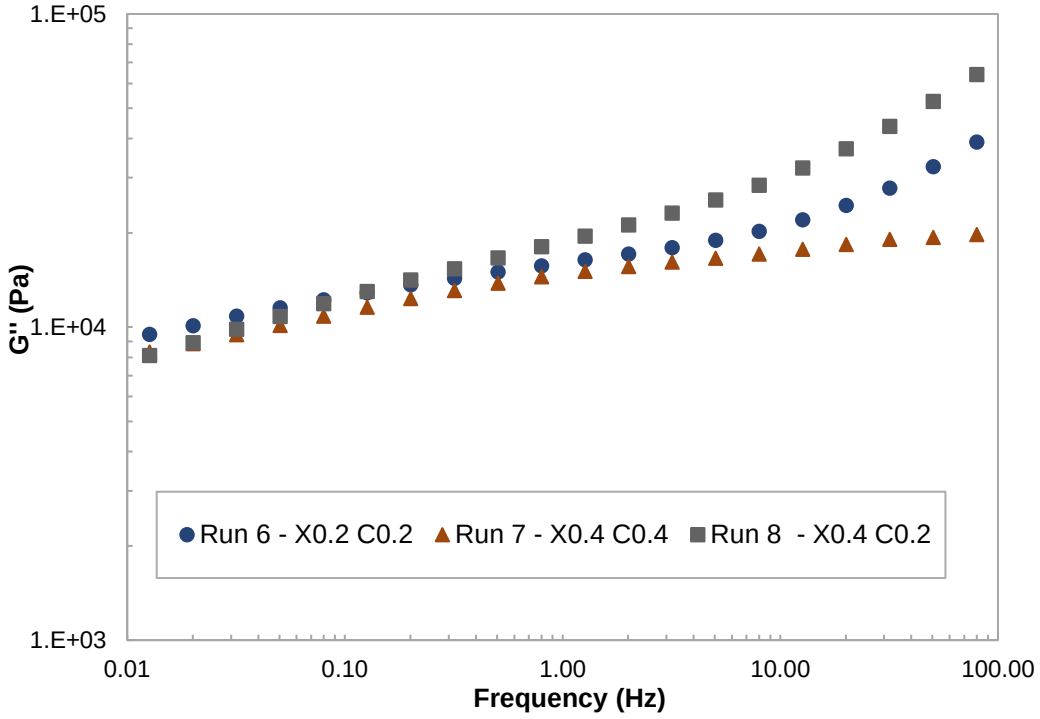

Figure 6.16 Loss modulus G" vs. frequency at 23 ℃ for Run 6 to 8.

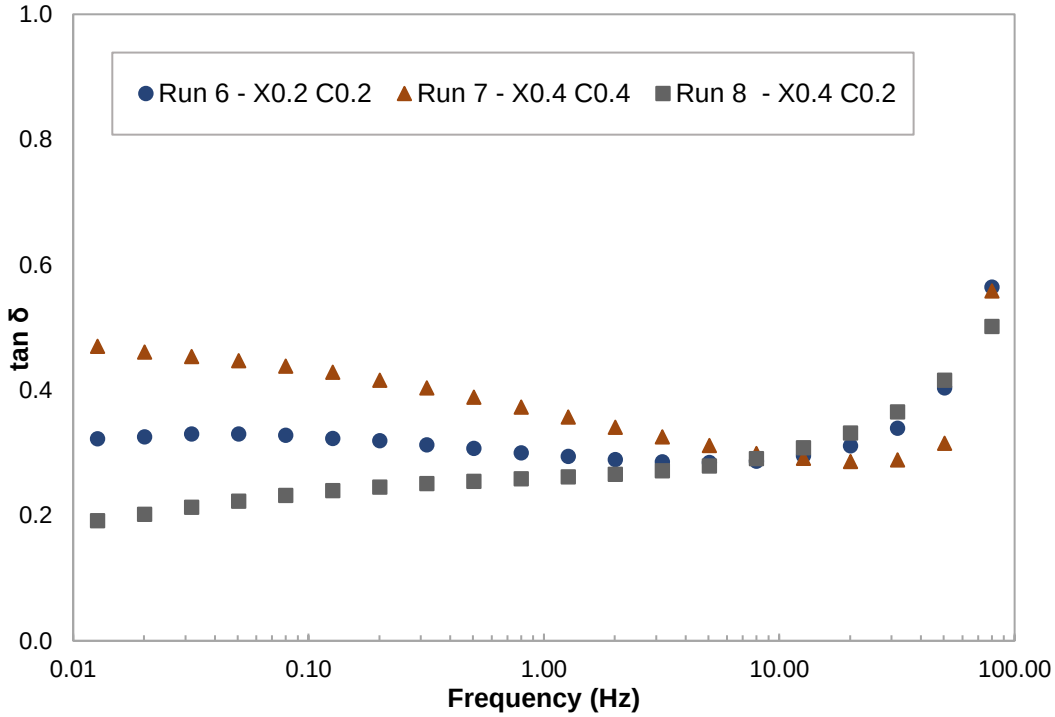

Figure 6.17 Tan δ vs. frequency at 23 ℃ for Run 6 to 8.

Conclusion

Crosslinker and CTA were used in a series of seeded, semi-batch emulsion polymerizations to produce SNP-based PSAs with a variety of adhesive and latex properties. Core-shell latex particles were achieved in all cases. By simultaneously varying the crosslinker and CTA concentrations, one can tune the acrylic shell polymer microstructure and achieve a range of adhesive properties. The addition of crosslinker and CTA had a negligible effect on polymerization kinetics, latex particle size and viscosity. The gel content of the latex polymers increased with crosslinker concentration and decreased with CTA concentration. An empirical model of gel content as a function of crosslinker and CTA

concentrations was derived, based on a 3^2 factorial design. Model predictions correlated closely with the experimental data.

Using the results from three different adhesive tests (tack, peel strength and shear strength), 3D response surfaces were generated and shown to be a useful tool for the design of SNP-based PSAs. The viscoelastic properties of the selected latex samples were measured and correlated well with the adhesive test results.

In summary, one can choose the appropriate amounts of CTA and crosslinker to formulate SNP-based latexes with targeted adhesive and latex properties as part of a more sustainable approach to PSA production.

Acknowledgment

Financial support for this work through the Natural Sciences and Engineering Research Council (NSERC) of Canada and EcoSynthetix Inc. (Burlington, ON) is gratefully acknowledged.

References

[1] R. Jovanović, M. A. Dubé, *J. Macromol. Sci. Part C* **2004**, *44*, 1.

[2] C. Creton, *MRS Bulletin* **2003**, 28, 434.

[3] M. A. Dubé, S. Salehpour, *Macromol. React. Eng.* **2014**, *8*, 7.

[4] T. Wang *et al.*, *Adv. Mater.* **2006**, *18*, 2730.

[5] R. W. Connelly, W. F. Parsons, G. H. Pearson, *J. Rheol. 1978-Present* **1981**, *25*, 315.

[6] L. Qie, M. A. Dubé, *J. Appl. Polym. Sci.* **2012**, *124*, 349.

[7] G. E. Fonseca, T. F. McKenna, M. A. Dubé, *Chem. Eng. Sci.* **2010**, *65*, 2797.

[8] R. Vendamme, N. Schüwer, W. Eevers, *J. Appl. Polym. Sci.* **2014**, *131*, n/a.

[9] Y. Zhang, M. A. Dubé, *Adv. Polym. Sci.* **2017**, 1, doi:10.1007/12_2017_8.

[10] M. N. Belgacem, A. Gandini, *Monomers, Polymers and Composites from Renewable Resources*, Elsevier, Oxford, UK **2008**.

[11] Y. Zhang, M. F. Cunningham, N. M. B. Smeets, M. A. Dubé, *Eur. Polym. J.* **2018**, *106*, 128.

[12] Y. Zhang, M. F. Cunningham, N. M. B. Smeets, M. A. Dubé, *Ind. Eng. Chem. Res.* **2019**, DOI:10.1021/acs.iecr.9b00332.

[13] J. Y. Charmeau, R. Berthet, C. Gringreau, Y. Holl, E. Kientz, *Int. J. Adhes. Adhes.* **1997**, *17*, 169.

[14] J. Garrett, P. A. Lovell, A. J. Shea, R. D. Viney, *Macromol. Symp.* **2000**, *151*, 487.

[15] S. Ren, M. A. Dubé, *Int. J. Adhes. Adhes.* **2017**, *75*, 132.

[16] C. Tan, T. Tirri, C.-E. Wilen, *Int. J. Adhes. Adhes.* **2016**, *66*, 104.

[17] J. Kajtna, J. Golob, M. Krajnc, *Int. J. Adhes. Adhes.* **2009**, *29*, 186.

[18] L. Qie, M. A. Dubé, *Macromol. React. Eng.* **2011**, *5*, 117.

[19] L. Qie, M. A. Dubé, *Eur. Polym. J.* **2010**, *46*, 1225.

[20] P. Chen *et al.*, *Polym.-Plast. Technol. Eng.* **2012**, *51*, 122.

[21] E. Mehravar *et al.*, *Macromolecules* **2018**, *51*, 9740.

[22] S. Roberge, M. A. Dubé, *Int. J. Adhes. Adhes.* **2016**, *70*, 17.

[23] W. Fan, M. Tosaka, S. Yamago, M. F. Cunningham, *Angew. Chem. Int. Ed.* **2018**, *57*, 962.

[24] J. Chauvet, J. M. Asua, J. R. Leiza, *Polymer* **2005**, *46*, 9555.

[25] Pressure Sensitive Tape Council, *Test methods for pressure sensitive adhesive tapes*. **2004**.

[26] S. Cummings, *PhD Thesis*, University of Ottawa, August, **2017**.

[27] G. Odian, *Principles of Polymerization*, John Wiley & Sons, Hoboken, NJ USA **2004**.

[28] D. Urban, L. Egan, *Polym. Dispers. Their Ind. Appl.* **2003**, 191.

[29] K. P. Menard, N. R. Menard, *Encycl. Polym. Sci. Technol.* **2015**, 1.

[30] E. P. Chang, *J. Adhes.* **1997**, *60*, 233.

[31] C. A. Dahlquist, *Treatise Adhes. Adhes.* **1969**, 319.

7. General Discussion, Conclusion and Recommendations

The production, as well as the disposal of petroleum-based polymeric materials have raised considerable environmental concerns.[1,2] Thus, it is necessary to develop alternatives to produce more sustainable polymeric materials. For that purpose, we chose starch nanoparticles (SNPs) to displace petroleum-based monomers in the production of latex polymers targeting adhesive applications. The idea is to enable the incorporation of SNPs into polymer latexes by forming a core-shell structure (see Figure 7.1). Ideally, the SNP cores will provide biocontent, while the acrylic polymers on the shell govern the latex properties. The resulting polymers should also present enhanced degradation rates which will result in far lower environmental impact.

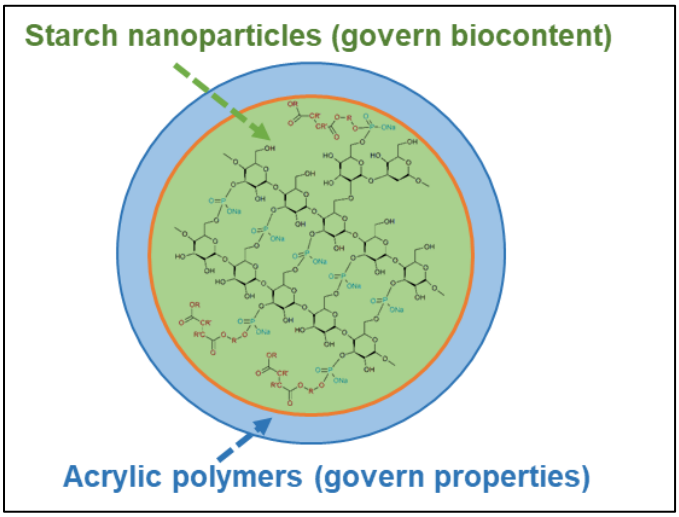

Figure 7.1 Concept of the core-shell particle morphology to increase bio-content of latex emulsions.

Emulsion polymerization was applied to produce bio-based polymer latexes in this project, because it uses water rather than organic solvents and therefore, is considered as a more sustainable way to produce polymer.[1,3] Typical emulsion polymerizations contain many components that influence both latex stability and polymer application

properties. Introducing SNPs into the emulsion system will inevitably affect latex stability and product properties.[4] A major challenge will be situating the highly hydrophilic SNPs within an organic shell in the presence of a continuous aqueous phase. In addition, it's difficult to achieve perfect core surface coverage, high solids content and high SNP incorporation due to the limited reactivity of SNPs. However, it is possible to overcome those challenges through the modification of SNPs and manipulation of the reaction formulation.

To achieve the core-shell particle morphology (i.e., starch core – synthetic polymer shell), a highly innovative methodology was developed (Figure 7.2). This includes the crosslinking of SNPs using a non-toxic crosslinker, sodium trimetaphosphate (step 1), attaching vinyl functional groups (i.e., C=C) with a functionalized sugar monomer (step 2), tuning hydrophobicity by introducing a "tie-layer" monomer, butyl vinyl ether (step 3), and finally achieving the core-shell morphology via a conventional semi-batch emulsion polymerization (step 4). This methodology allowed significant amounts of SNP encapsulation without destabilizing the latex nor deteriorating other latex properties at 15 wt.% SNP loading and 40 wt.% latex solids.[5] A series of controlled experiments was then conducted to identify the effects of various formulation parameters (e.g., STMP concentration, crosslinking time, BVE concentration) on the latex stability and latex properties such as particle size and distribution, viscosity, and microstructure (e.g., molecular weight, gel content). This also confirmed the necessity of each modification procedure.[5]

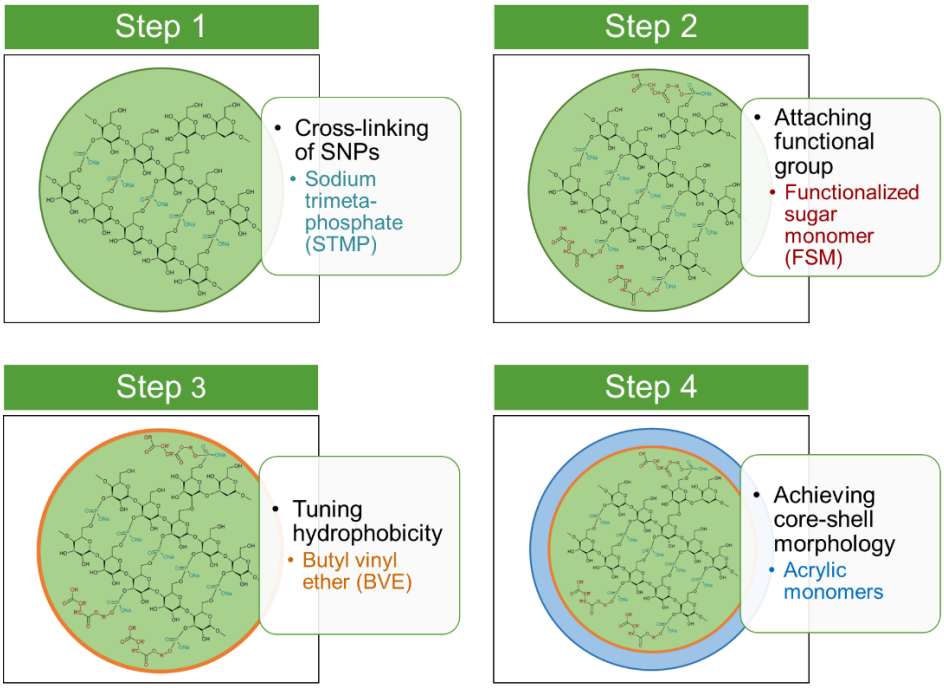

Figure 7.2 Methodology to achieve core-shell latex particle morphology.

To investigate the effect of SNP loading and latex solids on latex stability and latex properties (e.g., viscosity, particle size, adhesive properties, particle morphology), polymerization formulations with various SNP loadings and solids were tested.[6] Stable and low viscosity SNP-based latexes with up to 45 wt.% SNP loading and 55 wt.% latex solids were produced. The presence of a core-shell morphology was confirmed by STEM images (Figure 7.3). With the increase of the SNP loadings, the acrylic shell thickness (relative to the total particle diameter) decreased. Though SNP-based latexes with good adhesive properties can be achieved, it is inevitable that pushing the limits of SNP loading and latex solids will influence the latex adhesive properties.

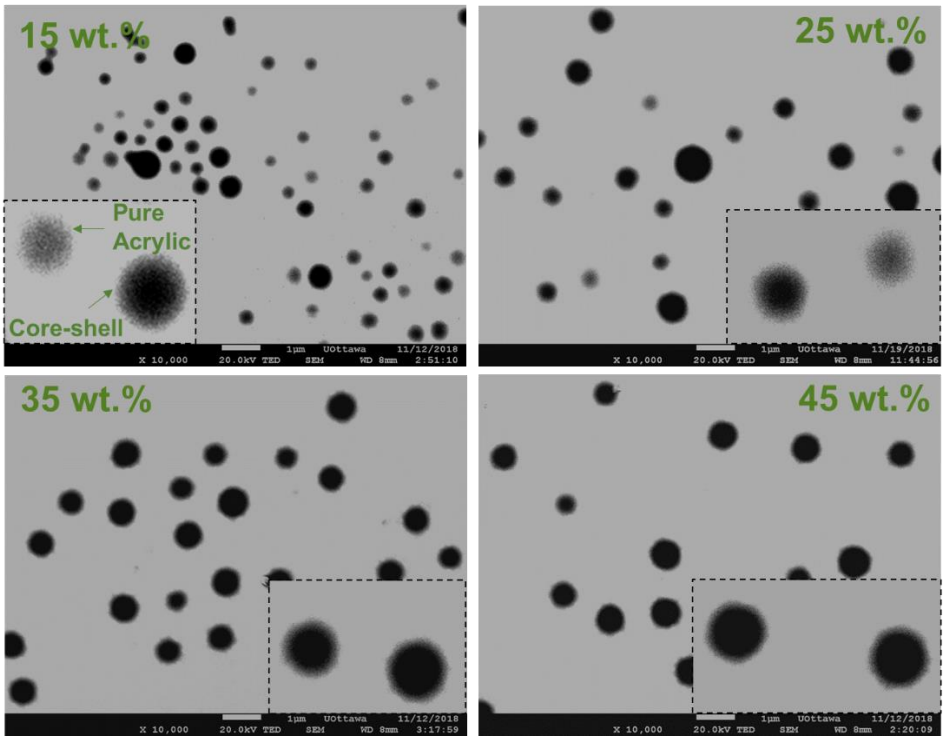

Figure 7.3 Latex particle morphology changes with SNP loadings.

The use of crosslinker and/or chain transfer agent (CTA) is considered an effective approach to manipulate polymer microstructure.[7,8] As the acrylic shell polymers contribute substantially to the adhesive properties of the SNP-based latexes, crosslinker and CTA were used simultaneously to tailor the microstructure of the acrylic shell polymer - in a sense, to "bring back" the properties of the SNP-free latex. Based on a 3^2 factorial design, a range of crosslinker and CTA concentrations was tested to understand their effects on adhesive and latex properties. There was no significant effect on the polymerization kinetics, particle size and viscosity with the addition of various amounts of crosslinker and CTA. Gel content of the latex polymers increased with increasing amounts of crosslinker and decreased with increasing amounts of CTA. Using the gel content results, an empirical model of gel content was proposed as a function of

crosslinker and CTA concentration. 3D response surfaces of tack, peel strength and shear strength were generated according to the adhesive testing results. The gel content model, as well as 3D response surfaces of adhesive properties, are useful tools for the design of SNP-based latexes with a variety of adhesive and latex properties by choosing the appropriate amounts of crosslinker and CTA.

Armed with the knowledge gained in this project, we can now produce SNP-based latexes for adhesive applications; however, some future possibilities can be explored:

1. With the methodology developed in the project, one can develop SNP-based latexes for a variety of applications (e.g., coatings, thermoplastics) by simply using different shell polymer formulations. For instance, to produce SNP-based latexes for coatings, one can simply replace the current acrylic polymer formulation (BA/MMA/AA, 93/5/2, mol/mol/mol) with a formulation used for coating applications (e.g., BA/MMA, 44/56, mol/mol).[9]
2. Though up to 45 wt.% of petroleum-based monomer was replaced by SNPs in this project, one can further improve the sustainability of the SNP-based latexes by replacing the petroleum-based acrylic monomers in the shell polymer formulations with renewable monomers. For example, vegetable-oil based acrylic monomers (e.g., fatty acids and derivatives)[10,11] and terpenes (e.g., limonene, α-pinene)[12–14] are good candidates as a replacement of petroleum-based monomers.

3. This thesis demonstrates a direct approach to use renewable monomers to achieve more sustainable polymer products. However, the sustainability of polymer production process goes well beyond that. As polymerization reactions are extremely exothermic, a great deal of energy is consumed in controlling reaction temperatures during polymerization reactions. Thus, one can maximize energy efficiency and make better use of the heat produced during polymerization to synthesize SNP-based latexes (or other bio-based latexes) by adopting an adiabatic polymerization strategy. Adiabatic polymerization is a polymerization process that involves no external heating or cooling system or, in some cases, only involves heating at the initial stages of the process.[15,16] For instance, initiators requiring relatively low temperatures (e.g., redox initiators) can be used to produce SNP-based latexes at room temperature.

In conclusion, we have successfully encapsulated SNP cores into latex polymers, have confirmed core-shell particle morphology, have studied the effect of SNP loadings and latex solids on latex stability and properties, and have explored approaches to tailor the properties of SNP-based latexes with the combination of crosslinker and CTA. This project concluded with the development of successful latex formulations based on industrial requirements for a high solids content (up to 55 wt.% solids) and high SNP content (up to 45 w/w%) with a range of latex and adhesive properties. It will eventually lead to one of the commercial polymer products containing the highest levels of renewable materials on the market. This will not only advance Canada's bio-economy and technology

strengths, but also reinforce Canada's position as a world-leader in novel, sustainable approaches to polymer production.

References

1. Y. Zhang, M. A. Dubé, *Adv. Polym. Sci.* **2017**, 1, doi:10.1007/12_2017_8.
2. M. N. Belgacem, A. Gandini, *Monomers, Polymers and Composites from Renewable Resources*, **2008**, Elsevier, *Oxford, UK*.
3. C. S. Chern, *Prog. Polym. Sci.* **2006**, *31*, 443.
4. R. Jovanović, M. A. Dubé, *J. Macromol. Sci. Part C* **2004**, *44*, 1.
5. Y. Zhang, M. F. Cunningham, N. M. B. Smeets, M. A. Dubé, *Eur. Polym. J.* **2018**, *106*, 128.
6. Y. Zhang, M. F. Cunningham, N. M. B. Smeets, M. A. Dubé, *Ind. Eng. Chem. Res.* **2019**, doi:10.1021/acs.iecr.9b00332.
7. L. Qie, M. A. Dubé, *Macromol. React. Eng.* **2011**, *5*, 117.
8. L. Qie, M. A. Dubé, *Eur. Polym. J.* **2010**, *46*, 1225.
9. B. J. Walekar, S. R. Mane, P. N. Bhosale, *Adv. Polym. Technol.* **2017**, *36*, 243.
10. S. Roberge, M. A. Dubé, *Int. J. Adhes. Adhes.* **2016**, *70*, 17.
11. S. Roberge, M. A. Dubé, *ACS Sustain. Chem. Eng.* **2016**, *4*, 264.
12. Y. Zhang, M. A. Dubé, *Macromol. React. Eng.* **2014**, *8*, 805.
13. Y. Zhang, M. A. Dubé, *Polym.Plast. Technol. Eng.* **2014**, *54*, 499.
14. S. Ren, E. Trevino, M. A. Dubé, *Macromol. React. Eng.* **2015**, *9*, 339.
15. S. Wang, E. S. Daniels, E. D. Sudol, A. Klein, M. S. El-Aasser, *J. Appl. Polym. Sci.* **2016**, *133*, 43037.
16. M. Goikoetxea, R. Heijungs, M. J. Barandiaran, J. M. Asua, *Macromol. React. Eng.* **2008**, *2*, 90.

Appendix A

Health and Safety Assessment

Laboratory activities including monomer distillation, preparation of pre-emulsion solution, and sample workup for characterization will be carried out under a fumehood with appropriate personal protective equipment to minimize any potential exposure to chemicals. All chemicals used in this project are listed in Table A.1 along with hazards and required personal protective equipment.

Table A.1 Potential chemical hazards and personal protective equipment

Compounds	**Hazards**	**Personal protective equipment**
Butyl Acrylate	Flammable liquid and vapour Cause skin irritation	Protective clothing and gloves, eye protection, and full-face respirator
Methyl Methacrylate	Highly flammable liquid and vapor Cause skin and respiratory irritation May cause an allergic skin reaction	Protective clothing and gloves, eye protection, and full-face respirator
Acrylic Acid	Very hazardous in case of skin contact (permeator), of eye contact (irritant, corrosive) Flammable	Face shield. Full suit. Vapor respirator. Be sure to use an approved/certified respirator or equivalent. Gloves. Boots
Sodium Trimetaphosphate	May be harmful if inhaled, or absorbed through skin May cause eye irritation	Handle with gloves and eye protection
EF-800	Cause eye irritation and may cause skin irritation	Protective clothing and gloves, eye protection

Potassium Persulfate	Oxidizing solids May cause eye, skin, and respiratory irritation	Protective clothing and gloves, eye protection
Hydroquinone	May cause moderate skin and eye irritant	Protective clothing and gloves, eye protection
Tetrahydrofuran	Flammable May cause mild skin and serious eye irritation	Protective clothing and gloves, eye protection
Chloroform-D	Toxic, carcinogen Moderate skin and eye irritant	Protective clothing and gloves, eye and face protection
Acetone	Highly flammable liquid and vapor Causes serious eye irritation May cause drowsiness	Protective clothing and gloves, eye protection
Starch Nanoparticles	May produce slight irritation to respiratory tract Prolonged exposure to eyes and skin may cause slight irritation	Protective clothing and gloves, eye protection Avoid breathing dust
Sodium Bicarbonate	No hazard May cause eye and skin irritation	Protective clothing and gloves, eye protection
Nitrogen	High pressure May cause suffocation by displacing the oxygen in air	Storage upright and secure cylinders all time while in use and use appropriate hand truck designed for cylinder